GEOPHYSICAL INSTITUTE

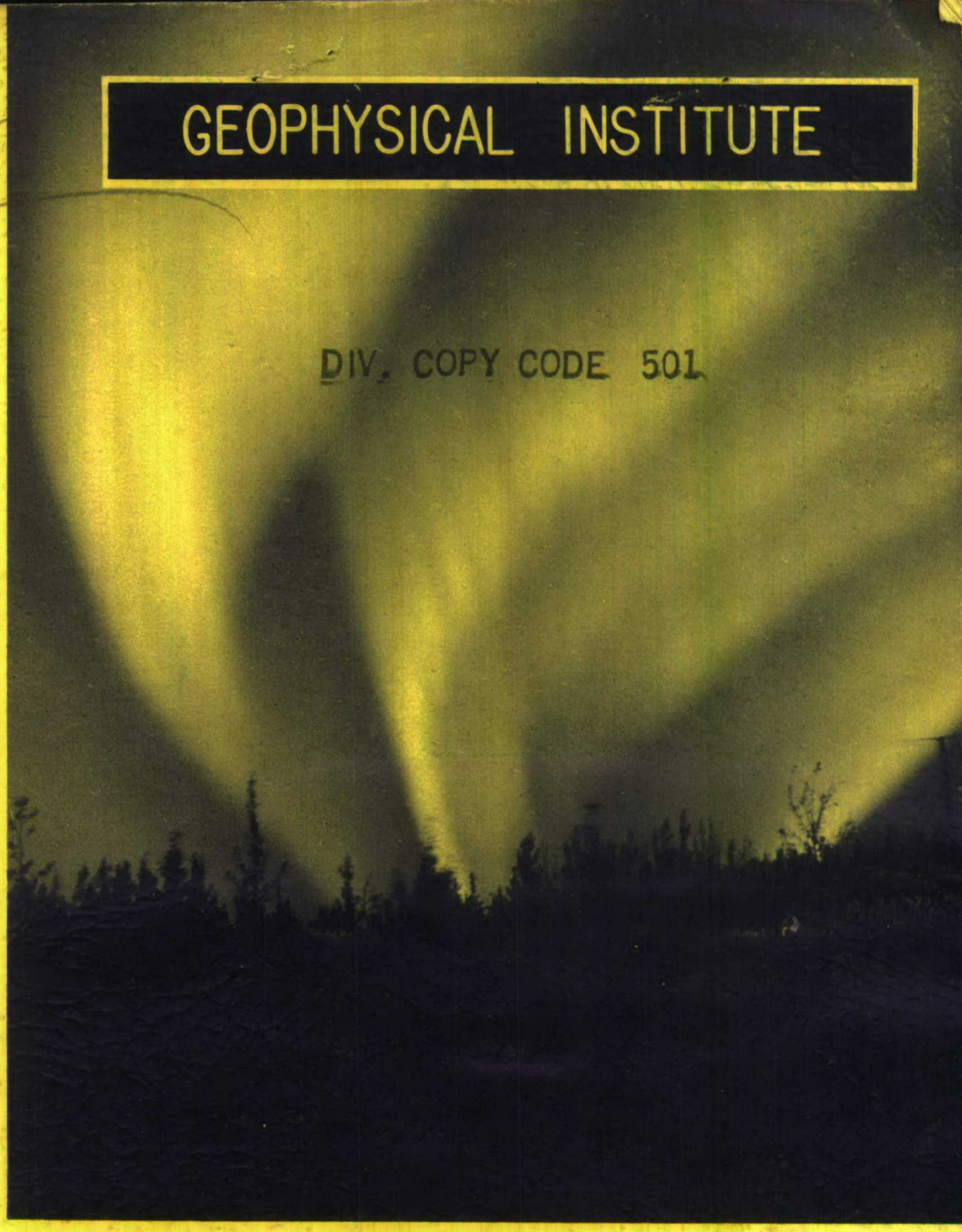

UNIVERSITY
OF ALASKA

COLLEGE
ALASKA

UAG-R138

THE SPATIAL AND TEMPORAL VIBRATIONS IN HIGH LATITUDE COSMIC NOISE ABSORPTION AND THEIR RELATION TO LUMINOUS AURORA

by

Z. A. Ansari

NSF Grant No. G14133

Scientific Report No. 4

MAY 1963

NATIONAL SCIENCE FOUNDATION
WASHINGTON, D. C.

GEOPHYSICAL INSTITUTE

of the

UNIVERSITY OF ALASKA

Scientific Report No. 4

THE SPATIAL AND TEMPORAL VARIATIONS IN HIGH LATITUDE COSMIC NOISE ABSORPTION AND THEIR RELATION TO LUMINOUS AURORA

by

Z. A. ANSARI

NSF GRANT NOS. G14133, GP947

MAY 1963

Principal Investigators:

R. Parthasarathy
H. Leinbach

Approved by:

C. T. Elvey
Director

Requests for additional copies by Agencies of the Department of Defense, their contractors, and other government agencies should be directed to the:

DEFENSE DOCUMENTATION CENTER (DDC)
ARLINGTON HALL STATION
ARLINGTON 12, VIRGINIA

Department of Defense contractors must be established for DDC services or have their "need-to-know" certified by the cognizant military agency of their project or contract.

All other persons and organizations should apply to the:

U.S. DEPARTMENT OF COMMERCE
OFFICE OF TECHNICAL SERVICES
WASHINGTON 25, D. C.

ABSTRACT

The spatial and temporal variations in cosmic radio noise absorption were investigated at College, Alaska, during 1962-1963 by means of riometers using one narrow beam antenna and two relatively broad beam antennas which were pointed at different directions along the magnetic meridian. The narrow beam antenna had a 12° beamwidth and was periodically swung in the magnetic meridian from 12° north of zenith to 12° south of zenith. Each of the broad beam antennas had a 26° beamwidth and was directed to 40° from zenith, one to the south and the other to the north. In order to explore the relation of the spatial variations in absorption with the differences in auroral luminosity existing in different directions at a given time, two λ 5577A photometers were operated in the two switching directions of the narrow beam antenna i.e. 12°N and 12°S. The information about the auroral coverage of the various antenna beams was obtained from all-sky photographs.

A simultaneous study of radio-wave absorption in relation to luminous aurora resulted in the conclusion that the nighttime radio-wave absorption observed at College, Alaska falls into the following two main categories.

The absorption belonging to Category I is observed at any time between 2000-0200 hrs, correlates well with the intensity fluctuations of λ 5577A, and is limited to luminous regions of the sky only. Included in the above category is the absorption associated with the quiet as well as bright and active phases of the display.

The absorption belonging to Category II is observed only in the post-midnight hours, does not correlate with the intensity fluctuations of λ 5577A and, most probably, is not limited to luminous regions of sky only. With the absorption making a transition from Category I to Category II, a 10-100 fold increase takes place in the ratio of absorption to λ 5577A intensity.

In order to explore the contribution of bremsstrahlung X-rays to the observed absorption of both categories, the X-ray intensity is calculated on top of the D-region assuming reasonable flux values of the primary electrons. Using the results of the generalized magnetoionic theory, it is shown that the contribution of X-rays to the observed absorption is at the most 2½% and therefore may be safely neglected.

The close association between radio-wave absorption and luminous aurora during absorption events of Category I suggests that the primary particles responsible for the absorption are approximately in the energy range 10-20 kev. It is shown that the absorption associated with the quiet phase of the auroral display is easily explained by a flux of 10^7-10^8 electrons cm^{-2} sec^{-1} in the above energy range. It is also shown that the transition from the quiet phase to the bright and active phase is the result of a momentary 10-100 fold increase in the flux of low energy electrons.

The lack of correlation between absorption and λ 5577A intensity fluctuations and the pronounced increase in the ratio of absorption to λ 5577A intensity observed during absorption events of Category II are indicative of a hardening of the primary particle energy spectrum, possibly due to the injection of a large

number of electrons in the energy range 30-100 kev. It is estimated that a flux of 10^6-10^7 electrons cm^{-2} sec^{-1} in the above energy range can adequately account for the observed absorption.

In the light of the above observations, the apparent discrepancy between the results of two rocket flights at Fort Churchill, one by McIlwain and the other by McDiarmid et al, is easily resolved.

This work was supported by National Science Foundation, Grants 14133 and 947.

ACKNOWLEDGEMENTS

The author is indebted to Dr. C. T. Elvey, Director Geophysical Institute and Vice President of research and advanced study, without whose keen interest and support this work would not have been possible.

It is a pleasure to acknowledge the most valuable advice received from Dr. H. Leinbach and Prof. R. Parthasarathy on the technical aspects of the study.

The author is indebted to Dr. L. Owren who was instrumental in introducing the author to cosmic noise absorption studies, and to Dr. W. L. Flock whose advice on the manuscript proved to be very helpful.

Helpful discussions with Dr. S. I. Akasofu and Messrs. A. E. Belon, G. J. Romick, W. B. Murcray are also gratefully acknowledged.

Messr. Pete Michalow and D. L. Chauvin provided valuable advice on transistor switching. The help of Mr. A. R. Franzke in building the transistor switches and also in the routine maintenance of the equipment is acknowledged with thanks.

The high quality of drawings is due to the meticulous care of Mr. D. C. Wilder. Mr. F. Danels is responsible for the excellent photographic reproduction of the drawings. Mrs. Carol Echols, Mrs. Nancy Curry and Mrs. Sharon Dean helped in computations, scaling and data reduction. The laborious task of typing the manuscript was ably handled by Mrs. Helen Linde.

This work was supported by the National Science Foundation, Grant 14133.

TABLE OF CONTENTS

TABLE OF CONTENTS (CONT'D)

TABLE OF CONTENTS (CONT'D)

TABLE OF CONTENTS (CONT'D)

TABLE OF CONTENTS (CONT'D)

LIST OF ILLUSTRATIONS

LIST OF TABLES

CHAPTER I.

RADIO-WAVE ABSORPTION PHENOMENA IN THE AURORAL ZONE

1.1 INTRODUCTION

The occurrence of polar blackouts at higher latitudes in association with bright auroral displays and violent magnetic storms, has been a well known phenomenon since the advent of short wave radio communication. Unfortunately, very little attention was paid to this phenomenon until the beginning of the International Geophysical Year, 1957-1958. The reason is not hard to find. Prior to the start of I.G.Y., or until 1953, the pulse reflection technique was the only method used widely for measurements of radio wave absorption. This method is not suitable for high latitudes where the high intensity and greater frequency of occurrence of absorption events create blackout conditions quite frequently. It is therefore easy to understand why most of the pre I.G.Y. work on polar blackouts is rather qualitative in nature. The work of Shain (1951) marks a turning point in the history of absorption measurements, as he was the first to measure absorption by using cosmic radio noise as a signal source. Although the cosmic noise method originated at a low latitude station, it made a tremendous impact in higher latitudes, where the need for a simple, reliable method of measuring absorption had been felt for some time. One great advantage of this technique is that it remains usable under even extremely disturbed conditions of the polar ionosphere. A detailed discussion of this method will be given in Chapter IV.

On the instrumental side many improvements have been made since the time of Shain's work at 18.3 Mc/s. By far the most important of these improvements are continuous refinements in (a) sensitivity, (b) stability and (c) power linearity of the receiving system as better electronic components became available. There are, however, two major improvements in the conceptual side of radio astronomical instrumentation. Dicke (1946) showed that by rapidly switching the receiver input between the antenna and a dummy resistor of the same impedance kept at a constant temperature and by detecting the difference output one could make the output very much independent of the receiver gain variations. In this method it becomes obvious that the closer the dummy resistor's temperature is to that of the antenna, the less susceptible is the output to receiver gain variations. Machin, Ryle and Vonberg (1952) extended this idea by keeping the dummy resistor at almost the same effective temperature as that of the antenna. This was achieved by replacing the dummy by a noise diode whose filament current was continuously varied by servo mechanism in order to maintain its effective temperature the same as that of the antenna. Little and Leinbach (1959) made further improvement by incorporating frequency sweep and minimum detection techniques in order to discriminate against narrow band interference. Later on they established a chain of such receivers (riometers) which since then have come into world wide use.

This development naturally led to a series of interesting studies which shed light on the phenomenon of absorption from an entirely new angle. This does not however mean that all the outstanding problems encountered in the understanding of absorption phenomenon have been resolved by these investigations. Several basic questions still remain unanswered, especially in the field of auroral absorption which is the main theme of the present investigation. In this experimental study an attempt will be made to obtain at least partial answers to some of the main problems.

1.2 CLASSIFICATION OF HIGH LATITUDE ABSORPTION

The high latitude radio-wave absorption may be classified into the following categories.

1. SCNA or the Absorption Following Solar Flares.

This type of absorption occurs at the time of major solar flares and is generally known as sudden cosmic noise absorption or SCNA. Immediately following the solar flare and SCNA the following ionospheric effects are observed.

a. SPA (Sudden phase anomaly)

The solar flare creates intense ionization in the D-region of the ionosphere and as a result the reflection of VLF waves takes place at a lower level.

b. SEA (Sudden enhancement of the atmospherics)

The signal strength of atmospherics at VLF frequencies is enhanced due to the higher reflection coefficient at oblique incidence.

Mitra and Jones (1954) attempted to explain SCNA and other associated effects as resulting from an over-all enhancement of D-region ionization caused by Lyman-α radiation from the flare. Friedman (1960) and Swift (1961) have shown the inadequacy of Lyman-α hypothesis. Recently acquired rocket data has now proved beyond doubt that the enhanced D-region ionization is almost entirely due to solar X-rays of 3-8 A .

2. Auroral Absorption

As its name suggests, the occurrence of auroral absorption is closely related to the occurrence of visual aurora during the night and also because it occurs with maximum frequency inside the auroral zone. Detailed discussion of this type of absorption will be given in section 1.3.

3. Polar Cap Absorption

Baily (1957) was the first to discover polar cap absorption on VHF ionospheric forward links in the arctic after the great cosmic ray producing flare of February 23, 1956. Later on Baily (1959) and Reid and Collins (1959) suggested that polar cap absorption could be explained if it is assumed that fast protons are emitted by the sun following major solar flares. It is now universally accepted that solar protons in 10-100 Mev range are responsible for polar cap absorption.

4. Sudden Commencement Absorption

Recently, yet another type of absorption phenomenon has been identified by Brown et al (1961). This absorption takes place at the time of sudden commencements of magnetic storms and

is designated as sudden commencement absorption or SCA. The onset of SCA is very sudden like that of SCNA, absorption increasing by 3-4 db within a few minutes. Unlike SCNA which occurs on the sunlit side of the entire globe, SCA can be observed on both the day as well as the night side of the earth. SCNA is a world wide phenomenon, but the occurrence of SCA appears to be limited to stations situated near the auroral zone maximum. Unlike SCNA, SCA is not accompanied by solar noise bursts. These differing diurnal and latitudinal patterns help in positive identification of the type of absorption. During a sudden commencement type of absorption event, Brown measured an X-ray burst over College by means of balloon-borne cosmic ray detectors. He attributes the X-ray burst to bremsstrahlung from electrons entering the upper atmosphere.

1.3 AURORAL ABSORPTION

The name auroral absorption is applied to an absorption phenomenon observed frequently at high and middle geomagnetic latitudes that shows large variations in space and time. The same name is also applied to daytime absorption showing characteristics similar to those described above, although no visual aurora may be associated with it. Thanks to the collective efforts of cosmic ray physicists all over the world the theory of polar cap absorption is based on a firm foundation. Unfortunately, the same statement cannot be made about auroral absorption which happens to be a far more complicated phenomenon and

which has received far less attention in the past. The reason for this state of affairs may be attributed partially to the preoccupation of ionospheric physicists and cosmic ray physicists alike with the study of polar cap absorption and partially to the complexity of the problem of auroral absorption.

As the aurorally associated absorption varies in an irregular manner with time, it is generally believed that it also varies irregularly in space. The patchiness of auroral absorption also follows from the fact that riometers spaced by a few hundred kms often show marked differences in absorption. One is therefore interested to know the scale size of the patches i.e. the minimum distance by which two riometers should be separated in order to get sizable differences in absorption. The patchiness of absorption may also be investigated by observing absorption in two different directions at one place. Obviously, this arrangement necessitates the use of antennas whose beamwidths are comparable to the angle subtended by an "average" patch at the receiving point. Therefore, one is forced to use antennas of a few degrees beamwidth only. As narrow beam antenna arrays are rather expensive to build it is convenient to use a single array and periodically switch the beam to different parts of the sky. However, for good performance of the antenna array the switching angle is limited to a few degrees from the normal position.

Perhaps the first published account of aurorally associated absorption is given by Appleton, Naismith, and Ingram (1937) and

is based on British radio observations at Tromsö, Norway during the second international polar year 1932-1933. Their equipment consisted of a receiver at Tromsö and a transmitter at Simavik, 10 miles away. They observed the equivalent heights at 2 Mc/s and 4 Mc/s and also the critical frequencies of the ionospheric layers. The authors found abnormal ionospheric effects associated with periods of high magnetic activity and auroral displays. They found a decrease in the reflection coefficient of the ionosphere with increasing magnetic activity. It was also noticed that the "no echo" conditions or what came to be known as polar blackouts were associated with the occurrence of severe magnetic storms and intense auroral displays. The occurrence of abnormal E region reflections was found to be associated with weak magnetic activity and seemed to precede the "no echo" condition.

On the assumption that the luminosity is proportional to the rate of change of intensity of the beam with respect to distance traveled, Harang (1946) has derived some interesting theoretical curves showing the luminosity produced by a bundle of cathode rays penetrating the earth's atmosphere. He has shown that with increasing speed of the cathode ray bundle the peak of luminosity shifts downwards. He also observed abnormal E layer reflections, at a frequency of 3.65 Mc/s, during auroral displays and came to the conclusion that the auroral luminosity and the abnormal reflections must be manifestations of the same phenomenon. The height of the abnormal E layer was found to be

within a few kilometers of the height of the auroral lower border. He also found that complete blackouts were associated with very strong auroral displays when they occurred at lower heights. Harang concluded that the region where radio waves are absorbed during blackouts must be close to the height interval where the lower borders of very strong auroral displays generally lie i.e. 80-90 km.

Heppner, Byrne and Belon (1952) investigated the association of radio wave absorption and E_s ionization with visual aurora at College, Alaska. They carried out visual observations of form, intensity and position of the aurora throughout the auroral season of 1950-1951 and paid special attention to aurora at the zenith. They found that the occurrence of blackouts was usually associated with pulsating aurora at the zenith in general and with pulsating draperies in particular. When there was no aurora in the entire sky they still found complete absorption in 13% of the cases considered. We can very easily explain these occurrences of heavy absorption with no accompanying aurora as being due to polar cap absorption, a phenomenon not known at that time.

A number of workers have made morphological studies of polar blackouts. Worthy of special mention are Wells (1947), Cox and Davies (1954) and Agy (1954). There seems to be a universal agreement among workers about the increasing frequency of occurrence of polar blackouts as the auroral zone is approached. Agy and Meek observed field strength recordings along the 90th

meridian and formulated the concept of the existence of an auroral absorption zone, which they showed to be very close to the visual auroral zone.

Little (1954) was the first to apply Shain's method of measuring radio wave absorption, using extra-terrestrial radio waves in the auroral zone. He monitored extraterrestrial radio waves at 65 Mc/s by means of a stable receiver connected to a twin Yagi array having a beamwidth of 26 degrees in the E plane and 50 degrees in the H plane. He showed that the frequency of occurrence of strong absorption at 65 Mc/s maximizes around midday with a minimum occurring during late evening hours. Little also pointed out the numerous advantages of the cosmic noise technique over normal echo sounding techniques which become unusable during polar blackouts.

The work of Little sparked a renewed interest among workers at high latitudes especially those at College, Alaska. The concentrated efforts in search of better experimental technique finally resulted in what is now known as the riometer.

1.4 X-RAYS AND ABSORPTION

While the cosmic noise technique was being developed by ionospheric physicists, the cosmic ray physicists were not sitting idle by any means. Meredith, Gottlieb, and Van Allen (1955) launched Geiger counters by means of rockoons (rockets launched from a balloon) up to 100 kms at places, with geomagnetic latitudes ranging between 54^{o} to 84^{o}. In most of the

launchings made in the auroral zone (geomagnetic latitudes ranging between 65^{o}-77^{o}) they detected an ionizing radiation much softer than cosmic rays, penetrating down to 50 km level. At first this radiation was interpreted as the high energy component of primary cosmic rays which was thought to penetrate deeper into the atmosphere because of its high energy. This interpretation required energies of 1 Mev for electrons and 20 Mev for protons which are rather improbable. In a subsequent paper Van Allen (1957) attributed the radiation to bremsstrahlung generated by primary electrons in the energy range, 10-100 kev.

Winckler and Peterson (1957) were the first to detect X-rays by means of a balloon during an auroral display at subauroral latitudes. They also showed a close correlation between X-rays and magnetic bays observed in the horizontal component of the earth's magnetic field.

Kinsey Anderson (1958) was the first to observe X-rays in the auroral zone with balloons. The soft radiation was observed in August 1957 at Fort Churchill during a magnetic disturbance but was not found to be definitely correlated with visual aurora.

With the discovery of soft radiation in the atmosphere following magnetic storms and auroral displays, an unexplained question immediately developed. There seems to be a general agreement that the observed X-rays are due to bremsstrahlung of electrons of $\beta = .25$-$.50$ which corresponds to 50-100 kev energy. The transit time of the solar corpuscles is typically of the

order of 20 hours which is equivalent to $\beta = .01$ or about 30 ev. The question arose as to how we can explain the presence of 50-100 kev electrons in a beam of 30 ev energy. It was quite obvious that there must be some mechanism for accelerating the electrons as the beam approaches the earth. Several acceleration mechanisms have been suggested by various authors but details will not be discussed here as the interest in the present study lies more with the effect of the electrons than their cause.

The various balloon groups are unanimous in reporting a strong correlation between X-ray bursts and aurorally associated absorption of extraterrestrial radio waves. Typically, the absorption event begins with the appearance of X-rays, and the detailed structure of the absorption event is reflected in the detailed response of the ion chamber. Heavy absorption is found to be associated with high intensity X-ray bursts. While at Minneapolis the X-ray bursts were found to be well correlated with visual aurora, at Fort Churchill, in the auroral zone, Anderson found no such relation.

A word of caution is necessary here for anyone who intends to use the data, i.e. fluxes etc. obtained by various balloon groups. The electron spectrum quoted by all the workers is inferred from bremsstrahlung observations, assuming a certain model, and therefore the results are not entirely unambiguous. In principle it is impossible to infer uniquely an electron spectrum from an observed photon spectrum.

A major step towards understanding the phenomenon of aurora and its associated effects was taken when McIlwain (1960) fired rockets into an auroral display, at Fort Churchill, Canada. He made two rocket firings, one into a quiescent glow of intensity I, and the other into a bright active arc. In both cases he found that a major portion of the auroral light was produced by electrons of less than 10 kev energy. A substantial part of the luminosity of the bright auroral display was found to be produced by nearly monoenergetic electrons of about 6 kev energy. The electron flux was found to be rapidly varying with time and the peak flux was about 5×10^{10} electrons/sec cm^2 ster.

1.5 PROBLEMS IN AURORAL ABSORPTION

Previous sections were devoted mostly to descriptions of the observed phenomena which are related to auroral absorption. In this section some of the outstanding problems shall be discussed which are not yet fully explained quantitatively. The purposes of this dissertation are to supplement existing observational data with new data obtained by means of improved techniques and to explain some of the outstanding questions by using available material.

1.5.1 Absorption and Visual Aurora

The relation between visual aurora and absorption is still not very clear. The question of whether absorption is more widespread than aurora or not is not settled yet. Some observations indicate a possible dependence of absorption on

the type of aurora present. The following three groups have worked on this problem to some extent.

a. Geophysical Institute, University of Alaska, [Little & Leinbach, (1958)]

b. Institute of Upper Atmospheric Physics, University of Saskatchewan, Saskatoon, Canada, [Alex Kavadas (1961)]

c. Norwegian Institute of Cosmic Physics in collaboration with Norwegian Defence Research Establishment [Holt & Omholt (1962)]

Of these, the first two have tried using an antenna having a much narrower beam in the North-South plane than in the East-West plane. The Canadian group was the first to try periodic switching of the main lobe of the riometer antenna 3^{o} North and 3^{o} South of the zenith.

In relating extraterrestrial radio wave absorption with visual aurora, it seems necessary to use antenna arrays which have narrow beamwidths not only in the North - South plane but also in the East - West plane. Another stringent requirement is that the signal picked up by the side lobes should always be a negligibly small fraction of that picked by the main lobe. Unfortunately the last mentioned requirement is not easy to satisfy for frequencies commonly used in auroral absorption work i.e. 27-50 Mc/s. For frequencies higher than 100 Mc/s both the requirements can be met conveniently but the absorption events become rarer since the absorption drops off as the square of the wavelength.

If the extraterrestrial radio waves were incident isotropically, it would have been a relatively simple matter to design an antenna for 27 Mc/s even, satisfying both the requirements. But unfortunately the incidence of radio waves is not isotropic. It is known that there are cold regions like the galactic pole in the sky and there are hot point sources like Cygnus and Casseiopia and also there is the still hotter galactic center. It may well happen that the main beam at some time of the day looks at a cold region while at the same time the side lobe receives the signal from a much hotter region, such as the galactic center. If the side lobe to main lobe power ratio of the antenna is greater than the ratio of the brightness temperature of the galactic pole to that of the glactic center, the signal in this situation will be dominated by the side lobe rather than by the main beam. The problem is further complicated when one tries to switch the beam electrically, as a result of which, the side lobe on one side of the main beam increases while the side lobe on the other side decreases in magnitude.

Past workers who attempted to relate radio wave absorption with visual aurora usually obtained the auroral information from all-sky camera records. One serious drawback of this approach is that the information extracted is essentially qualitative in nature. Ideally one should supplement all-sky camera data with those obtained by means of photometers which have beamwidths comparable to the beamwidth of the riometer antenna. This ideal setup would not only give qualitative

information, such as information on auroral forms (i.e. arcs, bands, draperies, etc.) but would also enable one to obtain quantitative data, such as luminosity values.

1.5.2 Physical Mechanism

The physical mechanism responsible for auroral absorption is not yet fully understood. Following are three different mechanisms which have been suggested by various workers.

1. Ionization by primary electrons proposed by Winkler, Peterson, Hoffman and Arnoldy (1959).

These authors believe that since the primary electrons carry 10^3-10^4 times more energy than the X-rays, the radio wave absorption should be primarily due to former.

The energy of the electrons precipitating in the auroral is such that they cannot penetrate the 100-90 km level of the atmosphere. The absorption on the other hand is believed to take place mostly in a region 60-90 kms. If this belief is accepted, it is not clear how the primary electrons can cause D region ionization when they are not even able to reach that level.

2. Ionization by X-rays.

Chapman and Little (1957), in trying to explain the fact that the aurorally associated absorption sometimes appears to be more wide spread than visual aurora, postulated the ionization of the D-region by X-rays which are emitted as bremsstrahlung of primary electrons.

3. Ionization by Lyman α radiation.

Bates (1955) pointed out that the auroral zone D-region can be ionized by Lyman α radiation emitted by auroral protons after they are neutralized to Hydrogen atoms in the upper atmosphere. However, it can be shown that the intensity of Lyman α radiation is too small to account for the unusually high absorption observed frequently during active auroral displays. Moreover, Montellabetti (1959) and Romick and Elvey (1958) have shown that H_β intensity decreases and becomes negligible when an auroral arc becomes suddenly active. It is also known that radio wave absorption is generally higher when violently active auroral forms are present in the sky. This condition implies that Lyman α radiation cannot be an effective ionizing agent for intense absorption events caused by bright and active aurora.

4. Ionization by auroral protons.

Omholt (1960) argued that auroral outbursts must be due to electrons, as the faintness of hydrogen lines during bright aurora rules out any appreciable proton contribution to the auroral luminosity. McIlwain (1960) measured the primary particle flux by firing a rocket into a bright auroral arc, and came to the conclusion that at least 75% of the auroral luminosity was due to electrons of 6 kev energy or less.

Although it is true that protons may not contribute appreciably to the auroral luminosity, yet at times they may have sufficient energy to substantially ionize the D-region. This

is especially true of certain daytime events which show a character which is typical of ionization by fast protons. Such events will be discussed in detail in Chapter VI.

Very little systematic work has so far been done to test the validity of these ionizing mechanisms quantitatively. Ideally, if the production and loss mechanisms of electrons at different heights throughout the lower ionosphere are known, one can calculate the electron density profile and the expected absorption, which can be compared with the observed one. But in practice the situation is much less favorable. Neither the production nor the loss rates are known with sufficient accuracy at various heights to enable one to calculate a reasonable electron density profile. During recent years several workers have experimentally investigated the photon and electron spectra and fluxes etc by means of balloon and rocket borne detectors in the auroral zone, with more and more refined techniques. Although the balloon and rocket results may not be 100 per cent accurate, it still seems worthwhile that these results should be used more and more in theoretical work.

1.5.3 The Breakup Phase of the Aurora, Associated Radio Wave Absorption, the Auroral Electrojet and the Auroral Hydrogen Emission.

The break-up phase of the aurora is a very spectacular phenomenon. Its geophysical effects seem to be equally spectacular. When a major break up occurs, the absorption suddenly increases and reaches its peak value within a few minutes. The peak absorption and the peak luminosity of the aurora occur

within a fraction of a minute. At the same time the H trace of the earth's magnetic field shows a pronounced dip which is explained by a westward auroral electrojet. Many workers have reported that the auroral hydrogen emission decreases abruptly at the time of auroral break-up. It is not quite clear why this happens and what causes it. Akasofu (1960) is of the opinion that there may be a constant flux of electrons and protons in homogeneous and quiet arcs. The decrease of hydrogen emission according to him may be attributed either to stoppage or to deflection of the proton flux.

1.5.4 Pulsating Absorption

Sometimes the auroral absorption shows period fluctuations with a period of a few minutes. A similar phenomenon is sometimes observed when the narrow beam antenna connected to the riometer is switched north and south periodically. In this situation the difference in absorption between the north and south fluctuates in a periodic manner. The physical mechanism responsible for this behavior is not well understood.

1.5.5 Aurora, Sporadic E and Auroral Absorption

Several workers have reported a relation between visual aurora and sporadic E [Harang (1946); Heppner, Byrne & Belon (1951); Hunsucker & Owren (1962)]. All the observations probably refer to the pre-break-up phase of the aurora, as black-out condition generally prevails during the post-break-up periods. Often the sporadic E trace shows group retardation,

which suggests that the pulse is returned by a normal refraction process like that effective in the daytime E layer. The peak electron density and the height in such cases can be deduced. In view of the strong connection between visual aurora and sporadic E, it seems worthwhile to calculate the expected absorption, using sporadic E data obtained by the ionosonde, and to compare it with the observed value.

1.6 Summary

In this chapter a brief description of observed phenomena was given and some of the outstanding problems connected with aurorally associated absorption were outlined. Succeeding chapters will be devoted to theory of ionospheric absorption, theory of bremsstrahlung, and ionization of the D-region by X-rays and electrons. Some of the problems outlined in this chapter will be discussed in detail in the light of fresh observational material.

CHAPTER II.

THEORY OF IONOSPHERIC ABSORPTION

2.1 INTRODUCTION

When a radio wave enters an ionized medium, its electric field imparts a sinusoidal component to the velocity of electrons and ions, which is superimposed on their random thermal motion. The former may be called the ordered component, because of its sinusoidal character, and the latter disordered because of its random nature. The oscillating ions and electrons, being accelerated charges, reradiate the energy supplied to them by the wave, the reradiated fields constituting the forward going wave. If the oscillating charges do not collide with each other and with neutral molecules, the energy extracted from the wave by ions and electrons is reradiated in toto and the wave progresses onwards unattenuated. In practice, however, this condition is not encountered as collisions always take place in an ionized gas. When an oscillating electron and a neutral molecule collide, the former loses its ordered energy almost completely. The loss of ordered energy implies that the energy imparted to the electron by the wave is not wholly reradiated. Thus, the amplitude of the forward going wave is diminished as compared to the incident wave.

According to the simple physical picture presented above, it is obvious that the absorption suffered by a wave should be roughly proportional to the collision frequency and to the electron density in the medium through which it passes. It is

also obvious that the absorption should be inversely proportional to some power of the frequency of the wave. This conclusion follows from the fact that, for a wave of higher frequency, electrons are able to make several oscillations between two consecutive collisions.

In this chapter several different methods of calculating the overall effect of collisions on absorption will be discussed. The first method given in section 2.2, essentially due to Lorentz, forms the basis of the classical Appleton-Hartree formula. The second method due to Huxley is an extension of the classical approach, using the idea of free paths in order to calculate the electronic drift velocities. The third and most satisfactory approach of Jancel and Kahan uses the Boltzmans' equation for electrons which is solved by Chapman-Enskog method. All the three methods hold only for a Lorentz gas consisting of two constituents such that

a) The mass of the molecules of the first constituent is greater than those of the second constituent

b) The effect of mutual collisions between the particles of the second constituent is negligible as compared to the collisions between the particles of the first constituent.

In case of the ionosphere, consisting of electrons and neutral molecules, both the requirements are satisfied for a slightly ionized gas. The ionic contribution is invariably of minor importance and is therefore neglected.

2.2 THE ABSORPTION COEFFICIENT

Let a plane wave of angular frequency ω be incident on an ionized medium. The electric field of the wave after it travels a distance s into the medium is given by

$$E_o \, e^{j\omega t} e^{-ks}$$

Where $E_o \, e^{j\omega t}$ is the incident field. The coefficient k is known as the absorption coefficient. If k varies along the path s, the corresponding expression for the electric field is given by

$$E_o \, e^{j\omega t} e^{-\int k \, ds}$$

From the discussion of the previous section it follows that the absorption coefficient, k, in general, is a function of the wave frequency, the frequency of collisions between electrons and neutral molecules, and the number density of the electrons.

2.3 THE AVERAGE EFFECT OF COLLISIONS

The average effect of collisions is to damp the oscillatory motion of electrons. In this section the average damping force acting on an electron as a result of collisions will be calculated, after Appleton and Chapman (1932).

The equation of motion of a free electron subject to the action of the oscillatory electric field of the wave of angular frequency ω, neglecting the effect of magnetic field, is given by,

$$m\ddot{x} = e \, E \, e^{j\omega t}$$

Integrating,

$$\dot{x} = \frac{eEe}{jm\omega}^{j\omega t} + c \ .$$

Applying this equation to a large number of electrons all of which made their last collision at time $t = t_1$,

$v = \frac{eE}{jm\omega} \left(e^{j\omega t} - e^{j\omega t_1} \right)$, where v is the velocity of each electron of this group.

One may then write $v = -\frac{jEe}{m\omega} \left(1 - e^{-j\omega\theta} \right) e^{j\omega t}$,

where $\theta = t - t_1$.

After Lorentz it is assumed that the times between collisions have a Poisson distribution. In other words, out of N electrons, the number of electrons which made collisions during the time interval θ, $\theta + d\theta$ is given by $\frac{N}{\tau} e^{-\theta/\tau} d\theta$, where τ is the average time between successive collisions. The average oscillatory velocity of the electrons is given by

$$\bar{v} = \frac{1}{N} \int_0^{\infty} \frac{-jEe}{m\omega} \left(1 - e^{-j\omega\theta} \right) e^{j\omega t} \frac{N}{\tau} e^{-\theta/\tau} d\theta$$

$$= \frac{eE e^{j\omega t}}{m(j\omega+\nu)} \ , \text{ where } \nu \text{ is the collision frequency .}$$

The effect of collisions can be taken into account in the motion of a single electron by introducing a frictional damping force proportional to the velocity of electron. The coefficient of the frictional term, g, is found by writing the equation

of motion ,

$$m\ddot{x} + g\dot{x} = e\,E\,e^{j\omega t}, \text{ from which}$$

$$\dot{x} = \left(\frac{eE}{j\omega m + g}\right) e^{j\omega t} = \left(\frac{e\,E\,e^{j\omega t}}{j\omega m + m\nu}\right),$$

which gives $g = m\nu$.

2.4 CLASSICAL EXPRESSION FOR REFRACTIVE INDEX AND ABSORPTION

The equation of motion of an electron subject to the action of an electromagnetic wave of angular frequency ω and under the influence of an applied magnetic field $\vec{B}$ is given by

$$m\dot{\vec{v}} = -m\nu\vec{v} + e\vec{E} + e\vec{v} \times \vec{B}$$

Maxwell's equations for the dielectric medium in which the electron is imbedded are given by

$$\text{Curl } \vec{H} = \epsilon_o \epsilon \dot{\vec{E}} \qquad \text{div } \vec{H} = 0$$

$$\text{Curl } \vec{E} = -\mu_o \dot{\vec{H}} \qquad \text{div } (\epsilon_o \epsilon \vec{E}) = 0 .$$

It is presumed that the medium has electric properties but no magnetic properties. This assumption implies that there is induced electric polarization but no magnetic polarization. Starting with the above relations and using the concept of characteristics waves, which propagate through the medium without changing their wave-polarizations, it is possible to get an expression for the complex refractive index n of the wave.

$$n^2 = 1 - \frac{X}{1 - iZ - \frac{1}{2} Y_T^2/(1-X-iZ) \pm \frac{1}{4} Y_T^4/\left[(1-X-iZ)^2 + Y_L^2\right]^{\frac{1}{2}}}$$

where

$$X = \frac{\omega_N^2}{\omega^2} = \frac{Ne^2}{\epsilon_o m \omega^2}$$

$$\omega_L = (\mu_o H e/m) \cos\theta$$

$$\omega_T = (\mu_o H e/m) \sin\theta$$

where θ is the angle between the direction of propagation and the magnetic field.

$$Y_T = \omega_T/\omega$$

$$Y_L = \omega_L/\omega$$

$$Z = \nu/\omega$$

In order to investigate the absorption suffered by a wave, one may write the complex refractive index separately in real and imaginary parts.

$$n = \mu - jX$$

The electric field of the wave in the medium is given by

$$E_o e^{j(\omega t - kz)} = E_o e^{j\omega(t - nz/c)}$$

$$= E_o e^{j\omega t} e^{-j\omega z/c (\mu - jX)}$$

$$= E_o e^{j\omega t} e^{-j\omega\mu z/c} e^{-\frac{\omega X z}{c}} .$$

The first factor on the right hand side indicates that the amplitude of the E field diminishes progressively as the wave

penetrates the medium. The exponent of the last term is called the coefficient of absorption and is usually denoted by k, where $k = \frac{\omega\chi}{c}$

For longitudinal propagation $Y_T = 0$ and

$$(\mu - j\chi)^2 = 1 - \frac{X}{1 - jZ \pm |Y_L|} .$$

Equating the real and imaginary parts,

$$\mu^2 - \chi^2 = 1 - \frac{X\,(1 \pm |Y_L|)}{(1 \pm |Y_L|)^2 + Z^2} ,$$

$$2\mu\chi = \frac{XZ}{(1 \pm Y_L)^2 + Z^2} ,$$

which gives $\chi = \frac{1}{2\mu} \quad \frac{XZ}{(1 \pm Y_L)^2 + Z^2}$,

$$k = \frac{\omega\chi}{c} = \frac{\omega}{2c\mu} \quad \frac{XZ}{(1 \pm Y_L)^2 + Z^2} .$$

For a non-deviative region $\mu \simeq 1$,

hence $k = \frac{2\pi}{c} \quad \frac{Ne^2}{\epsilon_o m} \quad \frac{\nu}{(\omega \pm |\omega_L|)^2 + \nu^2}$

Both N and ν are height dependent; therefore k is also a function of height. The power attenuation in a slab of thickness h is given by $e^{-2\int_0^h k\,ds}$

The absorption in decibels is given by $2 \times \log_{10} e \int_0^h k\,ds$, or

$$A(db) = 2 \times \log_{10} e \int_0^h \frac{2\pi}{c} \frac{Ne^2}{\epsilon_0 m} \frac{\nu}{(\omega \pm |\omega_L|)^2 + \nu^2} ds$$

2.5 OBJECTIONS TO THE CLASSICAL THEORY

Huxley (1940) has criticized the classical expression for the refractive index given independently by Appleton and Hartree on several grounds. His objections are summarized below.

In the equation of motion of an electron, the effect of collisions is taken into account by introducing a viscous damping force proportional to the velocity of the electron with the constant of proportionality g being $m\nu$. This equation therefore represents motion in a viscous rather than in a gaseous medium since the gaseous nature of the medium has not been taken into account. The classical theory neglects the thermal velocity distribution of the electrons. It assumes that when an electron and a heavy particle collide, the electron loses its momentum completely. Even with some other value of g, better results cannot be expected since the idea of a viscous force is itself not very sound for a gaseous medium.

2.6 HUXLEY'S IMPROVED THEORY

Only a brief outline of Huxley's improvement of magneto-ionic theory will be presented here in view of the fact that his earlier work has been more or less superseded by Jancel and Kahan's more elegant treatment.

The classical approach uses the differential equation of motion of an "average" electron to calculate the current.

In his improved theory Huxley (1951) does not make this assumption. Instead he calculates the average drift velocity of the electrons subject to the effect of sinusoidal electric-field of the wave and a constant magnetic field using the method of free paths. Starting with the average drift velocities, the components of the current density vector and the induced polarization can be calculated. The expression for the refractive index is obtained by using the above results in conjunction with Maxwell's equations, as is usually done in the classical approach. Following is a brief summary of Huxley's method of calculating average drift velocities of electrons using the idea of mean free paths.

When there is no applied electric field, the path of an electron, moving in a gas consisting of free electrons and heavier molecules, consists of a succession of straight segments with discontinuous changes of direction when a collision takes place. The length of each segment is given by τu where τ is the time of free flight and u the agitational velocity of the electron. When an electric field E is applied, the individual segments are no longer straight lines because each electron experiences a deflecting force, eE, which causes a displacement in its path during its free flight. The vector sum of such displacements taken over several free paths turns out to be a function of time and in general is different from zero, implying that the electron drifts under the action of the field.

The drift velocity can be calculated by accurate vector summation of the displacements suffered during all the free paths.

When the electric field is independent of time, Huxley found that the drift velocity is in the direction of the applied field. With an additional external magnetic field such is no longer the case. The expression for drift velocities is even more complicated in the presence of a sinusoidal electric field and constant magnetic field.

2.7 JANCEL AND KAHAN'S GENERALIZED MAGNETOIONIC THEORY

The mean free path method used by Huxley to calculate the average electron drift speeds has been criticized by Jancel and Kahan (1954). One of the weaknesses of Huxley's approach is that he disregards the velocity distribution of electrons. Huxley's formulas are applicable under the condition that the period of the incident electromagnetic wave ($\frac{1}{\text{frequency}}$) is sufficiently great in comparison with the time constant of decay of electron kinetic energy $1/2\ m u^2$ after the field is removed, enabling one to neglect the fluctuation of $1/2\ m u^2$ about its mean value during a cycle of the alternating field.

Jancel and Kahan's method consists of solving the Boltzman's equation in an anisotropic plasma with constant magnetic field and intense electric field.

The equations for the molecules and electrons are respectively

$$\frac{\partial f_1}{\partial t} + \vec{v}_1 \cdot \operatorname{grad}_{r_1} f_1 = c_{11} + c_{12}$$

$$\frac{\partial f_2}{\partial t} + \vec{v}_2 \cdot \operatorname{grad}_{r_2} f_2 + \vec{F}_2 \cdot \operatorname{grad}_{v_2} f_2 = c_{21} + c_{22}$$

Where f_1, f_2 are velocity distribution functions of molecules and electrons and $\vec{v_1}$, $\vec{v_2}$ their velocities. F_2 is the external force on the electron due to the action of the field. It is assumed that no external force acts on the molecules.

In the Boltzman's equation the term $\vec{v}$. grad$_r$ f takes into account the change in the velocity distribution function caused by diffusion. The diffusion term is zero when either the spatial gradient of the distribution function is zero or when the velocity of the particles is zero.

The distribution function of the electrons changes under the action of the applied field. The change in the distribution function as a result of an applied force is given by the scalar product of the force and the velocity gradient of the distribution function. The change in f as a result of the applied force is zero when either the force is zero or when the electrons are uniformily distributed in velocity space. Finally the distribution function can change as a result of collisions, and c_{11}, c_{12} represent the changes in f_1 due to interaction of molecules with molecules and electrons respectively. Similarly c_{21} and c_{22} represent the changes in f_2 as a result of collisions of electrons with molecules and electrons respectively. Since the electrons are fewer in number than the molecules, the term c_{22} would be negligible as compared to c_{21}. In case of a molecule and electron collision, it may safely be assumed that the speed of the molecule does not change appreciably. This assumption implies that c_{12} may be

neglected in comparison with c_{11}. The two Boltzman equations for molecules and electrons then reduce to the following.

$$\frac{\partial f_1}{\partial t} + \vec{v}_1 \cdot \operatorname{grad}_{r_1} f_1 = c_{11}$$

$$\frac{\partial f_2}{\partial t} + \vec{v}_2 \cdot \operatorname{grad}_{r_2} f_2 + \vec{F}_2 \cdot \operatorname{grad}_{v_2} f_2 = c_{21}$$

If homogeneous gases are considered the diffusion term may be neglected, i.e. $\vec{v}_1 \cdot \operatorname{grad}_{r_1} f_1 = \vec{v}_2 \cdot \operatorname{grad}_{r_2} f_2 = 0$.
Boltzman's equations then reduce to

$$\frac{\partial f_1}{\partial t} = c_{11} ,$$

$$\frac{\partial f_2}{\partial t} + \vec{F}_2 \cdot \operatorname{grad}_{v_2} f_2 = c_{21} .$$

The equation for molecules shows that the molecular distribution function is not effected by the presence of electrons and therefore may be assumed to approach Maxwellian distribution,

$$f_1 = n_1 \left(\frac{m_1}{2\pi kT} \right)^{3/2} \exp \left(-m_1 v_1^2 / 2kT \right)$$

under a state of thermal equilibrium.

The electron gas may be treated as a Lorentz gas for which the conditions are

(a) The mass of the molecule of the first constituent is greater than that of the second constituent.

(b) The effect of mutual collisions between the particles of the second constituent is negligible as compared to the collisions with the particles of the first constituent.

For a slightly ionized gas Chapman and Cowling have shown that $$c_{21} = \iiiint \left| f_1' f_2' - f_1 f_2 \right| g\, b\, db\, d\epsilon\, dv_1$$

Where f_1' and f_2' are the functions f_1 and f_2 for v_1' and v_2'. v_1, v_2 are the initial velocities and v_1', v_2' are the velocities after collision, g is the relative velocity given by $\left|\vec{v}_1 - \vec{v}_2\right| = \left|\vec{v}_1' - \vec{v}_2'\right|$ and b and ϵ are the impact parameters. The Lorentz force on the electron is given by

$$\vec{F}_2 = \frac{e_2}{m_2}\vec{E}\cos\omega t + \frac{e_2}{m_2}(\vec{v}_2 \times \vec{H}_o) = \vec{\Gamma}_2 \cos\omega t + \frac{e_2}{m_2}(\vec{v}_2 \times \vec{H}_o)$$

where ω is the angular frequency of the electromagnetic wave, $\vec{E}$ the electric vector of the wave and $\vec{H}_o$ the earth's magnetic field.

Jancel and Kahan develop f_2 in spherical harmonics containing a zero order term $f_2^{(0)}$ and terms involving $\vec{\Gamma}_2 \cdot \vec{v}_2$, $(\vec{H}_o \times \vec{\Gamma}_2)\cdot\vec{v}_2$ and $(\vec{H}_o \times \vec{H}_o \times \vec{\Gamma}_2)\cdot\vec{v}_2$ with $f_2 = f_2^{(0)} + \vec{f}_2^{(1)}\cdot\vec{v}_2$ For an arbitrary Γ_2, $f_2^{(0)}$ is not Maxwellian in general. However, in problems of radio wave propagation the electric field energy Γ_2^2 is negligible as compared to the thermal energy kT. Therefore $f_2^{(0)}$ may be considered Maxwellian. The average speed of the electrons is given by

$$\bar{v}_2 = \frac{1}{n_2}\int v_2 f_2\, dv_2 = \frac{1}{n_2}\int v_2 \left(f_2^{(0)} + \vec{f}_2^{(1)}\cdot\vec{v}_2 \right) dv_2$$

Using spherical coordinates with z axis taken in the direction of $\vec{f}_2^{(1)}$ it can be shown that

$$n_2(\bar{v}_2)_x = n_2(\bar{v}_2)_y = 0$$

$$n_2(\bar{v}_2)_z = \int_0^\infty f_2^{(1)} \frac{4\pi}{3} v_2^4\, dv_2$$

The total current $n_2 e_2 \bar{v}_2$ therefore can be calculated. Using the relation $I = \|\sigma\| E$ the conductivity tensor $\|\sigma\|$ is evaluated.

Jancel and Kahan were able to show that the classical results of Appleton and Hartree could be derived from their generalized theory under simplifying assumptions.

The expression for the refractive index in the general case however, is so complicated that it is of little practical use. Moreover, unless the law of collision frequency variation $\nu = \nu_m f(v)$ is known in the gas, most of the integrals occurring in the expression for refractive index cannot be evaluated.

Phelps, Fundingsland, and Brown (1951) had investigated the law of collision frequency variation as early as 1951 by increasing the conductivity of a decaying plasma after the electrons reached thermal equilibrium with the gas. They assumed that the collision frequency was proportional to some power of the electron velocity and evaluated the constant of proportionality and the exponent by equating experimental measurements of $\frac{\sigma_r}{\sigma_i}$ to the theoretical values.

In general, $\nu = \frac{v}{\ell} = v\, p_o\, P$

where P = probability of collision for momentum transfer

ℓ = mean free path

p_o = pressure normalized to zero, degree temperature.

Phelps et al assumed in particular that $\nu = a\, p_o\, v^h$ or $P = a v^{h-1}$ and found that $h = 2$ fits their results. This result agrees with the later results of Phelps and Pack (1959).

It seems that Jancel and Kahan were probably unaware of this measurement; otherwise they would have pushed their theory to a more useful stage.

2.8 SEN AND WYLLER'S IMPROVEMENT ON JANCEL AND KAHAN'S THEORY

The lack of practical applicability in Jancel and Kahan's approach was removed by Sen Wyller (1960) who incorporated in the generalized theory the laboratory results of Phelps and Pack on the velocity dependence of collision frequency in nitrogen.

The measurements of Phelps and Pack (1959) show that

$$\frac{N}{\nu(E)} = \frac{8.2 \times 10^6}{E} - \frac{5.9 \times 10^3}{E^2} \quad cm^3/sec \ .$$

Where E is the electron energy. It may be seen that the first term dominates even for electron energies as low as .001 electron volts and therefore we may write

$$\frac{N}{\nu(E)} \propto \frac{1}{E} \quad \text{or} \quad \frac{N}{\nu(E)} = \frac{C'}{E}$$

where C′ is a constant of proportionality. Let ν_m be the collision frequency corresponding to the most probable speed. This corresponds to E = kT

$$\nu_m = C'kTN$$

$$\nu(E) = C'EN$$

Dividing we get

$$\nu = \nu_m \frac{E}{kT} = \nu_m \frac{m_2 v_2^2}{2kT}$$

Using this value of collision frequency Sen & Wyller showed that the couplex index of refraction in the generalized theory is given by

$$\left(n - \frac{ick}{\omega}\right)^2 = \frac{A + B\sin^2\phi \pm \sqrt{B^2\sin^4\phi - C^2\cos^2\phi}}{D + E\sin^2\phi}$$

where $A = 2\epsilon_1(\epsilon_1 + \epsilon_{11})$

$B = \epsilon_{111}(\epsilon_1 + \epsilon_{111}) + \epsilon_{11}^2$

$C = 2\epsilon_1\epsilon_{11}$

$D = 2\epsilon_1$

$E = 2\epsilon_{111}$

n = real part of the refractive index

k = absorption coefficient

ω = angular frequency of the wave

ϕ = Angle between the direction of propagation and the magnetic field

$\epsilon_1, \epsilon_{11}, \epsilon_{111}$ are the fundamental elements of the dielectric tensor given by,

$$\epsilon_1 = (1-a) - ib$$

$$\epsilon_{11} = 1/2\,(f-d) + i/2\,(c-e)$$

$$\epsilon_{111} = \left[a - 1/2\,(c+e)\right] + i\left[b - 1/2\,(f+d)\right]$$

where

$$a = \frac{\omega_o^2}{\nu_m^2}\, C_{3/2}\left(\frac{\omega}{\nu_m}\right)$$

$$b = \frac{5\omega_o^2}{2\omega\nu_m}\, C_{5/2}\left(\frac{\omega}{\nu_m}\right)$$

$$c = \frac{\omega_o^2 (\omega - s)}{\omega \nu_m^2} \mathbb{C}_{3/2} \frac{\omega - s}{\nu_m}$$

$$d = \frac{5 \omega_o^2}{2 \omega \nu_m} \mathbb{C}_{5/2} \frac{\omega - s}{\nu_m}$$

$$e = \frac{\omega_o^2 (\omega + s)}{\omega \nu_m^2} \mathbb{C}_{3/2} \frac{\omega + s}{\nu_m}$$

$$f = \frac{5 \omega_o^2}{2 \omega \nu_m} \mathbb{C}_{5/2} \frac{\omega + s}{\nu_m}$$

The $\mathbb{C}$ integrals are given by the relation

$$\mathbb{C}_p (y) = \frac{1}{p!} \int_0^\infty \frac{x^p e^{-x}}{x^2 + y^2} dx$$

s is the gyrofrequency of the electrons given by $\frac{e_2 H_o}{m_2}$

and $\omega_o^2 = \frac{4 \pi n_2 e_2^2}{m_2}$

Sen and Wyller have shown that the generalized expression for refractive index reduces to the classical expression for ν = constant. They have also shown that if the collision frequency used in the classical expression is the same as the parameter ν_m used in the generalized theory, the difference between the corresponding absorption coefficients can be as high as 100 per cent. But taking $\nu_{AH} = 5/2 \ \nu_m$ for $\nu < .1 \omega$

they found that the disparity between the two formulas was reduced to about 5 per cent. Similarly for $\nu >> \omega$ the Appleton Hartree formula can be retained provided $\nu_{AH} = 3/2\ \nu_m$.

For cases between the two limiting cases, it is not possible to use a unique multiplying factor which would tend to minimize the disparity and therefore it is better to use the generalized formula. Chorbajian, Sugiura, and Parthasarathy (1962) have calculated the absorption in db/km using the Sen-Wyller formula for the height range 20-100 km and for values of propagation angle $\emptyset$ from 0 to 80 degrees. They have assumed ν_m values tabulated by Nicolet (1959). The calculations were made for N = 1, 1000, 10,000 for frequencies ranging between 1-50 Mc/s.

It is now generally believed that Nicolet's collision frequency values are a little too high. Kane (1959) made measurements of refractive index and the attenuation coefficient for 7.75 Mc/s by means of rockets fired into the D-region, from which using the Appleton-Hartree formalism obtained the electron collision frequency. In a later publication, Kane (1961) pointed out that the classical magnetoionic theory should not be used to deduce the collision frequency. He showed that if the generalized magnetoionic theory is employed, the deduced collision frequencies are approximately 2.5 times lower than those derived from the classical theory. The collision frequencies deduced by Kane are in good agreement with the laboratory measurements of collision frequencies in nitrogen made by Phelps and Pack (1959).

2.9 COMMENTS ON THE GENERALIZED THEORY

The generalized theory disregards two important processes of electron density variation, namely electron production and recombination. Most of the radio wave absorption takes place in the D region of the ionosphere where the recombination is very high. One is therefore faced with the question; is one justified in applying the results of the generalized theory to the D region? To be able to answer this question it is necessary to solve the following Boltzmans' equation which takes into account ionization as well as recombination.

$$\frac{\partial f_2}{\partial t} - \alpha + \beta v_2 + \vec{F}_2 \cdot \operatorname*{grad}_{v_2} f_2 = \iiint\!\!\iint (f_1' f_2' - f_1 f_2)\, g b\, db\, d\epsilon\, dv_1$$

Here $\alpha\, dv_2$ represents the rate of electron production per unit time with velocities in the range v_2, $v_2 + dv_2$, and $\beta f_2\, dv_2$ represents the rate of loss of electrons per unit volume in this velocity range due to recombination. α, β depend only on the magnitude of the electron velocity, v_2, and not on direction. Unfortunately it is not possible to integrate this equation.

Chapman and Cowling (1952) have considered a simpler case in which they have assumed the external force, F_2, to be zero. For the case for which an electron undergoes a large number of collisions, they found that the electron velocity distribution function is Maxwellian to a first approximation. For a second approximation, they impose the condition $\int_0^\infty (\alpha - \beta\, v_2) v_2^{\,2}\, dv_2 = 0$ which expresses a balance between ionization and recombination.

The second approximation gives a non-Maxwellian distribution in the general case.

In the case of cosmic radio waves incident on the ionosphere the electric field of the wave is extremely weak. Therefore it is reasonable to assume that the results of Chapman and Cowling for $F_2 = 0$ should also be applicable for a weak electromagnetic field. Also it should be noted that the terms pertaining to ionization and recombination have opposite signs which means that each of these processes tend to diminish the other's effect. Hence it is safer to assume a Maxwellian distribution for electrons in a gas which is undergoing both recombination and ionization than for one which is undergoing recombination alone.

CHAPTER III.

THE ELECTRON PRODUCTION AND LOSS MECHANISMS IN THE AURORAL IONOSPHERE

3.1 INTRODUCTION

The discovery of soft radiation in the auroral zone at Fort Churchill by Meredith, Gottileb and Van Allen (1955) prompted Chapman and Little (1957) to attribute the cause of aurorally associated radio wave absorption observed by means of a wide beam antenna to the ionization of the D-region by bremsstrahlung X-rays. Later on the X-rays were detected at much lower altitudes by means of scintillation counters which were flown in balloons. [Anderson (1958), Bhavsar (1961), Brown (1961) etc].

Anderson and Enemark (1960) were probably the first to obtain the energy spectrum of the primary electrons from the balloon data after applying necessary corrections. Several workers [(Bhavsar (1961), Brown (1961), Evans (1963)] have since followed Anderson's technique at different places in the auroral zone at different times and have come up with vastly different results.

Winckler, Peterson, Hoffman and Arnoldy (1959) inferred a flux of 0.6×10^6 electrons/cm^2/sec from the observed X-ray intensities, at balloon heights at Minneapolis on February 10-11, 1958. They argued that as the primary electrons carry about 10^3-10^4 times more energy than the X-rays, the former should be the prime cause of D-region ionization. Assuming energy of 100 kev or more for the primary electrons and considering the

process of attachment only, the above authors deduced equilibrium electron density of 1.24×10^4 electrons/cm^3 at 85 kms. It is now fairly well established that the auroral electrons have a steep energy spectrum therefore a flux of 0.6×10^6 for electrons of 100 kev energy seems to be an overestimation by at least an order of magnitude. Another very important point worth emphasizing here is that all the balloon observations refer to photon energies greater than about 22 kev and therefore provide no information about the flux of low energy X-rays. It will be shown in section 2.5 of this chapter that as far as ionization of the D-region is concerned X-rays of 1-10 kev energy are far more important than X-rays of much higher energy.

Chapman and Little (1957), who attributed the auroral zone D-region ionization during intense auroral displays to the action of X-rays, carried out rough calculations of the expected extra-terrestrial radio wave absorption assuming total X-ray photon flux of 10^5 photons cm^{-2} sec^{-1}. They assumed that about one electron in a thousand will give rise to a photon whose energy may be any fraction of the primary electron energy. The above authors however, disregard the continuous spectrum of the X-ray photons which can have a drastic effect on the rate of electron production. For a reliable estimate of the ionization created by bremsstrahlung X-rays, the following steps are necessary.

(a) The photon energy spectrum must be known at the top of D-region.

(b) The rate of electron production for each of the constituting energies must be calculated.

(c) The total rate of electron production must be determined by weighing the electron production rate in each energy range by the intensity carried in that range.

From the preceding discussion it should be quite obvious that the physical mechanism responsible for auroral absorption is still not fully understood and that a reassessment of the whole problem from a new viewpoint and with newly acquired data is quite in order. Chapter III is directed towards this end.

3.2 BREMSSTRAHLUNG

Fast moving electrical charges which are subjected to decelerating forces emit radiation which is known as bremsstrahlung or brake radiation. The classical treatment of bremsstrahlung, in the case of a charged particle moving in a straight line with the decelerating force parallel to the velocity vector, is relatively straightforward. The electric and magnetic fields due to the decelerated charge are calculated using Lienard-Wiechert potentials, which enable one to evaluate the Poynting vector, $S = \vec{E} \times \vec{H}$, representing energy flow per unit time. The rate of radiation of an accelerated charge is the amount of energy lost by it in a time interval dt' where t' is the retarded time. The rate of energy loss of the electron into a solid angle $d\Omega$ centered in a given angle θ is equal to radiation emitted in that direction. Equating the two, it is possible to get an expression for the directional rate of energy loss of the accelerated charge as a function of its acceleration and the angle θ.

For a precise calculation of the rate of energy loss it is necessary to know the variation of the velocity and the decelerating force with respect to time. A simple classical approach [for example see Panofsky and Philips (1956)] is to assume that the acceleration is constant while the electron slows down from u_o to 0.

Quantum mechanically it is said that if an electron with primary energy E_o passes through the field of a nucleus, there is a finite probability that a light quantum k will be emitted, with the electron making a transition to a state of lower energy E given by the relation,

$$E = E_o - k$$

Rigorous quantum mechanical formulas for bremsstrahlung cross sections have been worked out by Sommerfeld, Bethe, and Heitler etc., both for relativistic and non-relativistic electrons with varying degree of sophistication, ranging from the assumption of the Born approximation of scattering theory to the incorporation of screening by oribital electrons. For the purpose of this dissertation it suffices to use a simple non-relativistic expression for the total cross-section for the emission of a photon of energy k as given by Heitler (1954):

$$\sigma k \, d\left(\frac{k}{E_o}\right) = \bar{\sigma} \quad 8/3 \quad \frac{\mu}{k} \quad \ell n \left\{\frac{\sqrt{E_o} + \sqrt{E_o - k}}{k}\right\}^2 \frac{dk}{E_o} \quad ,$$

where μ = rest energy of the electron $\simeq$ 511 kev and

$$\bar{\sigma} = \frac{Z^2 \, r_o^2}{137} \quad ,$$

where r_o is the classical radius of the electron, and Z the atomic number of the target material.

This formula is valid only for non-relativistic electrons for which the following Borns' approximation holds.

$$\frac{2\pi Ze^2}{\hbar v_o} \ll 1 \quad , \quad \frac{2\pi Ze^2}{\hbar v} \ll 1$$

In this expression v_o and v are velocities of the electron before and after an encounter.

Even if Borns' approximation does not hold strictly it is still possible to use the above formula in conjunction with Sommerfelds' multiplying factor defined by the relation,

$$f(\xi, \xi_o) = \xi/\xi_o \left(\frac{1 - e^{-2\pi\xi_o}}{1 - e^{-2\pi\xi}} \right), \text{ where } \xi = \frac{Ze^2}{\hbar v} \quad , \quad \xi_o = \frac{Ze^2}{\hbar v_o} \quad .$$

The function $f(\xi, \xi_o)$ has a value close to unity for high and intermediate electron velocities but decreases rapidly as the electron velocity approaches zero. The expression for the total cross-section on the other hand, increases rapidly with decreasing photon energy and tends to infinity when the photon energy goes to zero. The intensity of the emitted X-rays which is proportional to $k\sigma_k$ diverges as the photon energy tends to zero. Physically this result is absurd as it is contrary to observations. Introduction of Sommerfelds factor avoids this difficulty as the product $f(\xi, \xi_o)\ k\sigma_k$ tends to a finite limit for extremely low photon energies. In this case the appropriate formula for the total bremsstrahlung cross-section is

$$\sigma_k\left(\frac{dk}{E_o}\right)=\left(\xi/\xi_o\right)\left(\frac{1-e^{-2\pi\xi_o}}{1-e^{-2\pi\xi}}\right)\ \bar{\sigma}\ 8/3\ \frac{\mu}{k}\ \ell n\left\{\frac{\sqrt{E_o}+\sqrt{E_o-k}}{k}\right\}^2\ \frac{dk}{E_o}\ .$$

$\beta << 1$

The formula of the total cross-section given above is now valid for all values of photon energies ranging between 0 to E_o. The present investigation, however, deals with the ionizing effects of the X-ray photons on the D-region of the ionosphere and it can be said with certainty that the contribution made by X-ray photons of less than 1 kev energy in this regard is negligibly small. Therefore it is assumed that the Born approximation holds and the simpler form of the cross-section is used throughout.

3.3 DIRECTIONAL INTENSITY OF X-RAYS

It is intended to calculate the flux of bremsstrahlung photons in a given direction starting with the assumption that a monoenergetic and monodirectional beam of electrons of flux I is incident on a small segment of the ionosphere. If the above problem were to be handled in a rigorous manner it would be necessary to start with the cumbersome expression for the differential cross-section as given by Heitler. However, in view of the uncertainties introduced in the calculations due to other approximations it is felt that such rigor is unnecessary here. In what follows, the directional intensity is calculated using the expressions for the total cross-section for the emission of a quantum of energy k and the polar diagram of X-ray emission.

Let N = number of molecules/cm^3 and

$\sigma_k \frac{dk}{E_o}$ = the total cross-section for the emission of a quantum of energy k due to bremsstrahlung process.

The average energy lost by an electron per centimeter path which goes into producing photons in the energy range k, k + dk is given by

$$Nk \ \sigma_k \ d \left(\frac{k}{E_o}\right)$$

The total number of photons in the energy range k, k + dk emitted in path length ds by a single electron is $N \sigma_k \frac{dk}{E_o} ds$* [Chamberlain (1961).]

The total number of photons emitted in the energy range k, k + dk per centimeter path per second by all the electrons is

$$IN \quad \sigma_k \frac{dk}{E_o} .$$

The polar diagram of X-ray emission has been worked out by Sommerfeld (1931) for a non-relativistic electron. This is given by

$$f(\theta) = \frac{\sin^2 \theta}{(1 - \beta \cos\theta)^4} ,$$

where $\beta = v/c$.

This expression gives the relative intensity of X-rays at a given angle θ with the electron path. In order to determine the absolute intensity it is necessary to determine the constant of proportionality A.

---

*At first glance it might appear that the expression for the total number of photons used here is not in agreement with that given by Chamberlain. However, it should be remembered that $\frac{\sigma_k}{E_o}$ of the present analysis is equivalent to $\phi (\nu_1/\nu)$ of Chamberlain's which explains the apparent difference between the two expressions.

The total number of photons produced in the energy range dk per cm path per second is obtained by integrating $\frac{A \sin^2\theta}{(1-\beta\cos\theta)^4}$ over the solid angle. The integral is

$$\int_0^{2\pi}\int_0^{\pi} \frac{A \sin^2\theta}{(1-\beta\cos\theta)^4} \sin\theta \, d\theta \, d\phi \ .$$

Equating this expression with the one obtained earlier determines the value of the constant of proportionality A, i.e.

$$\int_0^{2\pi}\int_0^{\pi} \frac{A \sin^2\theta}{(1-\beta\cos\theta)^4} \sin\theta \, d\theta \, d\phi = IN\sigma_k \frac{dk}{E_o} \ .$$

The integral on the left hand side is evaluated by parts (for the derivation see Appendix I) and is given by

$$\frac{8\pi A}{3(1-\beta^2)^2}, \text{ from which } A = \frac{3(1-\beta^2)^2}{8\pi} IN\sigma_k \ .$$

The non-relativistic expression for the total cross-section as given by Heitler (1954) is

$$\sigma_k = \bar{\sigma}\ 8/3\ \frac{\mu}{k}\ \ell n \left\{\frac{\sqrt{E_o} + \sqrt{E_o - k}}{k}\right\}^2 \ ,$$

where $\bar{\sigma} = Z^2 \times 5.7 \times 10^{-28}\ cm^2$.

Z is the atomic number of the target material and in the case of the ionosphere it may be taken as 7.3. Thus,

$$\sigma_k = Z^2 \times 5.7 \times 10^{-28} \times 8/3\ \frac{\mu}{k}\ \ell n \left\{\frac{\sqrt{E_o} + \sqrt{E_o - k}}{k}\right\}^2 \ .$$

The absolute intensity in the energy range dk at an angle θ from the electron path is given by

$$Z^2 \times 5.7 \times 10^{-28} \cdot 8/3 \ \frac{\mu}{k} \ \ell n\left\{\frac{\sqrt{E_o}+\sqrt{E_o-k}}{k}\right\}^2 \ 3\left(\frac{1-\beta^2}{8\pi}\right) \text{IN} \ \frac{\sin^2\theta}{(1-\beta\cos\theta)^4} \ \frac{dk}{E_o}.$$

Photons cm^{-2} sec^{-1} $sterad^{-1}$

Substituting the values of Z and μ we obtain

$$4.941 \ \ 10^{-24} \ 1/k \ \ell n \ \left\{\frac{\sqrt{E_o}+\sqrt{E_o-k}}{k}\right\}^2 \ (1-\beta^2)^2 \ \text{IN} \ \frac{\sin^2\theta}{(1-\beta\cos\theta)^4} \ \frac{dk}{E_o}.$$

Photons cm^{-2} sec^{-1} $sterad^{-1}$

3.4 AN ESTIMATE OF THE INTENSITY OF AURORAL X-RAYS

Several workers (Winckler, Peterson, Hoffman and Arnoldy 1959, Winkler 1960, Maehlum and O'Brien 1963) have expressed their doubt as to the ionizing effects of bremsstrahlung X-rays on the D region of the ionosphere on the grounds that the energy loss due to radiation is a negligibly small fraction of that due to collisions. Hence they argue that the intensity of X-rays produced is too small to account for the absorption measured by riometers during disturbed periods. In this section this contention is critically examined and the intensity of auroral X-rays is calculated using the flux data obtained by rockets, satellites and balloons.

It is necessary to emphasize here that all the balloon measurements of X-rays extend at most to 22 kev energy. The integral photon spectrum deduced by Bhavsar (1960) from his

balloon observations shows a very steep power law spectrum with an exponent of the order of 7 or more between 22-40 kev. It is therefore logical to suspect that the flux of low energy X-rays may be sufficiently high to ionize the D-region. The electron production curves given in section 3.5 make it quite clear that X-rays of 1-10 kev energy are much more efficient in ionizing the D-region than X-rays of higher energy. But so far no observations of X-rays in this region have been made by balloons because of high atmospheric absorption (photoelectric effect and Compton scattering). Moreover no estimates of the expected low energy X-ray flux have so far been made using primary electron flux data obtained from rockets and satellites. Therefore it seems to the author that the ionizing effects of bremsstrahlung X-rays can only be ruled out when either

(1) The intensity of 1-10 kev X-rays is actually measured at 95-100 km level and is found to be inadequate to explain the observed absorption or

(2) The intensity of 1-10 kev X-rays is calculated at 100 km level using reasonable values of primary electron flux and it is shown that the resulting electron production is too small to account for the observed absorption.

Of necessity the author has chosen the second approach.

As far as the ionization of the ionosphere D-region at a place is concerned, X-rays emitted vertically downwards in a cone of unit solid angle centered at the zenith are far more

effective in ionizing than those emitted at greater angles from the vertical. In this section, the intensity of the downward component of X-rays is calculated, assuming that the electron precipitation takes place over a large area of the ionosphere and that electrons hit the ionosphere at various angles from the zenith. It should be recalled that previous attempts (Anderson and Enemark 1960), disregard the angular distribution of the impinging electrons, the horizontal extent of the bombardment, and also the polar diagram of the X-rays emitted. The above authors use a simplified range energy relation. The calculations presented here are based on the following basic assumptions.

(a) A beam of monoenergetic electrons of 10 kev energy is incident over a large area at 120 kms height.

(b) Electrons move in straight lines and lose energy by collisions only and in accordance with Bethe's formula.

(c) X-rays produced in a small volume element $rdr\ d\theta \times 1\ cm^3$ are radiated in a given direction according to a $\sin^2\theta$ pattern where θ is the angle made with the electron path.

The energy loss of electrons from the top of atmosphere to 120 kms is neglected.

Consider a large area of electron precipitation at a height h above ground. Let M be a point at 100 km level as shown in Figure 1 where the intensity of down coming X-rays in the energy range k, k + dk per unit solid angle is to be calculated.

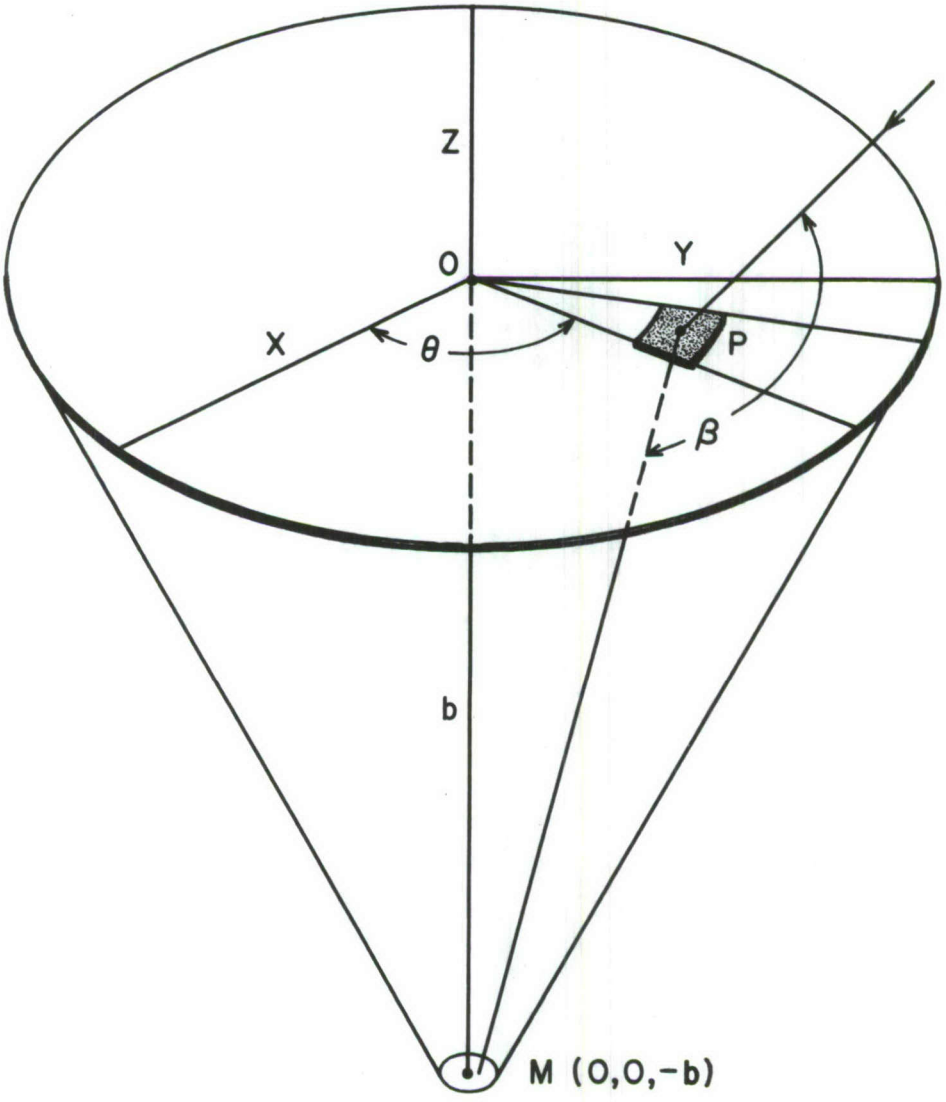

Fig. 1. Geometry for calculations of the intensity of bremsstrahlung X-rays.

The X-rays crossing the 1-cm^2 area at M downwards per sec per unit solid angle will be due to electrons which hit the level h in a circle of radius $\frac{b}{\sqrt{\pi}}$ where b is the vertical distance between the level h and the point M.

Take a right handed coordinate system XYZ with origin 0 as indicated in the figure. An electron with direction cosines ℓ, m, n hits the circle at the point P whose coordinates are (r cosθ, r sinθ, 0) where r is the distance OP. The coordinates of the point M are (0,0,-b). The direction cosines of the line PM are:

$$\frac{r\cos\theta}{\sqrt{r^2+b^2}} \;,\; \frac{r\sin\theta}{\sqrt{r^2+b^2}} \;,\; \frac{-b}{\sqrt{r^2+b^2}} \;.$$

The angle between the electron path and the line PM is

$$\phi = \cos^{-1}\left(\frac{r\ell\cos\theta + rm\sin\theta - bn}{\sqrt{r^2+b^2}}\right) \;, \quad \text{from which}$$

$$\sin^2\phi = 1 - \frac{(r\ell\cos\theta + rm\sin\theta - bn)^2}{r^2+b^2} \;.$$

Take an element of area r dr dθ centered at P. It may be recalled from the result obtained in section 3.3 that the total number of photons in the energy range k, k+dk produced in 1 cm^3 due to a flux of I electrons is

$$N\,\sigma_k\,I\,\frac{dk}{E}$$

Now consider an elementary solid of unit thickness and r dr dθ cross-section. The volume of the solid is r dr dθ cm^3.

The number of photons of energy range dk in the solid will be $N\ \sigma_k\ I\ \frac{dk}{E}\ r\,dr\,d\theta$. Out of these photons, the number which is radiated in a unit solid angle centered at an angle ϕ from the electron path is given by

$$3\left(\frac{1-\beta^2}{8\pi}\right)^2\ N\ \sigma_k\ I\ \frac{dk}{E}\ r\,dr\,d\theta\ \frac{\sin^2\phi}{(1-\beta\cos\phi)^4}$$

Since $\beta^2 \ll 1$ for 10 kev electrons this may be approximated to

$$3\left(\frac{1-\beta^2}{8\pi}\right)^2\ N\ \sigma_k\ I\ \frac{dk}{E}\ r\,dr\,d\theta\ \sin^2\phi$$

The solid angle subtended at the point P by 1 cm^2 area at M is $\frac{\cos\ 0M\ P}{r^2+b^2}$ radians where r and b are measured in centimeters. The number of photons in the energy range dk from elementary volume $r\,dr\,d\theta$ cm^3 crossing 1 cm^2 area at M per second is:

$$\frac{3}{8\pi}\ N\ \sigma_k\ I\ \sin^2\phi\ \frac{rb}{(r^2+b^2)^{3/2}}\ dr\,d\theta\ \text{or}$$

$$\frac{3}{8\pi}\ N\ \sigma_k\ I\left[1-\left(\frac{\ell r\cos\theta+m r\sin\theta-bn}{r^2+b^2}\right)^2\right]\frac{rb}{(r^2+b^2)^{3/2}}\ dr\,d\theta\ \frac{dk}{E}\ .$$

The intensity of X-rays at M due to electrons crossing a disc of 1 centimeter thickness and of b^2 cross-section is given by

$$\int_0^{2\pi}\int_0^{\frac{b}{\sqrt{\pi}}}\frac{3}{8\pi}\ N\ \sigma_k\ \frac{I}{n}\left[1-\left(\frac{\ell r\cos\theta+m r\sin\theta-bn}{r^2+b^2}\right)^2\right]\frac{br}{(r^2+b^2)^{3/2}}\ \frac{dk}{E}\ dr\,d\theta$$

photons cm^{-2} sec^{-1} $sterad^{-1}$.

After carrying out the integration (for details see Appendix II), the expression for intensity becomes

$$\frac{3}{8\pi} N \sigma_k \frac{I}{n}\left[2\pi\left(1-\frac{1}{\sqrt{1+\frac{1}{\pi}}}\right) - \frac{2\pi}{3} n^2 \left(1 - \frac{1}{(1+\frac{1}{\pi})3/2}\right) + \frac{1}{3}\left(\frac{(1-n^2)}{(1+\frac{1}{\pi})}3/2\right) - \frac{2\pi}{3}(1-n^2)\left(\frac{1}{\sqrt{\frac{1}{\pi}+1}} -1\right)\right]$$

The intensity turns out to be independent of ℓ and m which was to be expected. The intensity is also independent of b which is rather surprising.

After simplifying the expression in the brackets, the expression for intensity reduces to

$$\frac{3}{8\pi} N \sigma_k I \left[\frac{.761}{n} - .660\, n\right] .$$

For normally incident electrons, the factor in the brackets is .101, and for electrons incident at 60^o it is about 1.19. The above analysis shows that if the horizontal extent of the bombarded region is not taken into account, the deduced intensities would be overestimated by a factor of 10 for vertically incident electrons.

Similarly if the X-ray polar diagram is not taken into account by assuming that all X-rays travel in the forward direction, the X-ray intensities deduced would be overestimated by at least $\frac{8\pi}{3}$. The combined effect of neglecting the horizontal extent of electron precipitation and the X-ray polar diagram could result in an overestimation of the intensity by as much as two orders of magnitude.

Let $f(\alpha)$ be the distribution function of the zenith angles of the electrons striking the circular disc at the level h.

$f(\alpha)\, d\alpha$ = number of electrons - cm^2 sec^{-1} with zenith angles between $\alpha, \alpha + d\alpha$. If it is assumed that $f(\alpha)$ = constant = f between $\alpha = 0$ and $\alpha = \frac{\pi}{4}$ the expression for intensity becomes

$$\frac{1}{8\pi} N \sigma_k f \int_0^{\pi/4} \left(\frac{.761}{\cos\alpha} - .660 \cos \alpha \right) d\alpha$$

$$= \frac{f}{8\pi} N \sigma_k (.204), \text{ where } \cos\alpha = n .$$

The last expression shows that the contribution to the intensity from the disc is rather insensitive to the zenith angle variations of the impinging electrons provided the thickness of the disc is small enough for the energy losses of electrons passing through the disc at various angles to be negligible. The need for this limitation arises because of the fact that σ_k is a slowly varying function of energy and it can be treated as a constant only when the variation in energy is small. For actual calculations of the intensity only normally incident electrons were used. The unit solid angle cone was divided into slabs of such thicknesses that the energy loss of the electrons was of the order of 10 per cent of the incident energy. The photon intensity per kev range was calculated at 100 km level for k = 1 to k = 9 at 1 kev intervals. The absorption of photons between the level of production and the point M at 100 km level was taken into account by multiplying the intensities by the factor

$$e^{-\int_{100\ km}^{h_p} \mu_m(k)\,\rho\,(h)\,dh}\ ,$$

where h_p is the height where photons are originally produced and $\mu_m(k)$ is the mass absorption coefficient for photon of energy k.

O'Brien (private communication) has quoted a peak flux of 10^{10} - 10^{11} electrons cm^{-2} sec^{-1} in the energy range 9-10 kev.

Assuming a flux of 8.0×10^{10} electrons of 10 kev energy, the resulting X-ray intensities per cm^2 per sec per steradian per kev were calculated at 100 km level. The calculated intensities are given in Table 1.

Table 1.

X-ray energy kev	Intensity photons cm^2 sec^{-1} $Sterad^{-1}$ kev^{-1}
1	6.14×10^4
2	3.41×10^4
3	1.64×10^4
4	1.01×10^4
5	5.70×10^3
6	3.26×10^3
7	1.49×10^3
8	8.09×10^2
9	6.0×10^1

It seems obvious that the calculated intensities are too low to cause any appreciable ionization. For the sake of completeness, the electron production between 100-60 kms due to

X-ray spectrum given in Table 1 is calculated in section 3.5, Table 2, and it is shown in Chapter VII that it is much too small to account for the observed absorption.

3.5 ELECTRON PRODUCTION BY AURORAL X-RAYS

The theory of electron production by monochromatic radiation from the sun has been satisfactorily worked out by Chapman (1931). With slight modification, the results can be applied to the case of auroral X-rays. The only significant difference between auroral and solar X-rays is that the former are mainly produced in a thin layer of the ionosphere due to slowing down of electrons, whereas the latter originate from the sun.

Let h_o be the height above ground of the layer where X-rays of energy k electron volts and of intensity I_o are produced. The intensity of the X-rays as they travel downwards is reduced by the photoelectric effect and Compton scattering. For low energy X-rays of 5 kev or so the photoelectric effect is the most important absorbing mechanism but for higher energies the effect of Compton scattering is also significant. The intensity at a point h km above ground is given by

$$I_o \; e^{-\mu(k) \; (h-h_o) \sec \chi},$$

where it has been assumed that the point in question receives X-rays from a point source at h_o whose zenith angle is χ. $\mu(k)$, generally known as the absorption coefficient is a function of the photon energy k. In general

$$\mu(k) = \mu_{ph}(k) + \mu_c(k)$$

where μ_{ph} is the photoelectric coefficient and μ_c the Compton absorption coefficient. A more practical absorption coefficient

generally in use is the mass absorption coefficient μ_m which is defined by the relation

$$\mu_m = \frac{\mu}{\rho} \quad cm^2\ gm^{-1}$$

where ρ is the density of the absorber.

Expressed in terms of μ_m, the expression for the intensity becomes

$$I = I_o\, e^{-\int_h^{h_o} \mu_m \rho \sec\chi\, dh}.$$

$-\frac{dI}{dh} = \mu_m \rho \sec\chi\, I$ = Intensity lost per centimeter.

Let ω be the energy required to produce one electron-ion pair. For air the value of ω is close to 34 ev (Swift 1961). The number of electron-ion pairs q produced per cm^3 per second is

$$q = \frac{1}{\omega}\ \mu_m \rho I = \frac{1}{\omega}\ \mu_m \rho I_o\, e^{-\int_h^{h_o} \mu_m \rho \sec\chi\, dh},$$

provided I_o is measured in units of ev-cm^{-2}-sec^{-1}. If the intensity I_o is measured in ergs-em^{-2}-sec^{-1} the corresponding expression for q becomes

$$q = 1.835 \times 10^{10}\ \mu_m \rho\ I_o\ e^{-\int_h^{h_o} \mu_m \rho \sec\chi\, dh}\ cm^{-3}\ sec^{-1}.$$

Mass absorption coefficients for X-rays passing through air were calculated from the data given in the Handbook of Physics and Chemistry (Hodgman 1961) for X-ray energies of 2-100 kev according to the following expression.

$$\mu_m\ (air) = \frac{78.08\ \mu_m\ (nitrogen) + 20.95\ \mu_m\ (oxygen) + .93\ \mu_m\ (Argon)}{100}$$

Mass absorption coefficient of X-rays in air is plotted in Figure 2 as a function of energy. Using these values of μ_m, the electron production was calculated for I_o = 1 erg-cm^{-2}-sec^{-1}, for various X-ray energies and zenith angles assuming a height of 100 kms for h. The atmospheric density values were taken from the tabulations of ARDC model atmosphere (Minzner, Champion and Pond 1959). In Figures 3 and 4, q is plotted as a function of height for zenith angles 0°, 30° and 60°. It is quite apparent from these graphs that low energy X-rays of 1-10 kev are far more efficient in ionizing the D-region than X-rays of much higher energy. It should be noted that the peak production rate is almost the same for X-rays of vastly different energies but it occurs at a significantly lower altitude for X-rays of higher energy. The shape of the production curve also undergoes some change as the photon energy increases. It might be of some interest to compare the rate of electron production calculated here for the auroral X-rays with those obtained by Swift (1961) for solar X-rays in the energy range 1-9 kev. The curves plotted by Swift however, do not change their shape with energy. The change of shape of the production curve obtained here may be explained because of slightly higher values of μ_m used in the present analysis and also because the energy range is vastly different.

The electron production cm^{-3} sec^{-1} between 100-60 kms due to the estimated X-ray spectrum given in Table 1 was calculated using the rates of electron production for X-rays in the energy range 1-9 kev. The result is given in Table 2.

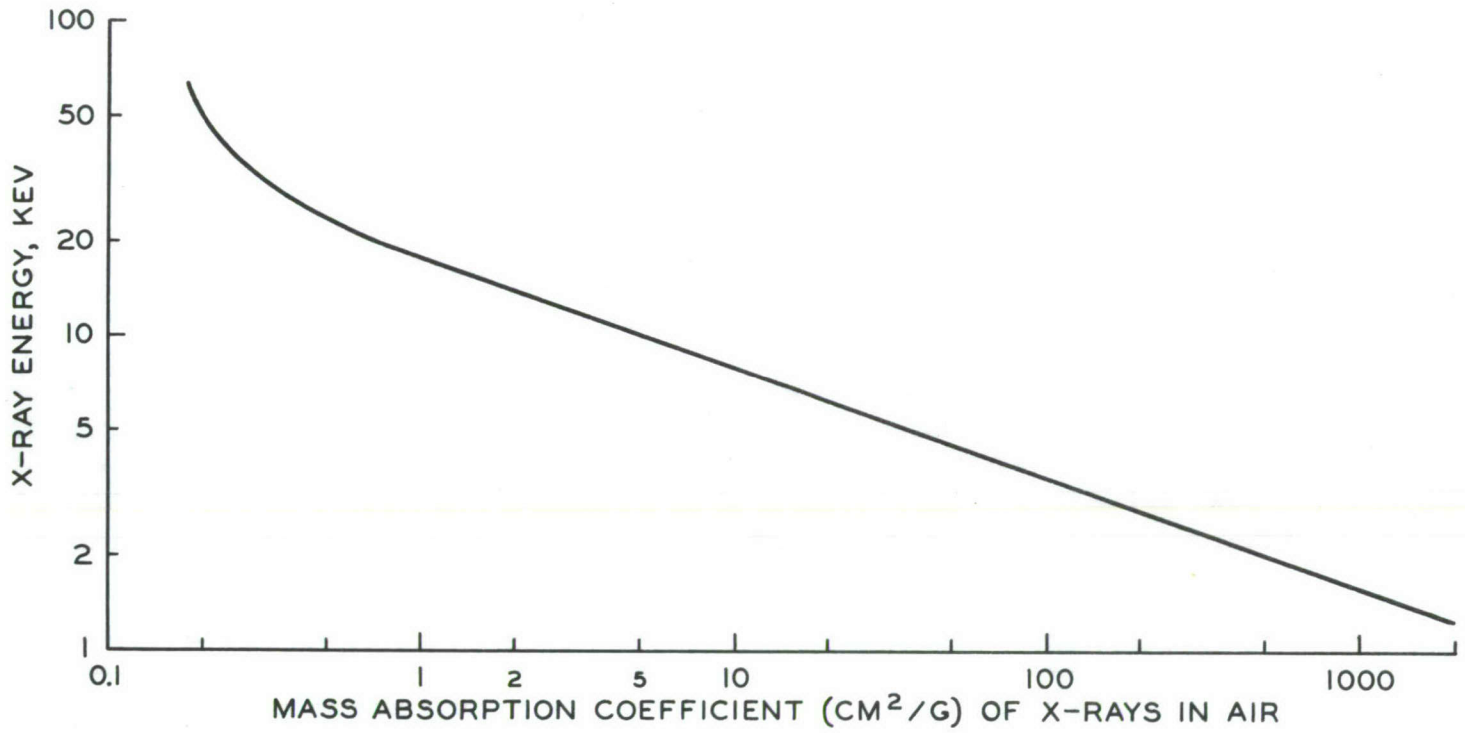
100
50
20
10
5
2
1
X-RAY ENERGY, KEV
0.1
1
2
5
10
100
1000
MASS ABSORPTION COEFFICIENT (CM²/G) OF X-RAYS IN AIR

Fig. 2.

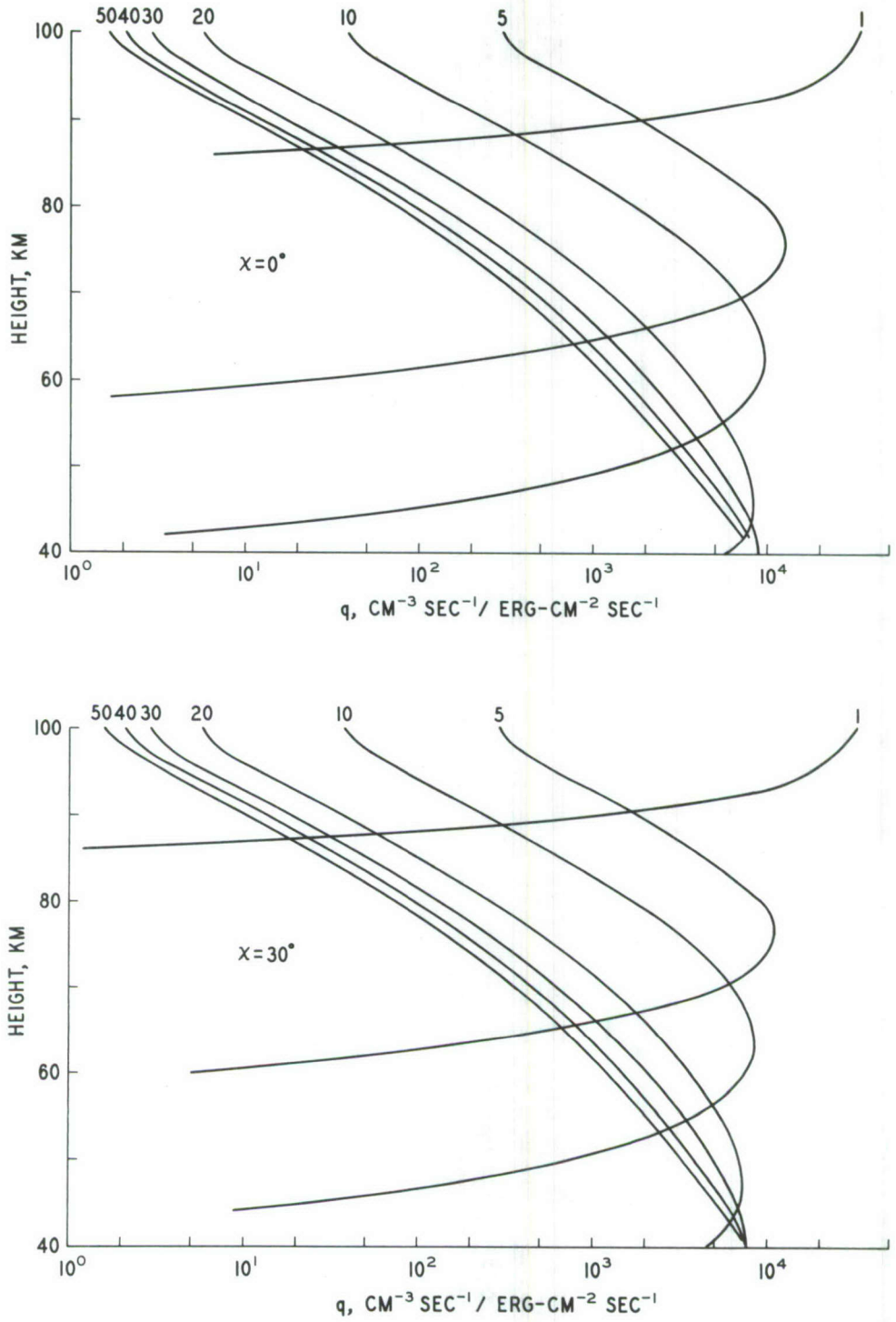

Fig. 3. Electron production by monochromatic X-rays of 1-50 kev energy incident on top of the D-region, at different angles.

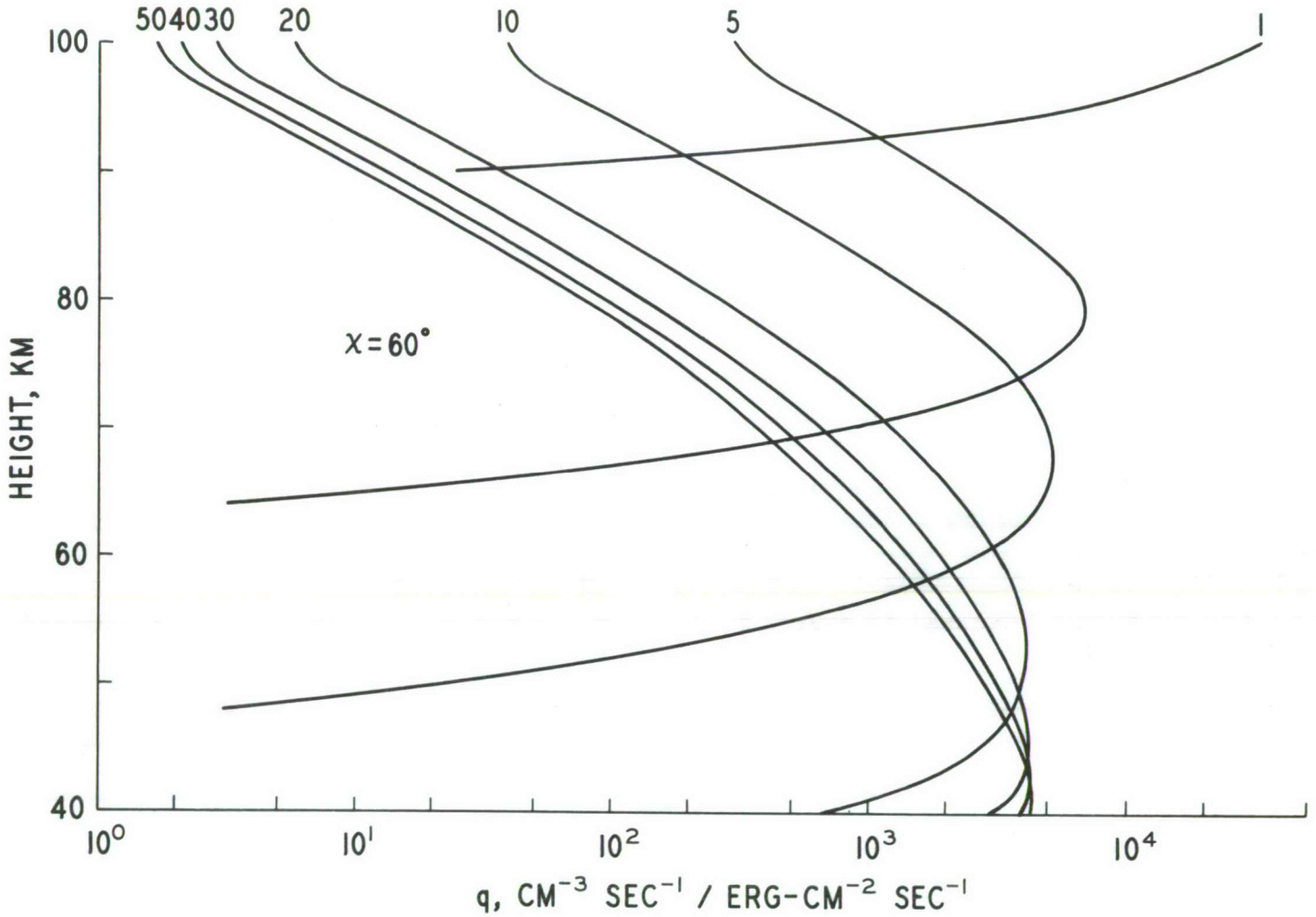

Fig. 4. Electron production by monochromatic X-rays of 1-50 kev energy incident on top of the D-region at 60^{o} from vertical.

Table 2.

Height km	q cm^{-3} sec^{-1}
100	3.86
98	3.50
96	3.50
94	3.21
92	2.86
90	2.76
88	3.25
86	3.25
84	3.05
82	3.03
80	3.03
78	2.42
76	1.98
74	1.59
72	1.31
70	1.09
68	.85
66	.62
64	.44
62	.29
60	.18

The electron production profile due to X-rays which are generated as bremsstrahlung of the 10 kev primary electrons.

3.6 ENERGY LOSS OF PRIMARY ELECTRONS

The energy loss of electrons in an absorber of atomic number Z and average ionization potential I is given by the following expression derived by Bethe (1933).

$$-\frac{dE}{dX} = \frac{2\pi Z e^4 N}{V^2 m}\left[\ell n \frac{V^2 m T}{2I^2(1-\beta^2)} - (\ell n 2)\left(2\sqrt{1-\beta^2} - 1 + \beta^2\right) + 1 - \beta^2\right],$$

where V and T are the velocity and the relativistic kinetic energy of the electrons and N is atomic number density of the absorber. I is usually treated as an empirical constant (Halliday, 1960) having the value of 80.5 ev for air. Fermi (1950) gives a value of 13.5 x Z for I which is close to 98.5 ev. The later value was adopted for the calculation of energy loss of electrons in air. The molecular number density per cm^3 as tabulated by Minzner, Champion and Pond (1959) was used for N. The ionosphere between 145 kms and 75 kms was divided into thin slabs in such a manner that the energy loss of electrons while passing through each slab was less than 10 per cent of the energy of the incident electron. Between 75 km and 100 kms, the region where all the primary electrons between the energy range 10-100 kev come to rest, the condition of 10 per cent energy loss necessitated a minimum thickness of 100 meters. On the other hand, between 145 and 125 kms, slabs of only 5 km thickness were found to meet the requirement. The energy lost by the electron in a slab was subtracted from its incident energy for calculating the energy loss due to the next slab. This process was repeated until the energy loss was greater than the

incident energy at which stage the electron had stopped. The energy loss of normally incident electrons of 6-100 kev energy was calculated in this manner and the energy of these electrons as a function of height is plotted in Figure 5. It should be noted that an electron of 6-10 kev energy loses energy rather slowly and over a wider height range as opposed to an electron of 100 kev energy which loses 90% of its energy in a layer only 10 kms thick. This explains why a high energy electron is much more efficient in ionizing the atmosphere it passes through as compared to an electron of much lower energy. It should be borne in mind that the calculations presented above completely disregard the effects of scattering and that of the earth's magnetic field.

3.7 IONIZATION BY PRIMARY ELECTRONS

The number of electron-ion pairs produced per cm^3 by an electron losing $\frac{dE}{d\chi}$ electron volts per centimeter is roughly $\frac{1}{\omega} \frac{dE}{d\chi}$ where ω is the energy in electron volts required to produce one electron-ion pair in air. For a flux of I electrons-cm^{-2}-sec^{-1}, the number of electron-ion pairs produced per cm^3 per second is given by

$$q = I \frac{dE}{d\chi} \frac{1}{\omega} \quad cm^{-3} \; sec^{-1} \; .$$

Some workers prefer to use $\frac{dE}{d\xi} = \frac{1}{\rho} \frac{dE}{d\chi}$ eV gm^{-1} cm^2, where ρ is the density of the absorber, instead of $\frac{dE}{d\chi}$. When values of stopping power $\frac{dE}{d\xi}$ (eV gm^{-1} cm^2) are available, the electron production is given by $q = I \rho \frac{dE}{d\xi} \frac{1}{\omega}$.

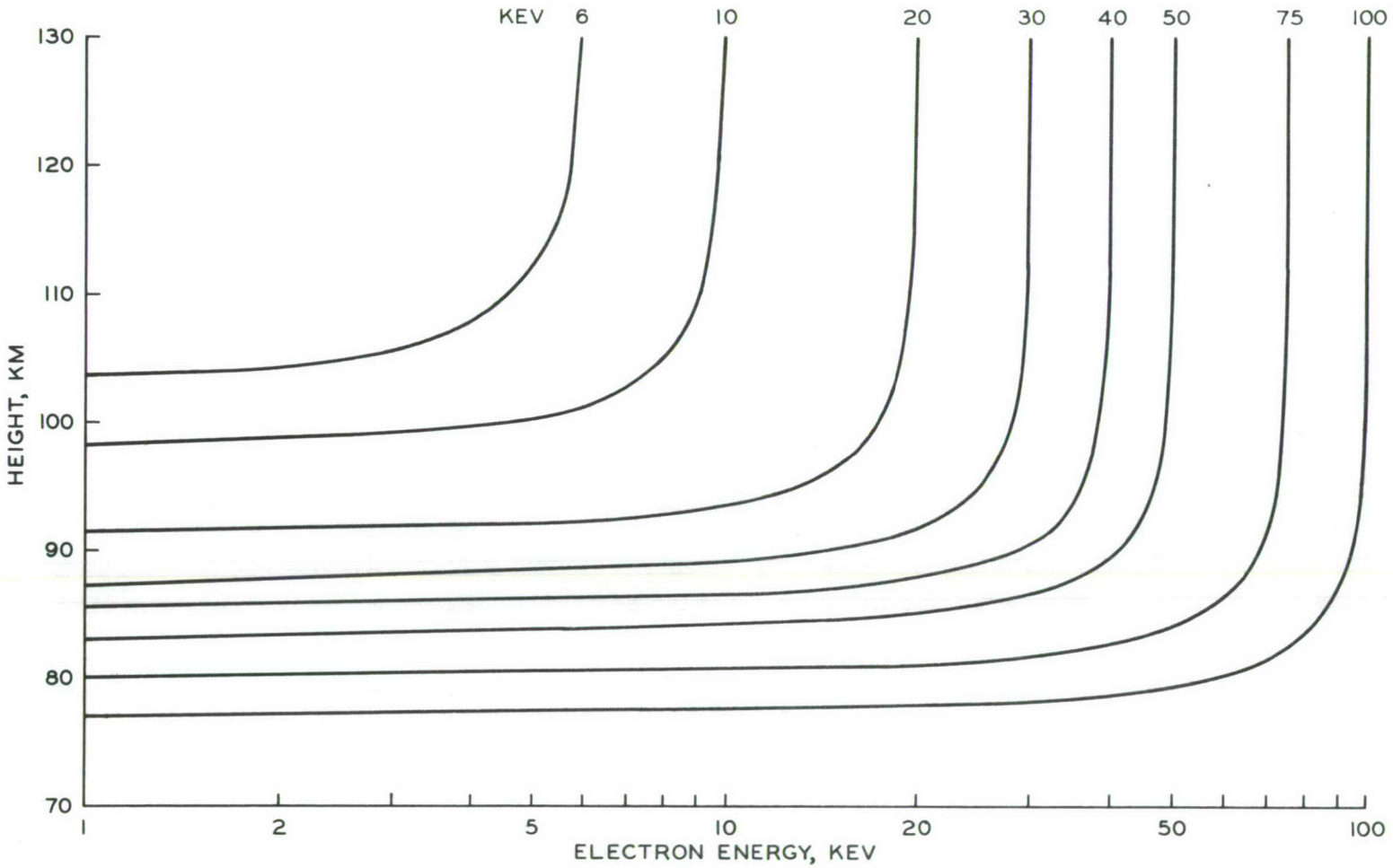

Fig. 5. Energy loss of monoenergetic electrons of 6-100 kev energy normally incident on the ionosphere.

Spencer (1955) has tabulated the values of stopping powers for electrons of .01 - 10 mev energy, incident on air at NTP in units of $mc^2\ gm^{-1}\ cm^2$. In order to convert these values into units of ev $gm^{-1}\ cm^2$, it is necessary to multiply the tabulated values by 5.11×10^5. Furthermore, in order to get the energy loss in electron volts per centimeter, the tabulated values should be multiplied by 5.11×10^5 times atmospheric density at NTP. i.e. 1.2250×10^{-3} gm cm^{-3} (ARDC model atmosphere).

The electron production function q was calculated for electrons of 6-100 kev energy using $\omega = 34$, and is plotted in Figure 6 as a function of height. As expected the high energy electrons create ionization at significantly lower heights than low energy electrons.

Omholt (1960) has made the statement that the ionizing efficiency of X-rays is the same as that of fast electrons. One obvious interpretation of this statement is that the ionization produced by a high energy electron is of the same order of magnitude as that created by an X-ray photon of the same energy. In order to check the validity of his statement the q function appropriate to a 50 kev electron and a 50 kev photon are plotted in Figure 7. The graph shows that between 85-100 kms electron production by primary electrons is greater than that by the X-ray photon by several orders of magnitude, where as between 40-85 kms the only contribution to the ionization comes from the X-rays.

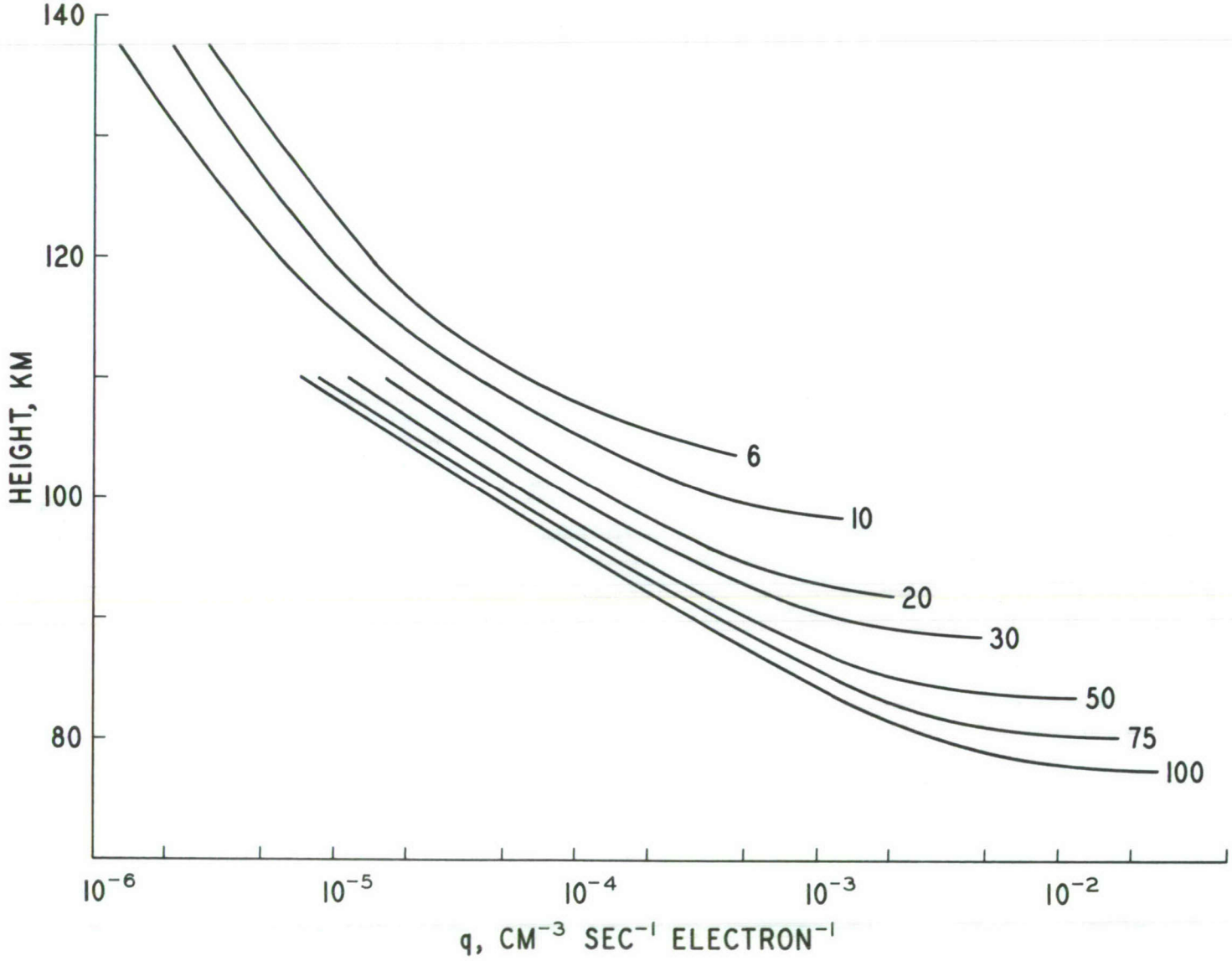

Fig. 6. Electron production by monoenergetic electrons of 6-100 kev energy normally incident on the ionosphere.

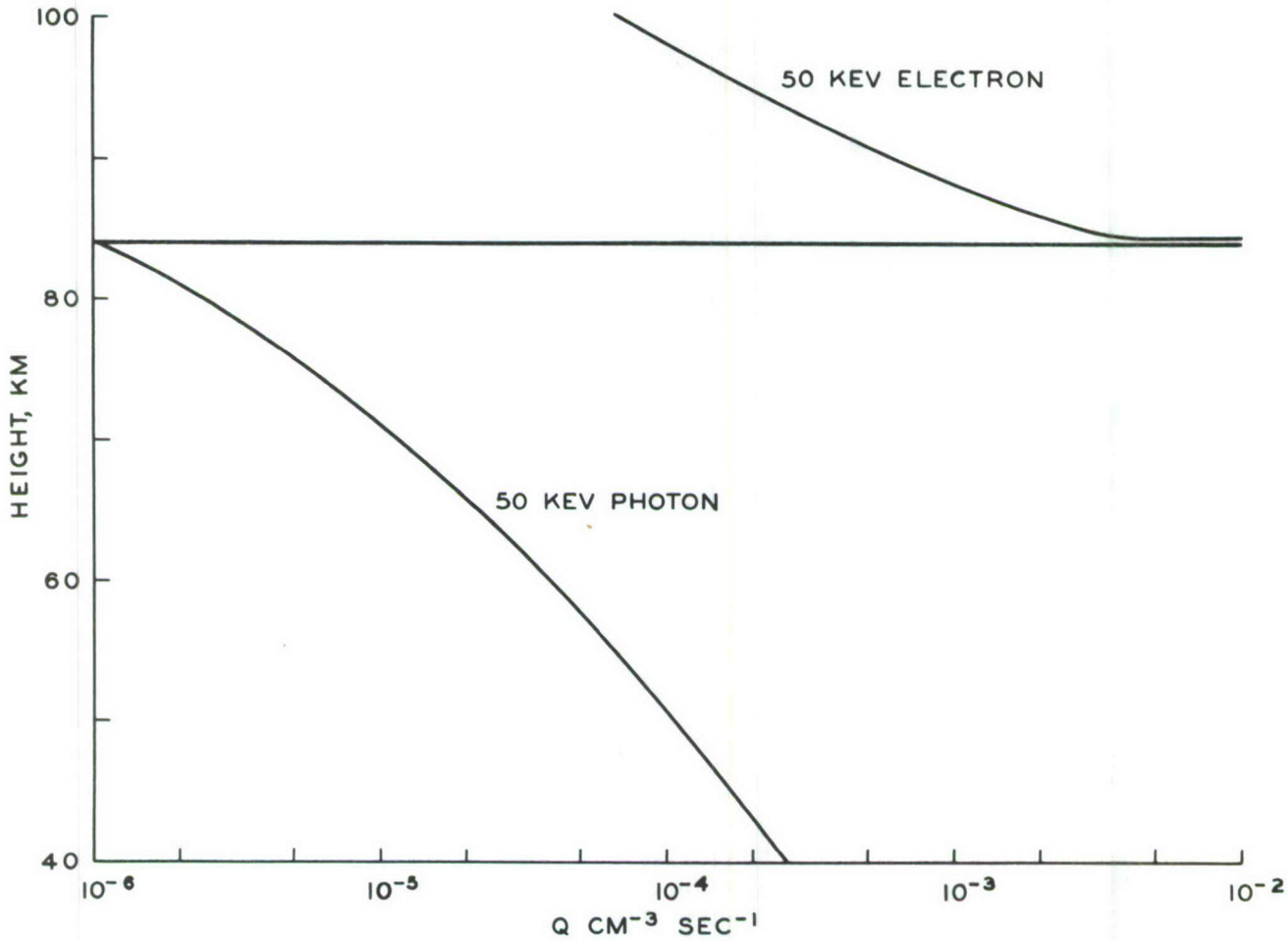

Fig. 7. Comparison of the electron productions by a 50 kev electron and a 50 kev photon.

The peak electron production by primary electrons is at least one order of magnitude greater than the peak production by X-rays. It appears from the graph that both processes complement each other.

3.8 THE RATE COEFFICIENTS AND THE EQUILIBRIUM ELECTRON DENSITY

The rates of variation of electron and negative ion density with time are given by the following equations respectively

$$\frac{dN_e}{dt} = q - \alpha_e N_e N_+ - \beta N_e n + \gamma N_- n + \gamma_1 \beta N_-$$

$$\frac{dN_-}{dt} = - \alpha_i N_- N_+ + \beta N_e n - \gamma N_- n - \gamma_1 \beta N_-$$

where α_i = coefficient of mutual neutralization of positive and negative ions

β = coefficient of attachment of electrons to neutral atoms and molecules

γ = coefficient of detachment of electrons from negative ions by collisions

n = number density of neutral particles

N_e = number density of electrons

N_- = number density of negative ions

N_+ = number density of positive ions

$\gamma_1 \beta N_-$ = the rate of loss of negative ion density due to photo-detachment

q = rate of electron production due to photo-ionization.

If the atmosphere is assumed to be electrically neutral, a further condition is imposed which may be written as

$N^+ = N_- + N_e$.

If in the equation of negative ions, it is assumed that the rate of disappearance of negative ions by mutual neutralization $\alpha_i N_- N_+$ can be neglected in comparison with the attachment and detachment rates $\beta N_e n$ and $\gamma N_- n$, the resulting equation is

$$\frac{dN}{dt} = \beta N_e n - \gamma N_- n - \gamma_1 \beta N_- .$$

Under dynamical equilibrium $\frac{dN}{dt} - = 0$ which reduces the above equation to

$$\beta N_e n = \gamma N_- n + \gamma_1 \beta N_-$$

or

$$\frac{N_-}{N_e} = \frac{\beta n}{\gamma n + \gamma_1 \beta} = \lambda ,$$

$$N_+ = N_e + N_- = (1+\lambda) N_e .$$

N_- and N_+ may be eliminated from the equation of electron density by using the above relations. The result is

$$\frac{dN_e}{dt} = \frac{q}{1+\lambda} - (\alpha_e + \lambda\alpha_i) N_e^2 - \frac{N_e}{1+\lambda} \frac{d\lambda}{dt} .$$

If conditions are such that the ratio of negative ion density to electron density is fairly constant, the term involving $\frac{d\lambda}{dt}$ may be neglected. Then

$$\frac{dN_e}{dt} = \frac{q}{1+\lambda} - (\alpha_e + \lambda \alpha_i) N_e^2 .$$

Under equilibrium condition $\frac{dN_e}{dt} = 0$

and $N_e = \sqrt{\frac{q}{(1+\lambda)(\alpha_e + \lambda\alpha_i)}}$

In the nighttime $q = 0$ and therefore

$$\frac{dN_e}{dt} = - (\alpha_e + \lambda \alpha_i) N_e^2 .$$

$\alpha_e + \lambda \alpha_i$ is known as the effective recombination coefficient. The values of λ to be used in the above equations are

$$\lambda = \frac{\beta n}{\gamma n + \gamma_1 \beta} \qquad \text{(day)} ,$$

$$\lambda = \beta/\gamma \qquad \text{(night)}$$

The two main processes of attachment are

(a) Three body collisional attachment to molecular oxygen. Molecular oxygen is the most effective third body for this reaction.

$$e + O_2 + O_2 \longrightarrow O_2^- + O_2$$

Process (a) is particularly dominant at lower altitudes.

(b) Radiative attachment to atomic oxygen.

$$e + O = O^- + h\nu$$

Process (b) is important at higher altitudes where atomic oxygen is relatively abundant. Molecular and atomic nitrogen is ineffective in forming negative ions in this process. Swift (1961) has plotted electron attachment as a function of altitude between 50 km and 113 kms. According to his graph, the attachment rate increases linearly with decreasing height between 110 and 95 kms. Between 95 kms and 86 kms, there is a slight decrease after which the attachment rate again increases linearly up to 50 kms.

Collisional detachment is characterized by the following reaction

$$O_2^- + O_2 \longrightarrow 2O_2 + e$$

$$O_2^- + O \longrightarrow O_3 + e$$

The coefficient of collisional detachment is very much uncertain. Swift (1960) has quoted a value of 10^{-18} (0_2). On the other hand Mitra (1952) has given a height independent value of 10^{-15} - 10^{-14} cm^3 sec^{-1}.

The reactions giving rise to radiative recombination are

$O + e \longrightarrow O^* + h\nu$ $\quad \alpha_e = 1.5 \times 10^{-12}$ cm^3/sec. Mitra (1952)

$O_2^+ + e \longrightarrow O_2^* + h\nu$ $\quad \alpha_e = 4.8 \times 10^{-8}$ cm^3/sec. for O_2 (Sayers 1956)

$N^+ + e \longrightarrow N^* + h\nu$

$N_2^+ + e \longrightarrow N_2^* + h\nu$ $\quad \alpha_e = 10^{-12}$ cm^3/sec. (Mitra 1952)

The recombination rate of electron to molecular oxygen is not very well known, because electrons are more effectively removed by attachment to neutral oxygen than by recombination. Mitra (1952) assumes that the recombination rate of electrons to molecular oxygen is of the same order of magnitude as that to atomic oxygen, i.e. 10^{-12} cm^3/sec. Sayers (1956) on the other hand gives a much higher value of 4×10^{-8} cm^3/sec.

The recombination rate of electrons to molecular nitrogen is fairly well known from the measurements of Bialecke and Dougal (1958) and Faire and Champion (1958). At D-region temperatures, the value of the recombination coefficient varies between 0.7×10^{-6} to 0.8×10^{-6}.

The reactions leading to dissociative recombination are:

$O_2^+ + e \longrightarrow O^* + O^{**}$

$N_2^+ + e \longrightarrow N^* + N^{**}$ $\quad$ reaction coefficient 10^{-8}-10^{-7} cm^3/sec

The reactions leading to mutual neutralization of positive and negative ions are

$$N_2^+ + O^- \longrightarrow N_2^* + O^*$$

$$N_2^+ + O_2^- \longrightarrow N_2^* + O_2^*$$

$$O_2^+ + O_2^- \longrightarrow O_2^* + O_2^{**}$$

$$O_2^+ + O^- \longrightarrow O_2^* + O^*$$

$\alpha_i = 10^{-7}$ cm^3/sec Mitra (1952) .

Photo-detachment of negative ions takes place according to the following reactions.

$$O^- + h\nu \longrightarrow O + e$$

$$O_2^- + h\nu \longrightarrow O_2 + e$$

The rate of photo-detachment, $\gamma_1 \beta N_-$ may be written as

$$\gamma_1 \beta \left[O^-\right] + \gamma_1' \beta' \left[O_2^-\right] = 10^{-1} \left[O^-\right] + 9 \times 10^{-2} \left[O_2^-\right] .$$

Mitra (1952)

Swift (1960) uses a slightly higher value of the photo-detachment rate given by the relation

$$\gamma_1 \beta N_- = 1.4 \left[O^-\right] + 0.44 \left[O_2^-\right] .$$

The adopted values of the rate coefficients are given in Table 3.

Table 3.

$\beta = 2.5 \times 10^{-30} N(O_2)$ cm^3/sec

$\gamma = 10^{-16}$ cm^3/sec

$\alpha_d = 5 \times 10^{-7}$ cm^3/sec

$\alpha_i = 10^{-7}$ cm^3/sec.

The nighttime values of $\frac{1}{(1+\lambda)(\alpha_d + \lambda\alpha_i)}$ calculated between 60-100 km in 2 km steps are given in Table 4. The equilibrium electron density at any height is thus easily found by the expression $\sqrt{\frac{q}{(1+\lambda)(\alpha_d + \lambda\alpha_i)}}$ when the electron production function q is known at that height.

Table 4.

Height km	$\frac{1}{(1+\lambda)(\alpha_d + \lambda \alpha_i)}$
100	1.90×10^6
98	1.86×10^6
96	1.80×10^6
94	1.70×10^6
92	1.60×10^6
90	1.44×10^6
88	1.25×10^6
86	1.08×10^6
84	8.20×10^5
82	5.99×10^5
80	4.13×10^5
78	3.73×10^5
76	1.92×10^5
74	1.24×10^5
72	8.20×10^4
70	5.29×10^4
68	3.39×10^4
66	2.16×10^4
64	1.40×10^4
62	9.26×10^3
60	5.99×10^3

The nighttime value of $\frac{1}{(1+\lambda)(\alpha_d + \lambda \alpha_i)}$

CHAPTER IV

THE EXPERIMENTAL TECHNIQUE OF STUDYING SPATIAL VARIATIONS OF AURORALLY ASSOCIATED RADIO WAVE ABSORPTION

4.1 INTRODUCTION

The conventional methods of measuring radio wave absorption depend on the availability of "echoes" from the ionosphere of pulses from a transmitter, on the ground. In the auroral zone the absorption is often so severe that most of the energy sent by the transmitter is absorbed, thereby making the above method of little practical use.

In the cosmic noise method originated by Shain (1951), the attenuation of cosmic noise in traversing the ionosphere is used to measure the absorption. Obviously this method requires the knowledge of the unattenuated strength of the cosmic noise. The strength of the cosmic noise signals received on a quiet day is used as a reference for this purpose. The absorption is computed by comparing the signal strength at a given time with the reference signal strength received at the same sidereal time.

Little (1954) was the first to realize the enormous potentialities which the cosmic noise method offered for high latitude radio wave absorption studies. Later, Little and Leinbach (1958) improved Shain's experimental technique by introducing a sensitive, self-balancing, noise-measuring instrument called the riometer, which since then has come into world-wide use.

A very important part of the absorption measuring device is the antenna. When a broad-beam antenna is employed, the noise

power entering the receiver is from a large area of the sky. Therefore if a riometer connected with a wide-beam antenna registers absorption, one can only say that absorption took place somewhere in the broad region of the sky from which cosmic noise signals were received. If one wishes to study the absorption suffered by radio waves in different directions or, in other words, the distribution of absorption across the sky, it is necessary to use narrow beam antennas pointed at various parts of the sky. As narrow beam antennas are rather expensive, it is convenient to employ a single narrow beam antenna and to electrically swing the beam to different parts of the sky. For good performance, however, it is possible only to swing the beam a few degrees of the normal position. Furthermore, the switching speed should be such that the change in absorption taking place in one switching cycle is negligibly small. For the study of events which show rapid fluctuations of absorption with time, it is necessary to use faster switching speeds. Unfortunately, switching speeds faster than one cycle per minute cannot be satisfactorily handled by a single riometer because of excessive fluctuations in the signal level and, therefore, for fast-onset events one is forced to use one riometer for each antenna position.

In order to investigate the relation between auroral occurrence and the absorption measured by means of a narrow beam antenna, it is necessary to use photometers which have beamwidths comparable to the beamwidth of the antenna. It is convenient to have photometers pointed in each of the positions where the

antenna beam is periodically directed. The all-sky camera data, when available, provides a qualitative supplement to the photometer data.

In this chapter, the experimental program for the study of spatial variations of radio wave observation and their relations with luminous aurora is described in detail.

4.2 THE RIOMETER

The riometer developed by Little and Leinbach (1958) is similar in design to the radiometer developed by Machine, Ryle, and Vonberg (1952), but with many improved features suitable for cosmic noise absorption measurements. As far as interpretation of data obtained during the present investigation is concerned, a brief description of the principles of operation of the riometer suffices.

In the riometer, the noise power from the antenna is continuously compared with that from a calibrated noise source. This comparison is accomplished by switching the receiver input alternately between the antenna and the local noise diode source at the rate of 340 cps. When the two noise signals are unequal, a 340 cps square wave, having an amplitude proportional to the difference between the two signals, results at the detector of the receiver. This square wave is amplified and then detected in a phase sensitive detector, whose d.c. output voltage is proportional to the difference between the two noise signals and whose polarity is determined by which of the two noise signals is the stronger. The d.c. output of the phase sensitive

detector is used to adjust the filament temperature of the noise diode so that the difference between the two noise signals is reduced. Thus the noise power from the antenna is continuously made equal to the noise power from the noise diode. The noise power output of a noise diode is directly proportional to the d.c. current flowing through it. Therefore the antenna noise power can be continuously recorded on a linear scale simply by recording the noise diode current.

4.3 REQUIREMENTS OF A NARROW BEAM ANTENNA FOR COSMIC NOISE ABSORPTION MEASUREMENTS.

The use of a narrow beam antenna for the reception of weak cosmic noise signals imposes rather stringent requirement on the antenna parameters, especially the main lobe to side lobe ratio. For unambiguous analysis of cosmic noise absorption data obtained from a narrow beam antenna, it is necessary that the power received by the side lobes should be a negligibly small fraction of that entering through the main beam at all times. In practice this requirement is difficult to meet in view of the fact that the brightness temperature of the sky varies enormously from one part of the sky to another. With the rotation of the earth, it may well happen at some time that the side lobe receives signal from a very hot region, such as those near the galactic plane, while the main beam is pointed toward a much colder region of the sky such as the galactic pole. In a case like this, if the main beam to side lobe ratio is not appreciably large, a major part of the power entering the receiver could be

from the side lobe. If the riometer showed absorption at this time, it would be impossible to specify the direction in which it was observed.

Shklovsky (1960) has quoted a range of 8500-67000k^{o} for the variation in brightness temperature from the coldest to the hottest region of the sky at 40 Mc/s. If the power gathered by the side lobe in a given direction is to be at the most 10 per cent of that gathered by the main beam, even when the former is pointed towards a hot region and the latter towards cold, it is necessary that the side lobe should be about 20 db down from the main beam. In practice this is an overestimate because for a vertically directed 4 x 4 array at College the main side lobe at 50^{o}-60^{o} from the zenith would never be pointed at the galactic center, and therefore the maximum ratio of the brightness temperatures encountered would be more like 5:1, which still requires that the side lobe be at least 17 db down from the main beam. More complications arise when one tries to swing the beam electrically a few degrees on either side of the zenith. In this case the side lobe structure in the plane of switching becomes unsymmetrical; the side lobes in the direction of switching diminish in intensity whereas those on the opposite side are enhanced. The magnitude of the unsymmetry is proportional to the switching angle. For a switching angle of 12^{o}, the increase in the side lobe level is of the order of 4 db. Therefore if the side lobe is required to contribute at the most 10 per cent of the total power when the beam is switched

to 12^{o} from the normal position, it is necessary that the side lobe in the normal position be at least 21 db down from the main beam. A narrow beam antenna of the above specifications is not hard to build for frequencies of the order of 100 Mc/s, but for much lower frequencies the size and the cost involved are excessive. Moreover, it should be borne in mind that the absorption is inversely proportional to the square of the frequency and hence the absorption events observed by means of a higher frequency riometer would be considerably weaker.

From the foregoing discussion it should be clear that, in the design of a narrow beam antenna, several compromises have to be made between many conflicting requirements.
These requirements are:

(a) Frequency: The frequency selected should neither be too high to defeat the purpose of the experiment nor too low to make the antenna cost prohibitive.

(b) Beamwidth: The beamwidth of the antenna should preferably be comparable to the angular widths of the auroral arcs whose absorption effects are to be studied.

(c) Side lobe level: The type of antenna selected must have the lowest side lobe level, commensurate with its cost.

(d) Separation of individual elements of the array: The separation between the elements of the array should neither be too small to cause interaction between adjacent elements and an unnecessary increase in the beamwidth nor too large to result in an increased number of side lobes.

(f) Switching angle: The switching angle of the antenna beam should neither be too small to make the observations redundant nor so large as to make one of the side lobes comparable with the main beam.

It should be obvious from the above summary that the cost of building the antenna and the funds available for it enter directly or indirectly into most of these requirements. With limited funds it is necessary to make compromises between many desirable features of the antenna.

In principle, it is possible to obtain lower side lobe levels by reducing the power fed to the outer elements of the array in accordance with Dolf-Techebyscheffs' optimum tapered feed. It should be remembered however, that such reduction always takes place at the cost of reduced gain and increased beamwidth, which are both undesirable.

Theoretical patterns were calculated for linear arrays, first of four dipoles and then of four Yagi antennas in which the currents were in the ratio 1/2 : 1 : 1 : 1/2. These patterns are given in Figure 8 for vertically directed and tilted beams. When the beam is swung by 12^{o}, it should be noted that the major side lobe of the dipole array is only 4 db down from the main beam, whereas in the case of Yagi array it is 6.5 db down. The above analysis suggested that Yagi antennas were preferable to dipoles.

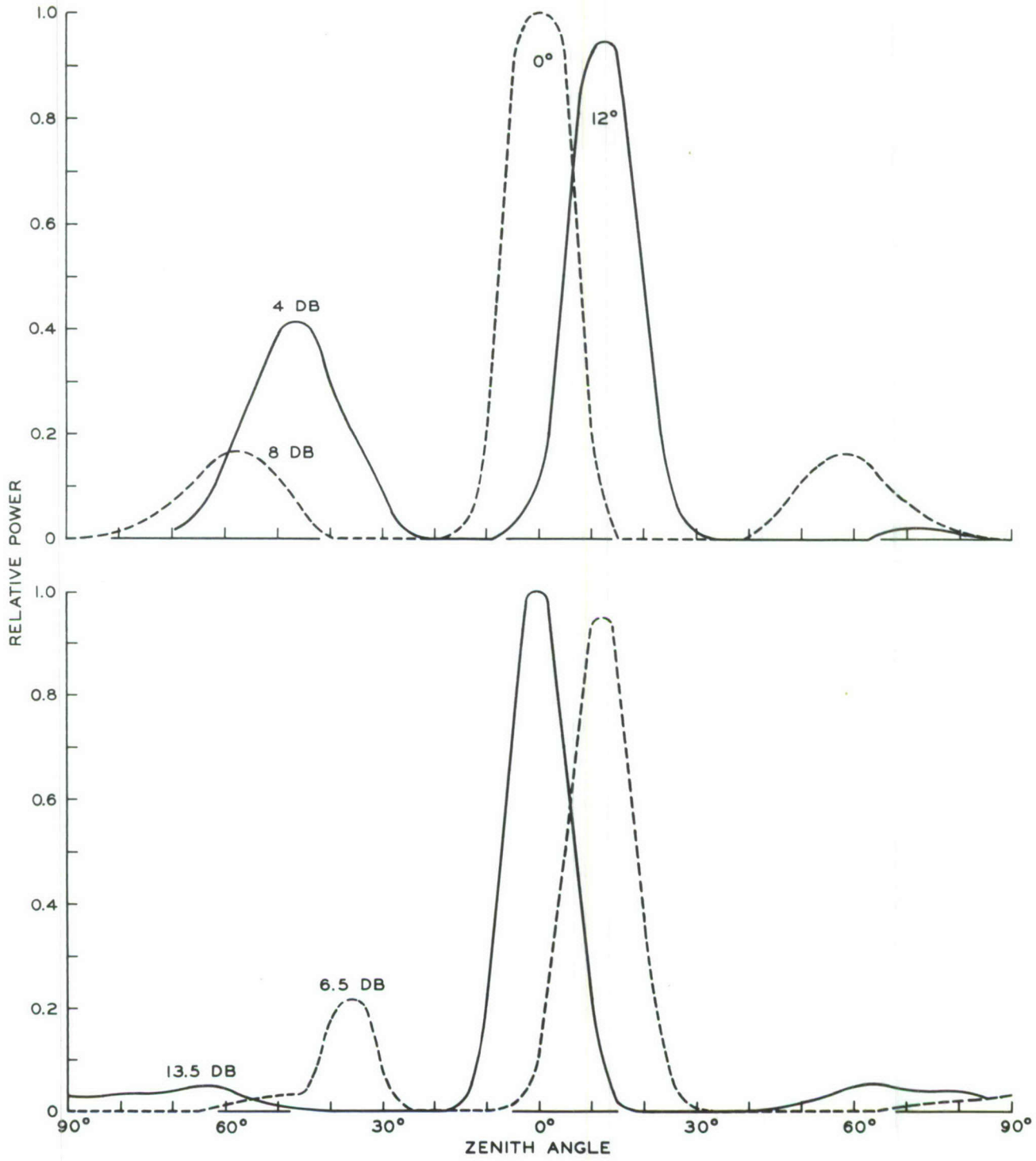

Fig. 8. Theoretical radiation pattern of a 4 element linear array consisting of (a) Dipoles (top), (b) Yagis (bottom) in which the currents are in the ratio $\frac{1}{2}$: 1 : 1 : 1/2.

4.4 THE ANTENNA ARRAY

After a careful consideration of the antenna requirements, the cost involved, the funds available, etc., a frequency of 36 Mc/s was chosen for the experiment. Yagi antennas were chosen as the elements of the array, rather than dipoles, because of their greater gain. An antenna spacing of 1.1λ was found to be the most suitable for the purpose of the experiment. A linear array of 4 Yagis, with 1.1λ spacing, was built in Australia by Thomas and McNicol (1960), and their results were found to be encouraging.

A switching angle of 12° on either side of zenith was chosen as a good compromise. Since a narrow beam was desirable both in the E and H-planes, it was decided to make a square array of 16 Yagis.

Before building the full sized array, a scale model of the same at 450 Mc/s was built and tested in the summer of 1961. The E-plane pattern of the model was measured on the ground by mounting the array vertically on a rotatable platform and by using it as a receiving antenna for the signal from a small transmitter located about 1000 feet away. The transmitting antenna was kept fixed and the rotation of the array with respect to the transmitting antenna was carefully determined by a theodolite mounted on the platform underneath the array. Keeping the transmitter power output constant, the output of the receiver was calibrated in millivolts for different positions of the array ranging between 0° - 90°, where the angles were measured from the position of maximum signal. Because of spurious reflections from large

radio astronomical telescopes at Ballaines Lake field site where the above experiment was carried out, only half of the E-plane pattern could be successfully determined. The results of the pattern measurement were found to be in close agreement with those of Thomas and McNicol (1960).

Figure 9 shows the structure of the antenna and the method of phasing and impedance matching employed. The 3-element Yagi antennas used are Telrex Model OS309/35 antennas, which have a gain of 9.5 db over a reference dipole, a front to back ratio of 23 db, an E-plane beamwidth of 56^{o}, and a nominal impedance of 52 ohms.

The feeds from all four antennas in each row were brought to points A, B, C, and D, by RG8AU coaxial cables. In order to keep the relative phase constant, the cable lengths used were taken as exact multiples of the wavelength at 36 Mc/s and were accurately determined by means of a VHF admittance meter. The impedance of 13Ω at points A, B, C and D was transformed back to 52 ohms by using a 1 : 4 transformation affected by using a 26 ohm quarter-wave line. The 26 ohm quarter wave line was obtained by joining two 52 ohm $\lambda/4$ lines in parallel. Thus the transformed impedance at points A', B', C', D' looking into the antenna is 52 ohms. In the case when the beam is pointed to the zenith, points A', B', C', D' are joined together, which results in an impedance of 13Ω . Using a 1:4 transformation again as before in the form of a 26 ohm quarter wave line a final impedance of 52Ω results. The method of impedance

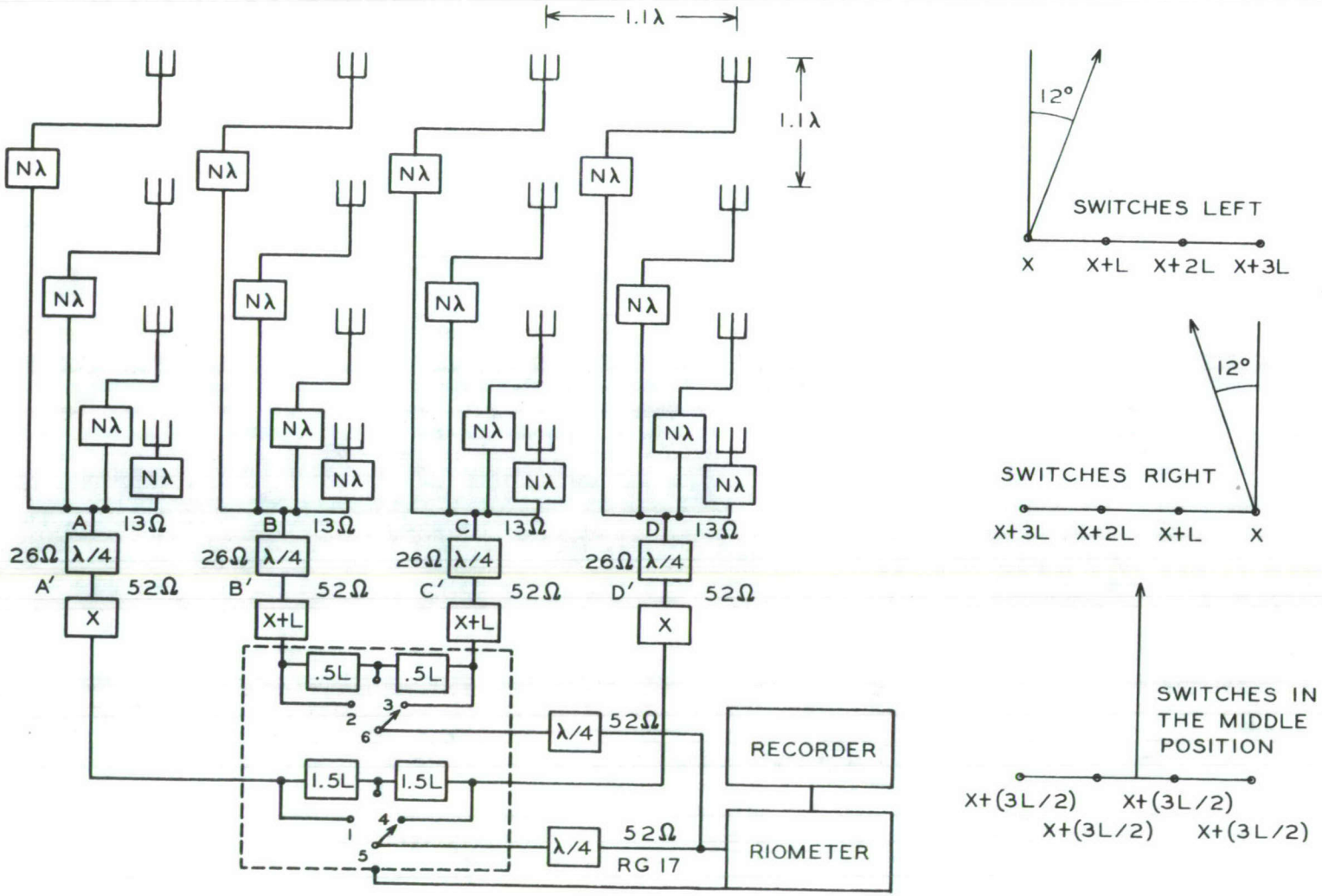

Fig. 9. Details of construction, impedance matching, and slow speed beam switching of the 4 x 4 Yagi array used for radio-wave absorption studies at College, Alaska.

matching when phase shifts are used to swing the beam is described in the following section.

4.5 BEAM SWITCHING

In principle the technique of beam switching employed is the same as that described by Starr (1953). Referring to Figure 9, it may be seen that the array construction starting from the individual antennas to points A', B', C' and D', is the same for the tilted beam as for the vertical case described in the previous section. When beam switching is incorporated, points A' and D' are joined to points 1 and 4 respectively, as shown in the figure by equal lengths of cables, and points 1 and 4 are joined together by a cable of length 3ℓ where

$$\ell = d\ (\sin \alpha)\ f,$$

where d = antenna spacing in wavelengths,

α = switching angle,

f = velocity factor of the cable ≈ 0.665 .

For a switching angle of 12° and antenna spacing of 1.1λ , the length ℓ for 36 Mc/s is given by

$$1.1\ \lambda \sin 12^{\circ} \times 0.665 \approx 4.1 \text{ feet.}$$

Similarly points B' and C' are joined to points 2 and 3 by cables of length $x + \ell$ and points 2 and 3 by a cable of length ℓ . Now consider the two switches, as shown in the figure to be connected to the main feed by an appropriate matching network at points 5 and 6. When both switches are to the left the path lengths of the feed are x, $x + \ell$, $x + 2\ell$, $x + 3\ell$ from left to right. This condition causes the beam to swing by

$\sin^{-1} \frac{\ell}{df}$ degrees to the right from the normal position i.e. when path lengths of the feed are equal. Similarly, when the switches are to the right, the beam switches to the left by an equal angle.

The impedance at points 5 and 6, looking into the array, is 26 ohms. In order to get a final impedance of 52Ω , the main feed is joined to points 5 and 6 by two $\lambda/4$ lines of 52 ohm impedance.

The above switching scheme allows one to swing the beam either to the right or to the left but there is no provision for pointing the beam straight up. The third position may easily be introduced by using two three position switches and by providing additional contacts at the mid-points of cables 2-3 and 1-4 for these switches (see Figure 9). When the switches are in the middle position, path lengths of the feed are all equal to $x + \frac{3\ell}{2}$, and therefore, the beam is pointed to the zenith.

4.6 SWITCHING TECHNIQUES

During early stages of the experiment, two coaxial relays used for switching were activated by a microswitch mounted on the shaft of a 1 rpm motor. For identification purpose, the on-off time of the microswitch was adjusted so that the beam pointed to the north for 35 seconds and to the south for 25 seconds. The main feed from the antenna was connected to a single riometer, and data pertaining to both positions were obtained from a single recorder. As the levels of the quiet

day signals in these directions are slightly different, the record appears in the form of a rectangular waveform whose amplitude varies according to the difference in the signal level between the two directions. The broader portion of the rectangular waveform corresponds to the $12^{o}N$ position and the narrow portion corresponds to the $12^{o}S$. The two absolute amplitude levels of the rectangular waveform represent the signal levels from north and south.

The mechanical relays were soon found to be unsatisfactory because of corrosion of contacts and resulting impedance variation. Because of corrosion and excessive wear the contacts had to be cleaned every few days for reliable operation. In order to avoid this inconvenience, the transistor switch of Figure 10 was built. The switch uses 2N1307 transistors and has an insertion loss of the order of 1/4 db.

The numbers labeled on the switch diagram correspond to connections with the array of Figure 9. The switch S, showed in Figure 10, is used to provide a negative voltage to the base of the transistors. With the top section of the switch S closed, the transistors marked T_2 and T_4 conduct, joining point 3 to point 6 and point 4 to point 5. When the bottom section of the switch is closed, T_1 and T_3 conduct, connecting 1 to 5 and 2 to 6.

4.7 FAST SPEED SWITCHING

The slow speed switching scheme described in the previous section was found to be adequate for absorption events which

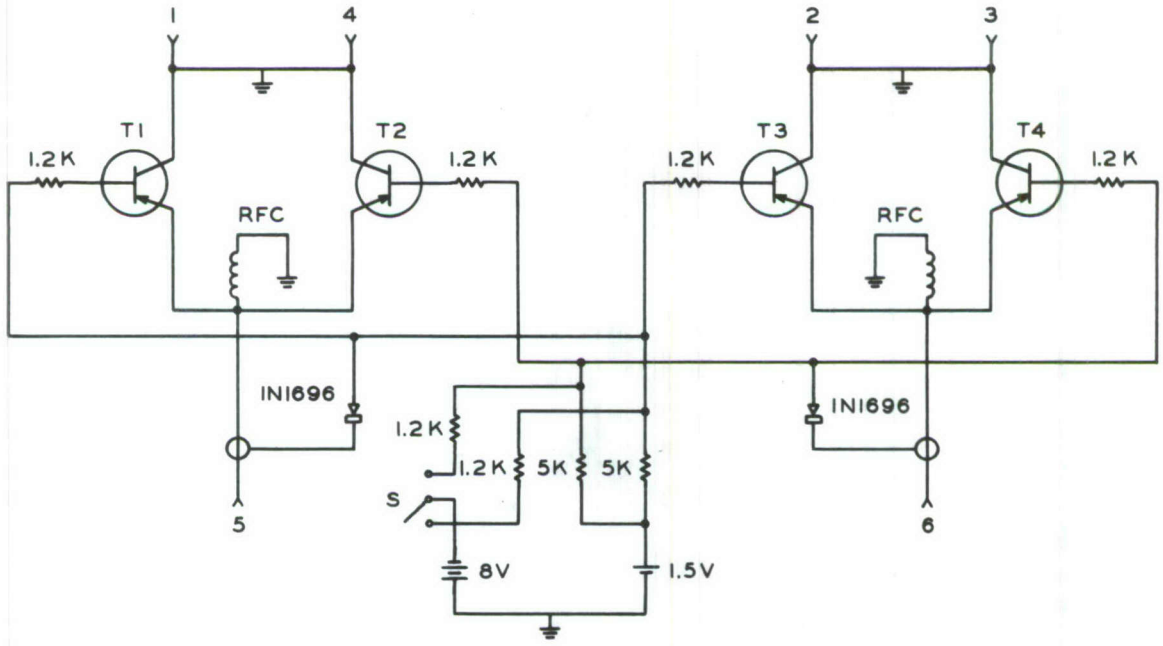

Fig. 10. Slow speed transistor switch used for antenna beam switching. The numbers in Fig. 10 represent connections of the transistor switch with the array of Figure 9.

show little variation in one switching cycle. Often, the absorption events in the auroral zone have extremely sharp onsets which require much faster switching. A high speed switching scheme built in the fall of 1962 and still currently in use is shown in Figure 11. Two riometers with separate feeds and two separate recorders are used in this arrangement. When points 5 and 6 are joined to points 3 and 4 respectively and when points 7 and 8 are disconnected from 1 and 2, the riometer marked N receives a signal from the north and the recorder marked N registers the signal. At the same time, as points 7 and 8 are not connected to the antenna, the riometer marked S does not receive any signal and therefore recorder S registers zero deflection. When points 7 and 8 are joined with 2 and 1, and at the same time 5-6 are disconnected from 3-4, the riometer S receives a signal from the south while recorder N shows zero deflection. The only objectionable feature of the above scheme is that both recorders have to go through unnecessary fluctuations several times every minute which makes the record difficult to scale. To avoid this trouble, the riometer not being used was momentarily put out of operation by breaking its servo loop. When the servo loop of a riometer is broken, the output signal slowly approaches its quiescent level. If the switching is fast enough and if both riometers are muted in the off cycle in this manner, the recorders will draw continuous traces.

Details of fast switching and of the muting device are shown in Figure 12. Every 10 seconds the magnetic reed switch actuates the multi-contact relay, which in turn performs the following operations.

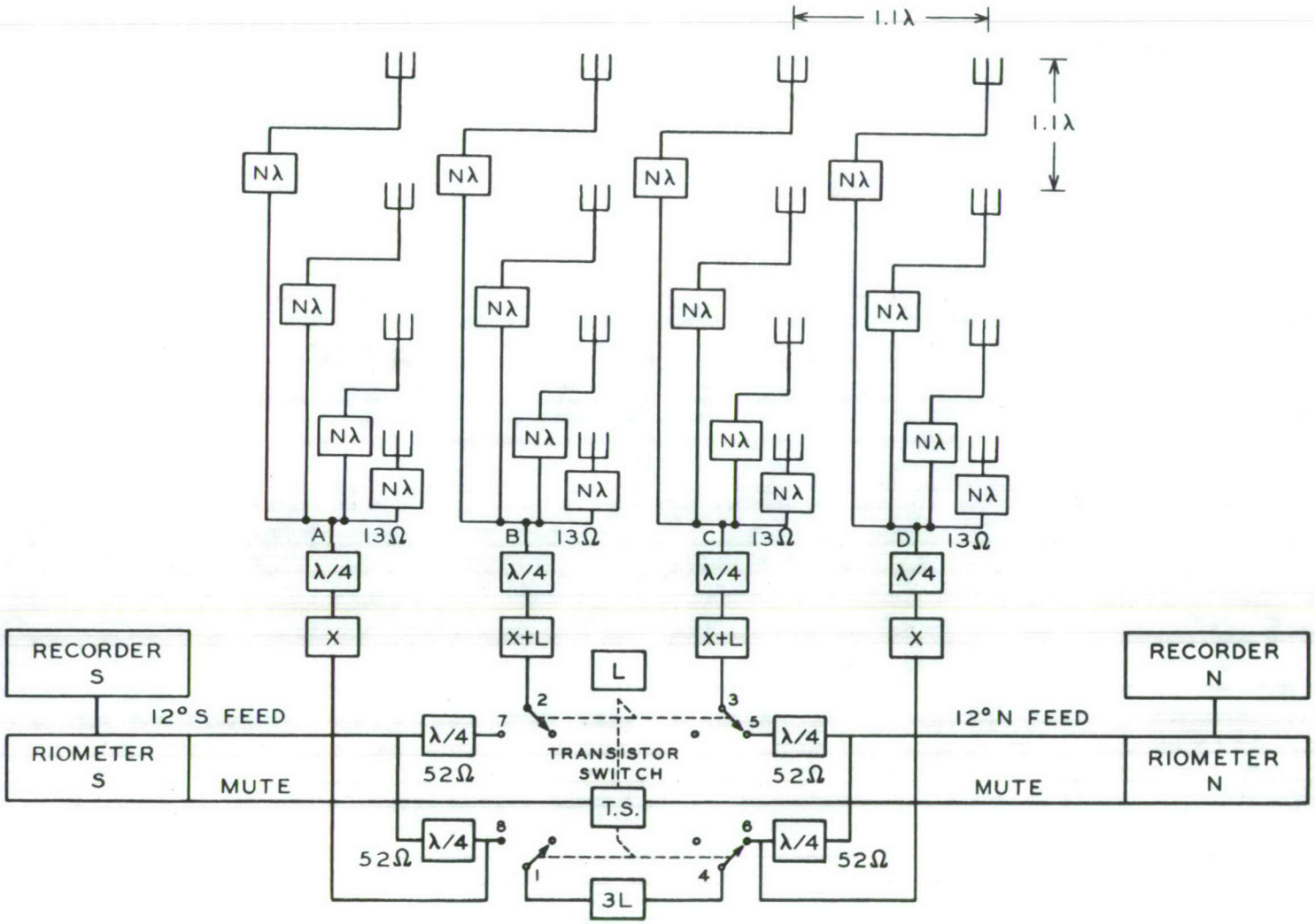

Fig. 11. Fast speed beam switching technique used with the 4 x 4 Yagi array for studying rapidly varying absorption events.

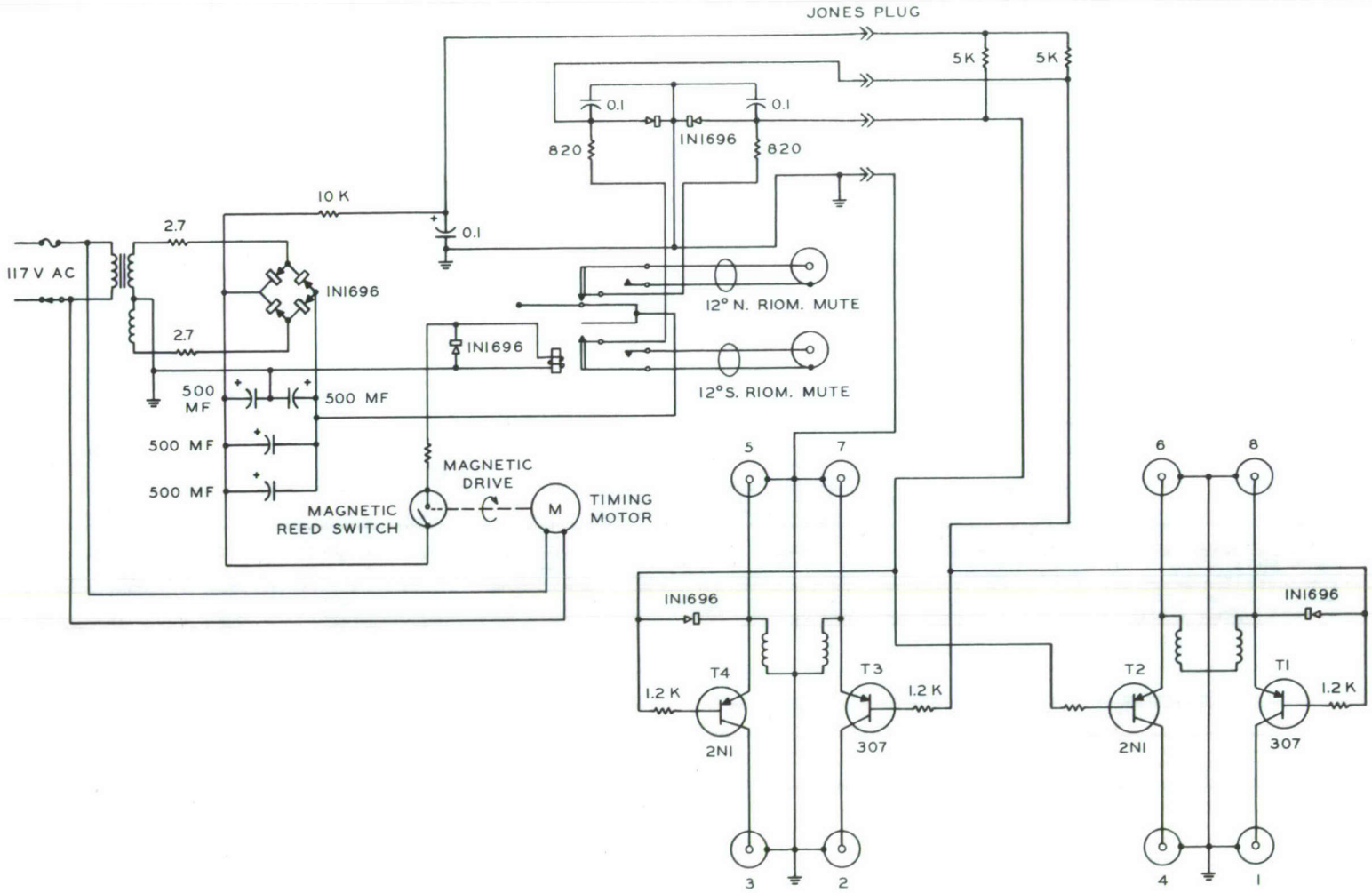

Fig. 12. Fast speed transistor switch used for antenna beam switching. The numbers in Fig. 12 represent connections of the transistor switch with the antenna configuration of Fig. 11.

(a) It switches a negative voltage to the base of transistors 1 and 2 (or 3 and 4) and switches the negative voltage from the base of transistors 3 and 4 (1, and 2). The above operation joins 2 to 7 and 1 to 8 (or 3 to 5 and 4 to 6) and disconnects 3, 5 and 4, 6 (or 7 and 1, 8).

(b) It mutes the south riometer (or the north) and at the same time de-mutes the north riometer (or the south).

The relay is so adjusted that operation (b) is followed by operation (a) by a second or so. This ensures that the riometers do not receive the RF signal from the array in the muted position.

4.8 ANTENNA RADIATION PATTERN

After building an antenna array one is immediately faced with some obvious questions as follows. Is the main beam of the antenna really pointed in the direction it is supposed to be? What are the beam widths and the magnitudes of the side lobes relative to the main beam both in E as well as H planes?

To be able to answer the above questions fully, it is necessary to carry out full scale antenna pattern measurements by flying a transmitter in an aircraft and receiving the signal through the array. Prior to this experiment, it became possible to get a reliable answer to the first question by using the point source Cassiopeia A as a reference. The angular distance of Cassiopeia A from the center of the main beam for both the 12^{o}S and 12^{o}N positions of the antenna was calculated as a function of sidereal time and plotted in Figure 13. In the 12^{o}S

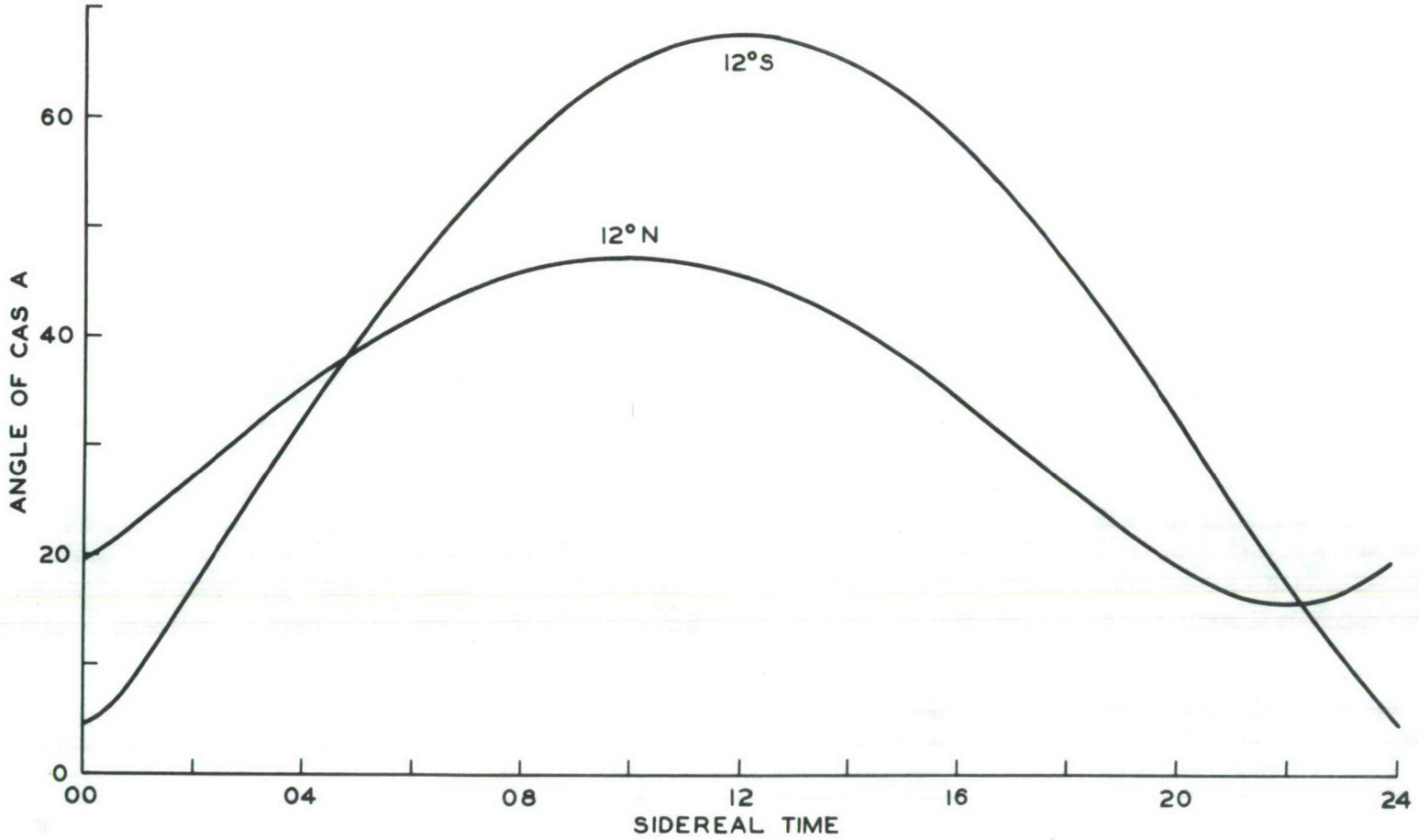

Fig. 13. The angle of Casseiopia A from the expected position of the main beam of the array plotted as a function of sidereal time for each of the two switched positions. Note that at 00 sidereal time Cas A passes through the half power beam of 12^{o}S switched position of the array.

position, it should be noticed that Cassiopeia A passes through the main beam at about 00 hrs sidereal time, and being a point source, must give rise to violent scintillations. It was gratifying to see that scintillations did occur at the above time which proved that the beam in the "12°S" position was indeed pointed in the vicinity of 12°S.

In order to measure the level and the position of the side lobes, a small transmitter was flown at 5000 feet over the array, and the signal was received by a SP600 receiver connected to the array. Another SP600 receiver was connected to a reference dipole erected in the vicinity of the array. The position of the aircraft was determined by two theodolites and was marked on the recorder. The radiation pattern of the array was measured in all the three positions namely 0°, 12°S, 12°N, both in the E and H planes first with uniform feed and next with optimum tapered feed. Ideally, the true radiation pattern of the array can only be obtained when the pattern of the antenna on the aircraft is known. However, the use of a reference dipole accomplishes this requirement. Unfortunately, during the course of the experiment, the receiver connected with the dipole apparently developed some trouble and showed irregular fluctuations on the recorder and receiver connected with the array. These fluctuations were interpreted as fluctuations of the reference dipole receiver gain which necessitated complete rejection of those data.

The experiment revealed that the E-plane of the array was unfavorable for switching the beam as the major side lobe in

that plane is only 4.3 db down from the main beam. To correct this unusually high side lobe level, all the 16 antennas were turned through 90° in order to take advantage of the lower side lobe to main lobe ratio in the H-plane. The radiation pattern, measured in the changed configuration of the array, with switching in the H-plane, showed a definite improvement over the previous arrangement. Thus it should be remembered that data prior to August 3, 1962 pertains to the period during which the switching took place in the E-plane of the array and that after August 3, 1962 the switching took place in the H-plane of the array. In both cases, for the sake of continuity of data, the magnetic meridian was used as the switching plane.

Additional information gained by the experiment concerns the choice between Dolf-Tchebyscheffs' optimum tapered feed and the uniform feed. It was found that by employing an optimum tapered feed, minor lobes could be wiped out, but the major side lobe at 55°, which happened to be the main source of trouble as far as the interpretation of the data is concerned, remained totally unchanged. The insertion of attenuators used in the tapered feed, moreover, caused a definite broadening of the main beam and a considerable decrease in the gain. Based on these results, the decision made was in favor of the uniform feed as the tapered feed was found to do more harm than good.

In order to obtain rough estimates of the power ratios of the main beam to the side lobe, it was necessary to assume a radiation pattern for the antenna mounted on the aircraft. The

level of the side lobes given in Table 5 are based on the assumption that the aircraft antenna radiated isotropically and as such these could be in error by as much as 25% depending on the true radiation pattern. The effect of changing distance of the aircraft from the array has been taken into account in the calculated side lobe strengths given in Table 5. The assumption of isotropic radiation by the aircraft is admittedly a weakness of the experiment. However, it should be borne in mind that the knowledge of the true level of the side lobe is neither necessary nor helpful for the interpretation of riometer data obtained by using the array as the receiving antenna. Even if the measured side lobe levels were to be in error by as much as $\pm$ 2b the interpretation of absorption data would essentially be the same.

The E-plane radiation patterns of the antenna in the 12^{o}S position, with uniform and tapered feeds, are shown in Figure 14. It should be noted that the side lobe structure is highly unsymmetrical; the side lobe in the northerly direction is only 4 db down from the main beam, whereas, in the south it is almost absent. The use of tapered feed eliminates the minor lobes but at the cost of significant broadening of the main beam and considerable reduction in gain, while the power ratio of main beam to major side lobe remains unaffected. Figure 15 shows the H-plane radiation pattern of the same array with uniform and with tapered feeds. As pointed out earlier, the side lobe structure becomes unsymmetrical only in the plane of switching, whereas, in a plane normal to the switching plane it remains unchanged.

Table 5.

Antenna Position	Switching Plane	Plane of Flight	Beam Width	Major Side Lobe Position Angle from Zenith	Power Ratio of Main Beam to Major Side Lobe in db
12°S	E	E	10°	40°	4.3
12°S	E	H	12°	55°	12.1
12°N	H	H	12°	40°	6.0
12°N	H	E	10°	55°	9.5

The characteristics of the narrow beam antenna array used in cosmic noise absorption studies at College, Alaska.

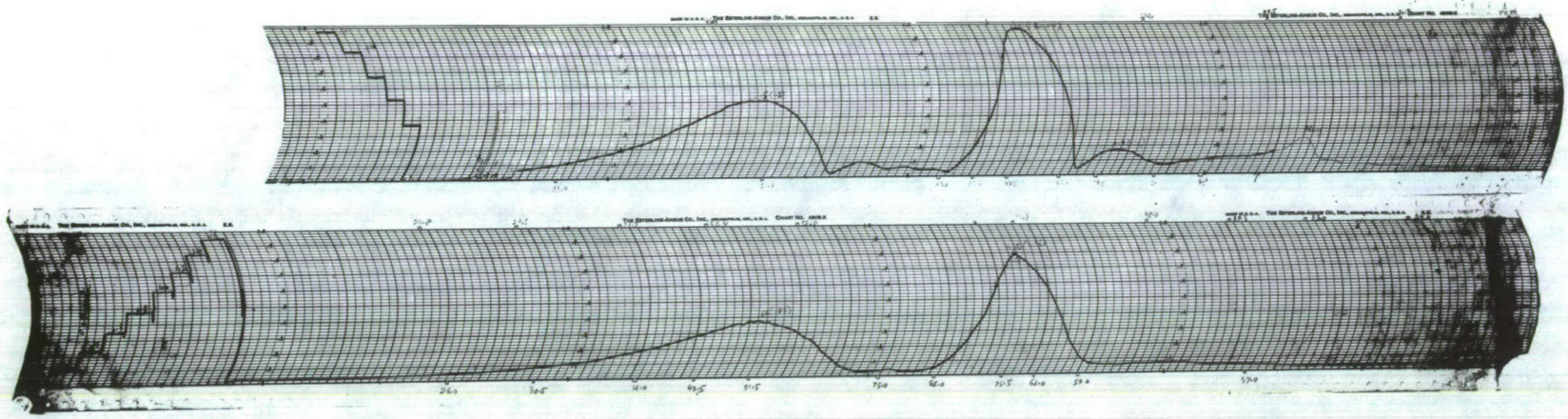

Fig. 14. Measured E-plane radiation pattern of the 4 x 4 Yagi array when the beam is swung by 12° in the E-plane, from the normal position. Top: uniform feed, Bottom: optimum tapered feed. The technique of reducing the currents of the outer elements of the array wipes out minor lobes at the cost of significant broadenning of the main beam, while the level of major side lobe of the array remains unchanged.

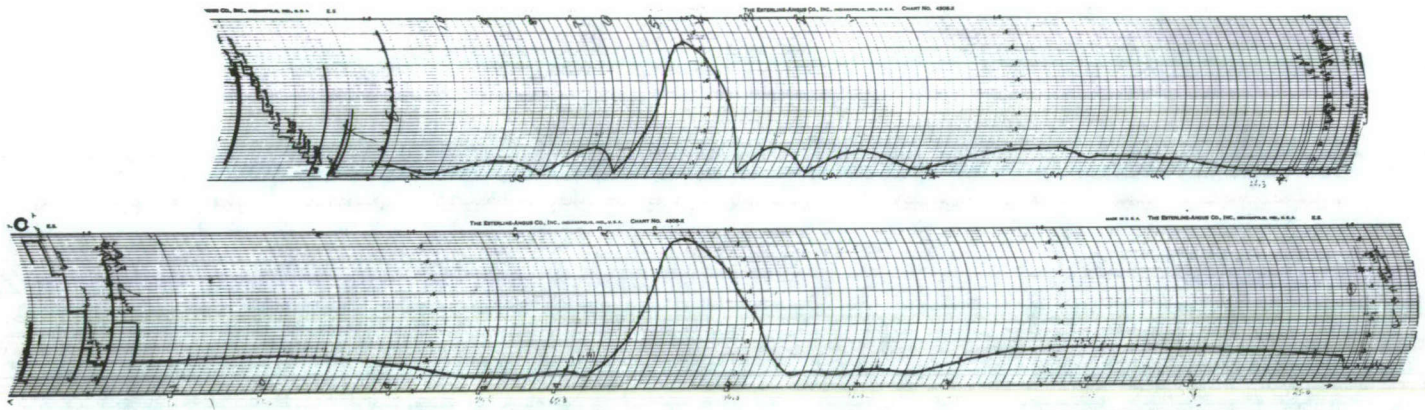

Fig. 15. Measured H-plane radiation pattern of the 4 x 4 Yagi array when the beam is swung in the E-plane. Top: uniform feed, Bottom: optimum tapered feed. The side lobe structure remains symmetrical in the H-plane when the beam is swung in the E-plane and vise versa. The technique of tapered feed wipes out minor lobes at the cost of significant broadenning of the main beam while the major lobes remain unchanged.

Figure 16 gives the radiation pattern of the array in the E and H planes with uniform feed when the antenna elements are aligned east-west instead of north-south and when the switching takes place in the H-plane. Notice the significant reduction in the side lobe to main beam ratio in comparison with the old arrangement of Figure 16.

In spite of the improvement brought about by the above mentioned changes, the level of the 40°N side lobe in the 12°S position of the array and that of the 40°S side lobe in the 12°N position of the array is of sufficient strength to cause interpretational problems at times when strong signals originate from that direction. To avoid this possibility, two oblique antennas were installed, one pointed at 40°N and the other at 40°S. These antennas were alternately switched in and out of a third riometer once every minute. The antennas selected for this purpose were Telrex twin 6 element Yagi T6EY-3 antennas whose half-power beam widths in the E and H planes of 26° and 49° are comparable to the half power beamwidths of the major side lobe of the array. The third riometer and associated antennas not only provide additional information at greater angles from zenith but also serve as a "side lobe monitor" by keeping a record of the absorption taking place in the direction of the side lobes.

4.9 PHOTOMETERS

The green auroral line of atomic oxygen, λ5577A, was monitored throughout the auroral season of 1962-1963, in both the

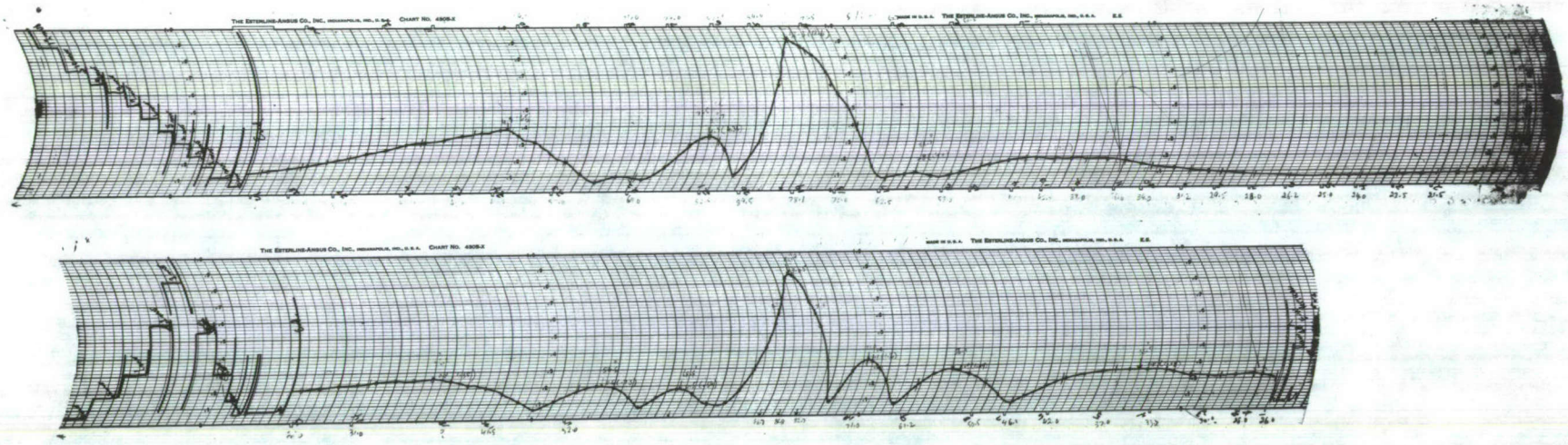

Fig. 16. Measured radiation patterns of the 4 x 4 uniformily fed Yagi array when the antenna beam is swung in the H-plane. Top: H-plane radiation pattern, Bottom: E-plane radiation pattern. Note that by the change of the switching plane a considerable reduction in major side lobe to main beam ratio was obtained in the H-plane as compared to the arrangement of Fig. 13. However, the E-plane radiation pattern is now poorer as compared to that of Fig. 14.

12^{o}S and 12^{o}N directions, by photometers which had a field of view of about 6^{o}. Both photometers used 5819 multiplier photo tubes and exactly similar d.c. amplifiers. The two λ5577A filters used were not exactly identical; the one used in the south had a wider bandwidth than the one in the north.

Shutters installed over both photo tubes automatically closed for a minute once every hour, thereby determining the dark current level. The overall system gains of the two photometers were equalized according to the following procedure. On a clear night when no aurora was present, both photometers were operated for a few minutes on various gain settings of the d.c. amplifier between 1 and 10. Next, the photometers were interchanged and the above procedure was quickly repeated with the previous north photometer now pointing to the south and vice versa. Assuming that light conditions had not changed in the meantime, it was possible to get a relative calibration between the two photometers. It was found that gain settings of 2, 3 on the 12^{o}S system corresponded very nearly to 5, 6 respectively on the 12^{o}N system. It should be remembered that the above statement holds only for clear nights with no aurora. In presence of aurora it was found that the 12^{o}S photometer was more sensitive than the 12^{o}N, even when the former was operated on a gain setting of 2 and the latter at 5.

The top of each photometer was protected from snow by transparent covers made of thin lucite. The snow covers were examined each day in order to make sure that they were free of

snow. Heating elements mounted a few inches from the cover helped eliminate ice formation on the snow covers.

4.10 MEHTOD OF ANALYSIS

Continuous records of 12°S and 12°N absorption were obtained from 31 March 1962. On October 8, 1962 fast speed switching with separate riometers for the north and south positions was started. Simultaneously, 40°N and S "side lobe monitors" were brought into service, and the operation of the 12° north and south photometers started. Daily calibration of all the riometers was carried out at closely spaced noise diode current intervals, throughout the duration of this investigation. Time marks obtained from WWV signals were daily put on all five recorder charts. All recorders were operated at a chart speed of 6"/hour.

In order to calculate absorption at a particular time the following procedure was used. The cosmic noise signal obtained during the quiet period of a month was plotted against sidereal time. From this plot, a so called "quiet day curve" was determined each month which represented the cosmic noise signal under absolutely quiet conditions during that month. In an extremely disturbed month, when there was no sufficiently quiet period, the quiet day curve of the previous month was used. The absorption in decibels is given by the following relation:

$$\text{Abs (db)} = 10 \log \frac{I_Q}{I_D}$$

where I_D = the level of the cosmic noise signal at a given time,

I_Q = the quiet day level of the cosmic noise signal at the same sidereal time.

Most of the absorption events which occurred between 31 March 1962 to March 1963 were analyzed in this manner. Weak events with absorption less than a db were excluded from the analysis.

The relative intensities of the λ5577A line in the 12^{o}S and 12^{o}N directions were scaled from the records for selected nights. For comparison with all-sky camera records, nights with zero cloud cover were selected during the period October 1962 to February 1963 from the records of the U.S. Weather Bureau. The all-sky camera records for these nights were scanned and a second list was made of nights which showed bright aurora during some part of the night. The 12^{o} north and south riometer records for these nights were analyzed in detail and a simultaneous study of absorption, relative auroral intensity, and antenna beam coverage of aurora was made.

For special absorption events, the photometer data was scaled even when the night was cloudy. In particular, since the break-up of aurora was easily recognizable even under cloudy skies or heavy snow-fall, many auroral break-up events which occurred during October 1962 to March 1963 were studied in conjunction with riometer data.

In order to study the variation of the characteristics of the absorbing region in space and time, riometer records for all four positions namely 12^{o}S, 12^{o}N, 40^{o}S and 40^{o}N were studied simultaneously for all major events which occurred during the period of investigation. Figure 17 shows the original riometer records of one such event which was observed on October 10, 1962.

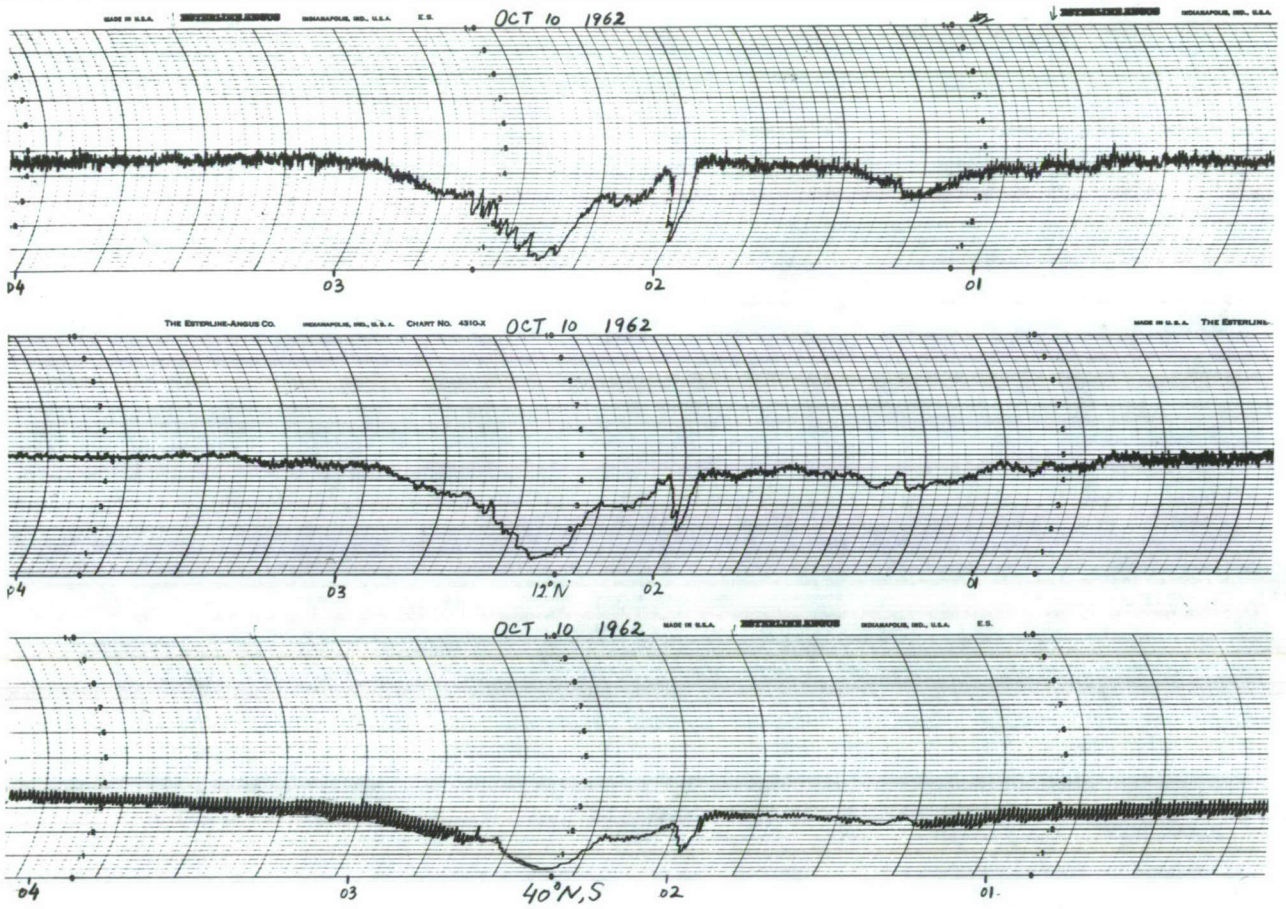

Fig. 17. Sample records of Oct. 10, 1962 showing a typical auroral absorption event recorded on all three riometers. The traces from top to bottom are 12°S, 12°N and 40°N,S.

4.11 PROBABLE ERRORS

The riometers used for 12^{o}N and 40^{o}N,S positions were conventional vacuum tube riometers, whereas, a transistorized commercially built riometer was used for the 12^{o}S position. The respective current ranges of the vacuum tube riometers were 0 to 4 ma and 0 to 5 ma respectively. Daily calibrations enabled the disturbed day cosmic noise signal to be determined with a probable error of $\pm$.1 ma. The current range of the transistorized riometer was 0 to 1 ma and the corresponding probable error was of the order of $\pm$.02 ma or less. The calibration of the transistorized riometer was extremely stable and did not show any noticeable change throughout the period of this investigation. Both vacuum tube riometers and especially the 12^{o}N riometer showed considerable changes in calibration, even within a period of a few days. The data obtained by the 12^{o}N riometer had to be rejected frequently when the signal level showed sudden variations because of changes of calibration. Because of the greater stability and higher reliability the 12^{o}S riometer data were used extensively for detailed study of absorption and visual aurora.

The probable error, expressed in decibels in the calculated values of absorption, depends to a large extent on the probable error in measuring the disturbed day current, I_D, and to a lesser degree on the probable error in the choice of the quiet day current I_Q. Extra care was therefore exercised in scaling records of disturbed period with extremely low I_D. For these periods, it was possible to scale the 12^{o}S riometer records with

a probable error of ± 0.01 ma and the vacuum tube riometer records within a probable error of ± .05 ma.

It is estimated that the probable errors in the calculated values of absorption are given roughly by the values of Table 6.

Table 6.

Absorption db	Probable error db
1-2	± 0.1
2-3	± 0.2
3-4	± 0.3
4-5	± 0.4
5-6	± 0.5
6-7	± 0.7
7-8	± 0.9
8-9	± 1.0
9-10	± 1.3

The probable error in time is of the order of ± 1/2 minute.

4.12 THE TECHNIQUE OF RESOLVING THE AMBIGUITY INTRODUCED BY THE SIDE LOBES OF THE ANTENNA ARRAY.

The results of the antenna radiation pattern measurements given in Table 5 indicate that the major side lobe of the array is only 6 db down from the main beam even after the improvement brought about by the change in the switching plane. The 6 db side lobe level obtained in practice is indeed far from the 20 db level required by theory for unambiguous analysis. One obvious problem that confronts the investigator at this stage is the interpretation of the data.

A major step towards correct interpretation was the installation of "side lobe monitors" as mentioned in section 4.8. In this section, the technique of resolving the ambiguity introduced in the absorption measurements as a result of contamination from the side lobes of the antenna array, is discussed in detail. In particular, if the relative contributions of the major side lobe and the main beam to the total cosmic noise signal are known, it will be shown by simple calculations presented below that the true absorption can be accurately estimated.

Let the total undisturbed cosmic noise signal as measured by the antenna array in one of its switched positions be 1 ma. Suppose X ma is the contribution to the signal level made by the major side lobe

Further let A = The apparent absorption in decibels measured by a riometer connected to the array

A' = The absorption in db in the direction of the major side lobe as measured by the "side lobe monitor",

A_t = The true absorption measured by a riometer connected to an ideal antenna having the same beam-width as the array in use but no major side lobe.

The true absorption A_t may be calculated in terms of A, A' and X from the following relation:

$$X\ 10^{-A'/10} + (1 - X)\ 10^{-A_t/10} = 10^{-A/10} ,$$

which gives $A_t = 10 \log_{10} \left(\frac{1 - X}{10^{-A/10} - X\ 10^{-A'/10}} \right)$.

The two extreme cases are:

1. $X = 0$ which gives $A_t = A$,
2. $X = 1$ which gives $A_t = 0$.

The above analysis shows that the true absorption as measured by an ideal array would lie somewhere between 0 and A depending on the magnitude of X, i.e. on the fractional contribution to the cosmic signal level by the major side lobe of the array. In practice, X is a function of sidereal time and its value can only be determined unambiguously at a given sidereal time when the ratio of the average brightness temperature in the direction of the major side lobe, and that in the direction of the main beam of the array, is known accurately. At high latitudes, as at College, the ratio of the average brightness temperatures in the two directions cannot always be obtained with sufficient accuracy on account of the paucity of brightness-temperature contours. Moreover, the above method is too cumbersome to be used when a large volume of data is to be analyzed.

While investigating the patchiness of auroral absorption, one is sometimes more interested in knowing the difference in radio-wave absorption between two adjacent areas of the sky rather than the true values of absorption themselves. It will be shown here, by a few examples, that for certain cases the apparent difference in absorption between 12^{o}N and 12^{o}S directions is a lower limit of the true difference. In such cases the true difference in absorptions is always greater than, or at the most equal. to the apparent difference.

In Figure 18 the absorption observed on November 15, 1962 in the 12^{o}N and S and the 40^{o}N and S positions are plotted. At

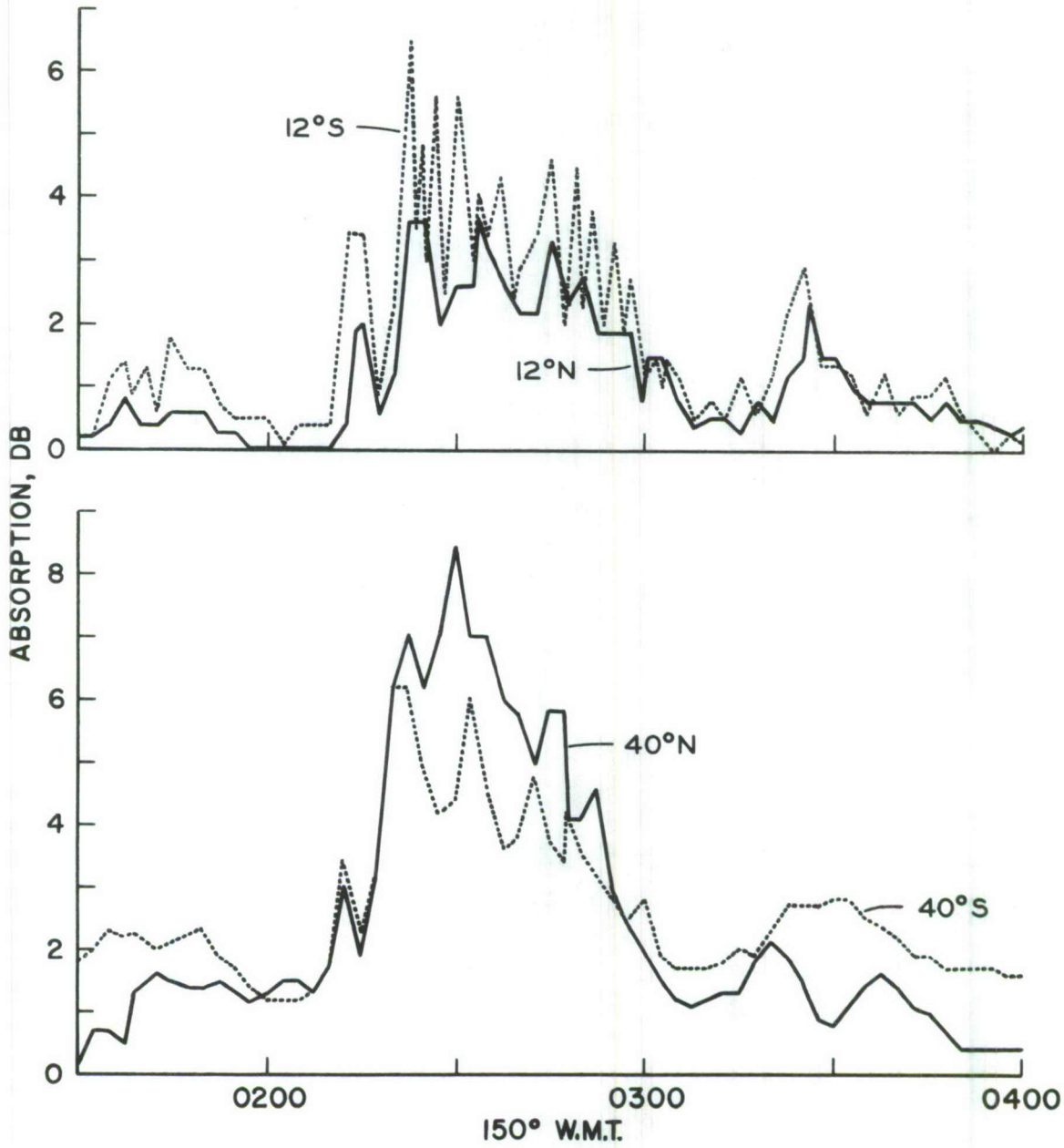

Fig. 18. The absorption event of Nov. 15, 1962 showing genuine differences in absorption between 12^{o}N and 12^{o}S, because of relatively small side lobe contamination.

0135 hrs the absorptions observed in various directions were as follows:

$A_{40^\circ N} = 0.7$ db
$A_{40^\circ S} = 2.3$ db
$A_{12^\circ N} = 0.4$ db
$A_{12^\circ S} = 1.1$ db

As there was only 0.7 db absorption in the direction of the major side lobe in the 12° south position of the array, one concludes that the observed absorption of 1.1 db must be very close to the true absorption in the 12° south direction. On the other hand, the observed absorption of 0.4 db in 12° North could be higher than the true absorption in that direction on account of the fact that at that time the major side lobe in that position of the array was showing the relatively high absorption of 2.3 db Combining the two results, one finds that the true difference in absorptions between the 12°N and 12°S directions at that time must be at least equal to the observed difference of 0.7 db.

The above reasoning may always be applied whenever,

Case I, $A_{40^\circ N} \gg A_{40^\circ S}$ with $A_{12^\circ N} > A_{12^\circ S}$

or when $A_{40^\circ S} \gg A_{40^\circ N}$ with $A_{12^\circ S} > A_{12^\circ N}$,

Case II, $A_{40^\circ N} \approx A_{40^\circ S}$.

Consider the observed absorptions at 0211 hrs which were:

$A_{40^\circ N} = 2.3$ db
$A_{40^\circ S} = 2.3$ db
$A_{12^\circ S} = 1.8$ db
$A_{12^\circ N} = 0.2$ db

As the absorptions in the direction of the major side lobes were equal it is reasonable to assume that A_{12^oS} and A_{12^oN} were equally contaminated as a result of their contribution. If so, the observed difference of 1.6 db between 12^oS and 12^oN should represent the true difference.

Case III, The Trend of the Absorption Graph.

In some cases, if the trend of the absorption graph is studied carefully, it is possible to remove the ambiguity caused by the side lobe contribution.

For example, consider the trend of the absorption graph between 0320 - 0325 hrs on November 15, 1962 (Figure 18).

During this period, A_{40^oN} shows a pronounced decline from 2.1 to 1.5 db, while A_{40^oS} shows a slow rise from 2.3 to 2.7 db. During the same period, both A_{12^oS} and A_{12^oN} showed relatively fast rises from 1.2 to 2.9 db and from 0.5 to 1.5 db respectively. The fact that A_{12^oS} was increasing rapidly while A_{40^oN} was showing a pronounced decrease, rules out the possibility of contamination of the former by the latter. Therefore one concludes that the increase observed in A_{12^oS} between 0302 - 0325 hrs must be a genuine increase in 12^oS direction.

4.12.1 Ambiguous Cases

In general, cases to which none of the above criterions are applicable, must be classified as ambiguous.

The absorption event of October 14, 1962, plotted in Figure 19, is a clear example of such ambiguous cases.

Between 0930-1220 hrs, absorption measured by the 40^oN riometer was greater than that measured by the 40^oS riometer.

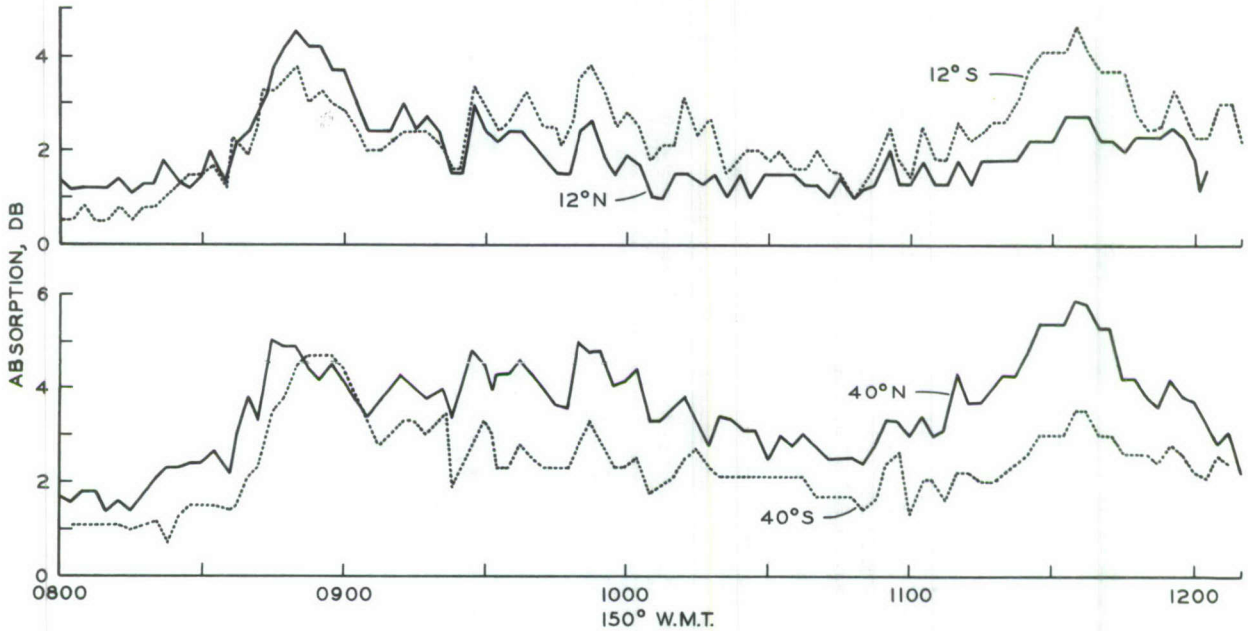

Fig. 19. The absorption event of Oct. 14, 1962 showing fictitious differences in absorption between 12°N and 12°S caused by strong side lobe contamination.

During the same period, the absorption measured by the 12°S riometer was higher than that measured by the 12°N riometer. A possible explanation of the peculiar absorption pattern is, that during the above period a major contribution to the total cosmic noise signal in the 12°S position of the array came from the side lobe situated at 40°N. If so, the absorption measured by the 12°S riometer does not represent the true absorption, and therefore the observed difference between the 12°N and 12°S riometers also does not represent the true difference.

By the same token, if at some time the absorptions observed by the 12°N and 12°S riometers are found to be equal while large differences exist between absorptions observed by the 40°N and 40°S riometers, it does not necessarily follow that the true absorptions in the former directions are equal. In order to illustrate the above point, absorption observed at 0925 hrs on October 14, 1962 (Figure 19) will be considered. The magnitudes of the observed absorption were:

$A_{12^\circ S} = 1.6$ db

$A_{12^\circ N} = 1.5$ db

$A_{40^\circ N} = 4.0$ db

$A_{40^\circ S} = 2.2$ db

It is likely that the apparent absorption of 1.6 db observed by the 12°S riometer was higher than the true absorption on account of the fact that a relatively high absorption of 4.0 db was taking place in the direction of the major side lobe of the antenna array. Thus, the true 12°S absorption in the

above case, may have been anywhere between 0 and 1.6 db depending on the magnitude of the side lobe contribution.

4.12.2 Summary

Cases in which a reasonable estimate of the true difference in absorption between $12^{o}N$ and $12^{o}S$ can be obtained are:

1. $A_{40^{o}N} \gg A_{40^{o}S}$ with $A_{12^{o}N} > A_{12^{o}S}$

2. $A_{40^{o}S} \gg A_{40^{o}N}$ with $A_{12^{o}S} > A_{12^{o}N}$

In these cases, the true difference in absorption between the $12^{o}N$ and $12^{o}S$ directions is greater than or equal to the observed difference.

3. $A_{40^{o}S} \approx A_{40^{o}N} \approx 0$

In cases when both the $40^{o}N$ and S riometers show negligible absorption while relatively high absorption is observed by the $12^{o}N$ or $12^{o}S$ riometer, the observed differences between the latter represent the true differences.

4. $A_{40^{o}N} \approx A_{40^{o}S} > 0$

For cases in which the $40^{o}N$ and S riometers record equal absorption of 2-3 db, it is reasonable to assume that both main beams of the array are equally contaminated by the presence of the side lobes. In such cases, the observed difference between $A_{12^{o}N}$ and $A_{12^{o}S}$ should represent the actual difference.

Cases in which it is not possible to get a reliable estimate of the difference in absorption between $12^{o}N$ and $12^{o}S$ riometers are:

1. $A_{40^\circ N} > A_{40^\circ S}$ with $A_{12^\circ N} < A_{12^\circ S}$

2. $A_{40^\circ S} > A_{40^\circ N}$ with $A_{12^\circ S} < A_{12^\circ N}$

The graphs presented in Chapter V and VI indicate that a large percentage of cases fall under the ambiguous category. This condition explains why a statistical analysis of the differences in absorption between $12^\circ N$ and $12^\circ S$ was not attempted.

CHAPTER V.

RADIO-WAVE ABSORPTION AND VISUAL AURORA

5.1 INTRODUCTION

The experiment described in the previous chapter was performed primarily with a view to getting answers to the following basic questions.

(a) It is generally believed that the auroral ionization is patchy. If so is it possible at times to detect significant differences in absorption between two adjacent areas of the sky?

(b) When these differences are observed during darkness, is it possible to explain them in terms of differences of auroral luminosity "viewed" by the two antenna beams? In general, is it true that the absorption is more widespread than the auroral luminosity? If so, is it possible to isolate the background component of the absorption?

(c) If a close association is found between auroral displays and radio-wave absorption in general, is it possible to identify the absorption associated with each of the various phases of the display?

If the above identification could be made with reasonable certainty, it would seem to follow that gross features of auroral displays may be deduced by riometers connected to narrow beam antennas pointed at different parts of the sky.

(d) Is there a significant change in the ratio of absorption to auroral luminosity from one phase of the display to another? Significant changes in the above ratio if consistently observed would indicate a change in the primary electron energy spectrum.

In an attempt to answer some of the questions raised above, a detailed study of radio-wave absorption in four different directions from College was made for selected events in conjunction with λ5577A intensity variations and all-sky photographs. In the selection of events for detailed study, more emphasis was laid on typical absorption events in order to bring out the normal features, if any, of aurorally associated absorption. Some of the events that showed unusual features have also been included in the analysis in order to point out the departures from a normal pattern.

In order to give a rough idea of the comparative areas of the sky to which the absorption measurements discussed in this chapter refer, the areas intercepted by the half power cones of 12^{o}S,N and 40^{o}S,N antennas in the magnetic meridian are shown in Figure 20.

It should be remembered that at right angles to the magnetic meridian, the half power beamwidths of 40^{o}N,S antennas are significantly broader and those of 12^{o}N,S antennas slightly narrower than the beamwidths shown in Figure 20.

5.2 IDENTIFICATION OF VARIOUS FEATURES OF A TYPICAL AURORALLY ASSOCIATED ABSORPTION EVENT.

Referring to the sample records given in Figure 17, it may be seen that in a typical nighttime event, observed at College, Alaska, four distinct phases are recognizable which are described below.

Phase 1: In this phase of the event, absorption slowly varies with time and the peak absorption seldom exceeds 1-2 db at

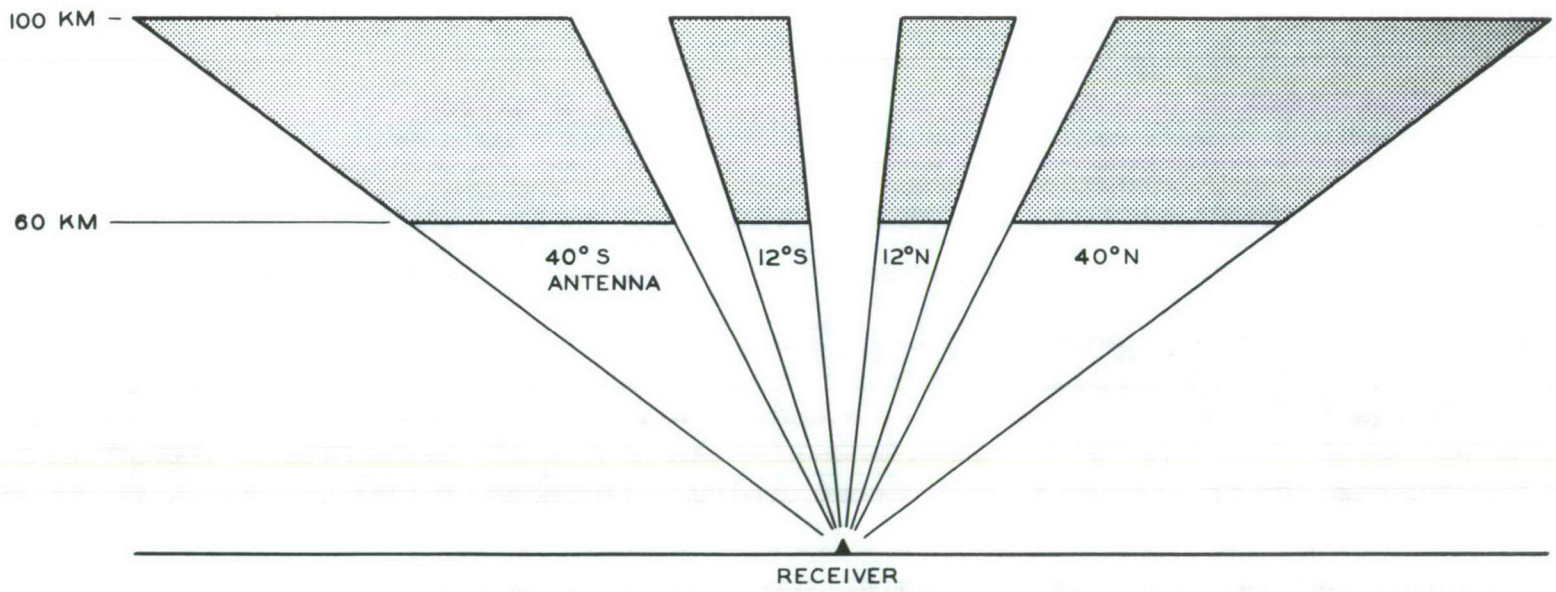

Fig. 20. Half power beamwidths in the magnetic meridian of 12° North, and 12° South switched positions of the 4 x 4 Yagi array and of 40° North and 40° South "side lobe monitors".

36 Mc/s. Referring to the absorption event of October 10, 1962 shown in Figure 17, phase 1 lasted from 0100-0130 hrs. Later in this chapter it will be shown that phase 1 is associated with the quiet or pre-break-up phase of an auroral display. Hence, the absorption encountered in phase 1 may also be called pre-break-up absorption.

Phase 2: Phase 2, the shortest of all phases, lasts for a few minutes and is the easiest of all to identify on account of its sharp onset. The rate of absorption increase is usually of the order of 2-4 db/min. Phase 2 lasted from 0157.5-0200 hrs in the event of October 10, 1962. Later in this chapter, it will be shown that phase 2 is invariably associated with the break-up phase of the auroral display. Throughout the present investigation, the self explanatory term of sudden absorption increase or SAI has been used for the absorption observed in phase 2 of an event.

Phase 3: The third phase of the absorption event includes a sharp recovery from the SAI followed by irregular decreases and increases in absorption. Phase 3 is associated with the post break-up phase of the auroral display.

In Figure 17, phase 3 started from 0200 hrs but its later portions were masked by the onset of the fourth phase. Other examples will be given later in this chapter which will establish the existence of the third phase.

Phase 4: The fourth phase of the absorption event is characterized by a relatively slow rate of absorption increase of the order 0.5-1 db/min which persists for a long period of time.

The recovery also is very slow and gradual. During this phase, extremely high absorption is observed which varies relatively slowly with time. The fourth phase lasted between 0215-0300 hrs in the event of October 10, 1962.

The fourth phase of an absorption event appears to be quite distinct from other phases in the following respects.

(1) Although the other phases are observed at any time between 2000-0200 hrs during the night, the occurrence of the fourth phase is invariably limited to post-midnight hours.

(2) The ratio of absorption to auroral luminosity is much higher than that found in the earlier phases.

(3) The absorption and auroral intensity fluctuations are not very well correlated.

The example of the auroral event of October 10, 1962 was primarily selected for the simple reason that all four phases of the event occurred in a relatively short period of time and were easily recognizable. However, it should not be inferred that all aurorally associated absorption events necessarily follow the pattern observed on October 10, 1962. For instance, during quiet nights when inactive auroral arcs are present, only the first phase may be observed but no second, third or fourth phases. It will be shown later that what appears to be the fourth phase may be an independent event as its occurrence does not depend on the occurrence of the earlier phases.

For the purpose of identification,the absorption in the fourth phase will be referred to as SVIA or "slowly varying intense absorption" throughout this investigation.

5.3 INVESTIGATION OF THE RELATION BETWEEN AURORAL LUMINOSITY AND ABSORPTION DURING VARIOUS PHASES OF AN ABSORPTION EVENT.

The previous section was devoted to the classification of the various phases of an absorption event, the classification being based primarily on the differing characteristics exhibited by the event at different times. In this section these phases of the absorption events are compared with the fluctuations of auroral luminosity as measured by photometers. Figure 21 shows the original records for 12^{o}N,S riometers and photometers obtained on October 16, 1962. All phases of the absorption event are easily identifiable, especially, the slowly varying intense absorption phase (SVIA) which lasted for a long time during this event. Note that the SAI (sudden absorption increase) observed by both riometers happened exactly at the time of sudden brightenning of aurora or break-up which drove both photometers off scale. The photometers remained off scale most of the time in the third or the post-break-up phase of the event. However, as soon as the SVIA started and the absorption started to increase, both photometers showed pronounced recoveries. A tremendous increase in the ratio of absorption to auroral luminosity is especially striking at the peak of SVIA. The fluctuations in absorption on both the north and south riometers appear to be entirely uncorrelated with the auroral intensity fluctuations observed by the respective photometers, in the SVIA phase.

The original 12^{o}S riometer and photometer records for December 18, 1962, shown in Figure 22, provide a remarkably

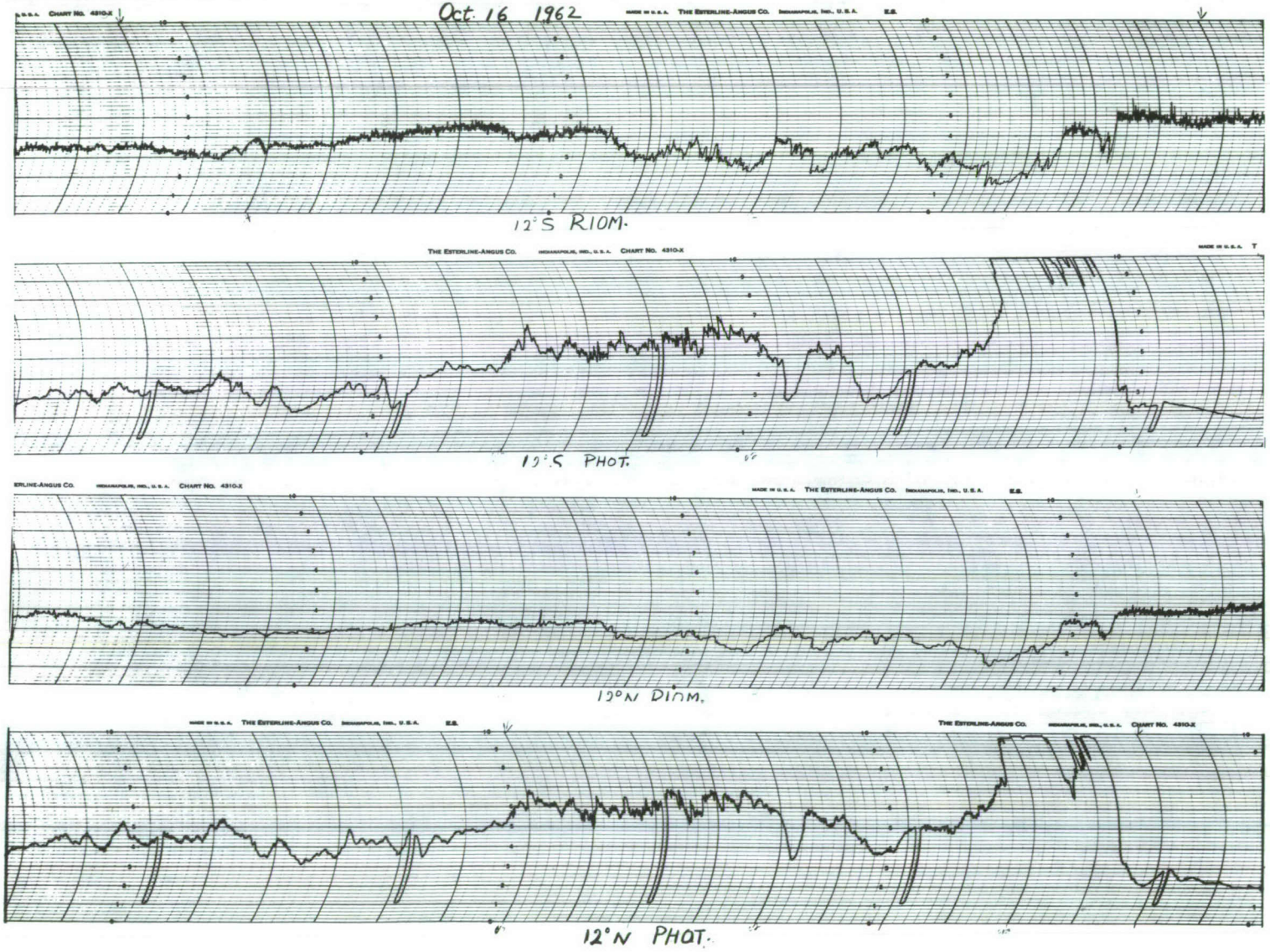

Fig. 21. Simultaneous records of 12° North, 12° South riometers and photometers obtained during the auroral event of Oct. 16, 1962. The traces from top to bottom are; 12°S riometer, 12°S photometer, 12°N riometer and 12°N photometer.

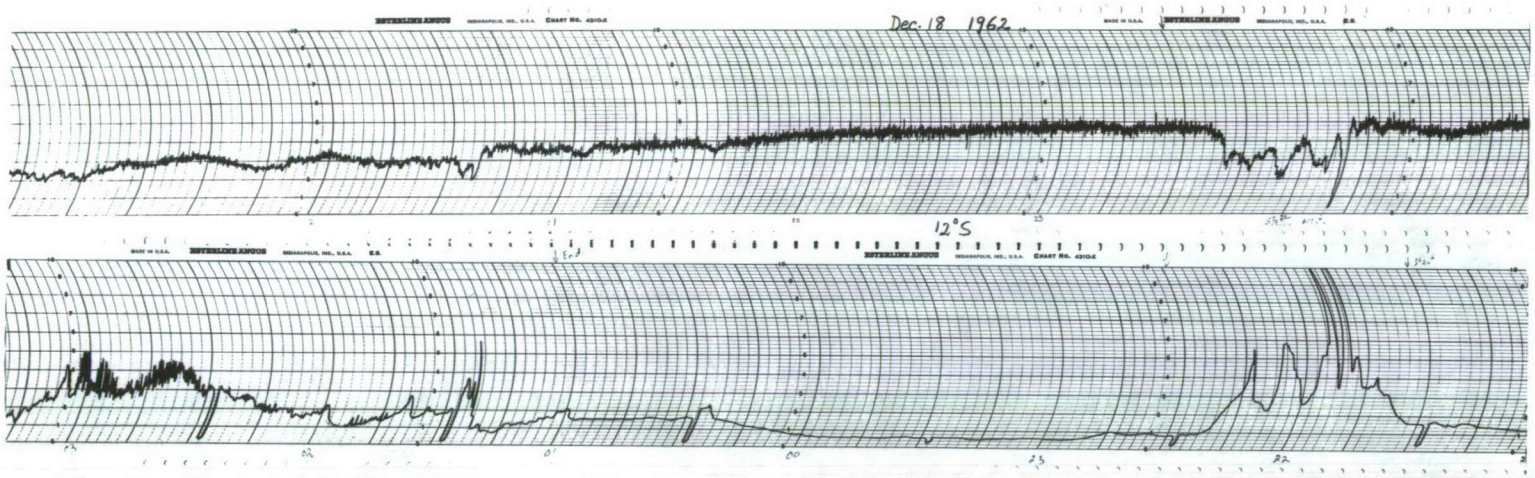

Fig. 22. Simultaneous records of 12°S riometer and 12°S photometer obtained during the short but intense auroral event of Dec. 18, 1962 showing almost one to one correspondence between absorption and auroral luminosity. Note that the pulsating auroral luminosity recorded towards the end is not associated with any significant increase in absorption. This is contrary to the generally held belief that pulsating aurora is associated with strong absorption.

clear example of an almost one-to-one correspondence between absorption and auroral intensity peaks. It should be noted that the above event was observed in pre-midnight hours and therefore, according to the statement made in section 5.2, contained the first three phases of absorption only. The fourth phase or what will be referred to as the slowly varying intense absorption phase was not observed during this night. The two insignificant peaks on the riometer trace between 2140-2148 hrs constitute the first phase of the event or the pre-break-up phase. The break-up phase or SAI was the most spectacular phase of this event and lasted for only a minute or so. The rate of absorption increase was more than 10 db/min during the SAI. The third phase or the post-break-up phase lasted from 2150 to about 2225 hrs and was characterized by irregular changes of absorption which are well correlated with auroral luminosity fluctuations.

The preliminary conclusions from Figures 21 and 22 are as follows:

(1) In the early phases of an aurorally associated absorption event i.e. in the pre-break-up, break-up and post-break-up phases, the absorption and auroral luminosity fluctuations are very well correlated.

(2) The slowly varying intense absorption phase is not a regular feature of an absorption event as it is sometimes present and sometimes not. When it is present it invariably occurs during the post midnight hours. The absorption and auroral luminosity fluctuations in this phase appear to be

entirely uncorrelated, and the ratio of absorption to auroral luminosity is considerably higher than that during the SAI.

5.3.1 The Event of October 10, 1962

The absorption and the relative intensity of λ5577A, both observed in the 12°S direction, during the auroral event of October 10, 1962 are shown in Figure 23.

The 12°S riometer recorded a maximum absorption of 0.6 db during the interval 0145-0155 hrs. During the time interval 0157.5-0200 hrs, a sudden increase in absorption (SAI) from 0.4 to 10 db was observed. The rate of increase of absorption was approximately 4 db/min. A considerable increase in the intensity of the green auroral line took place suddenly in the above period as shown by Figure 23.

In the post break-up phase, between 0200-0202.5 hrs, the absorption decreased from 10 to 0.8 db and the auroral intensity also exhibited a sharp decline.

The slowly varying intense absorption phase appeared to have started at 0215 hrs and to have reached its peak at 0222.5 hrs. The auroral intensity showed a minor peak during the above period. Referring to Figure 23, the ratio of absorption to auroral intensity appears to be significantly higher in the latter part of the event (SVIA) than in the former (SAI). The plot of 12°S absorption shows several irregular fluctuations in the latter part of the event which were not accompanied by fluctuations of the auroral intensity. Once again the above observation lends support to the view that absorption and

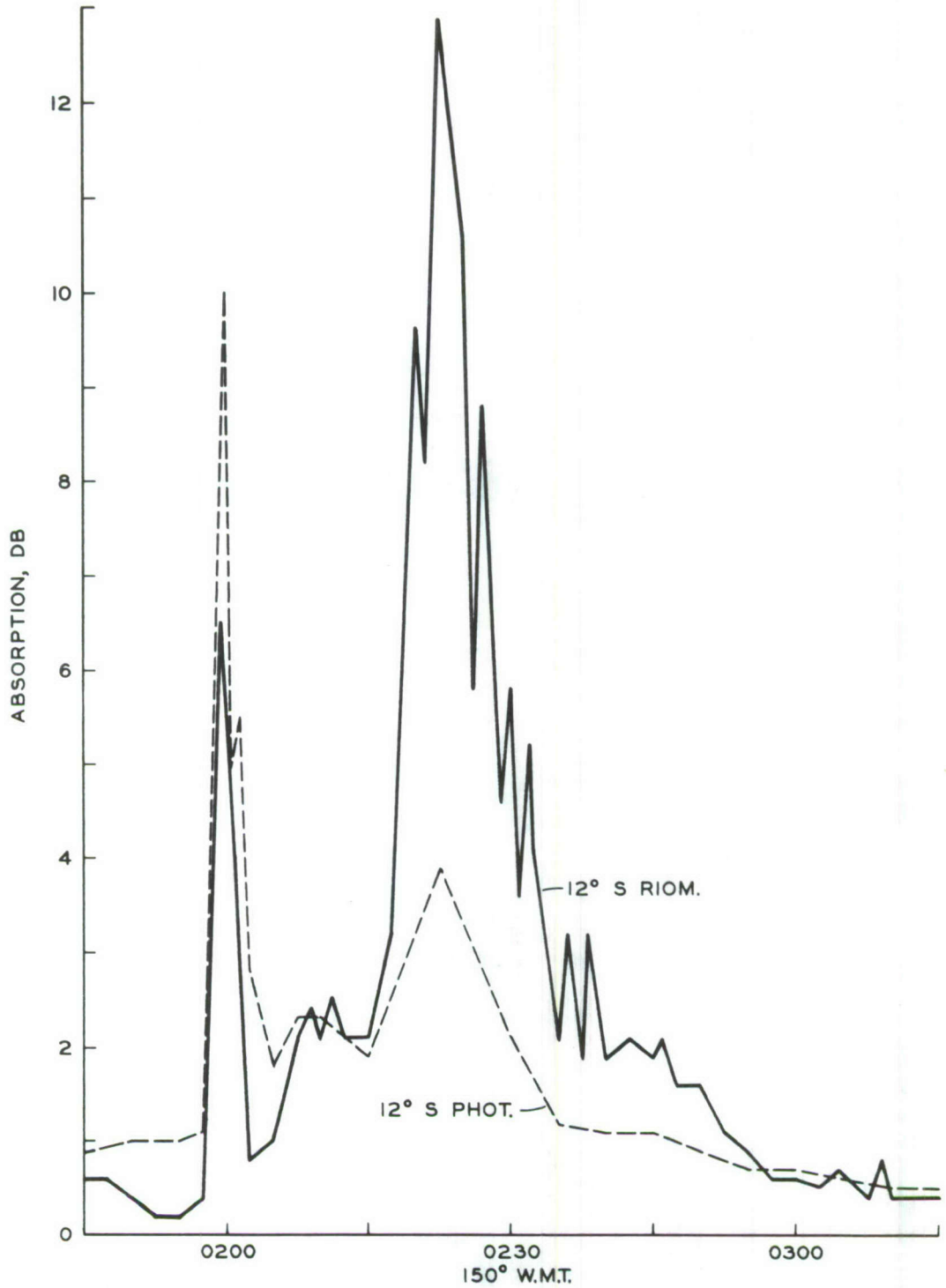

Fig. 23. Variation of absorption measured by 12°S riometer and the relative λ 5577Å intensity observed by 12°S photometer during the auroral event of Oct. 10, 1962.

auroral luminosity fluctuations are poorly correlated in the SVIA phase.

The wide spread character of the event of October 10, 1962 is portrayed in Figure 24 which gives a plot of absorption in 12°N,S and 40°N,S directions. It should be noticed that although the general shape of the absorption graph is the same for all four directions, the absorption in the 12°S direction showed irregular fluctuations between 0215-0240 hrs which were not observed in any other direction. The fact that these fluctuations did not appear in the 40°N direction, rules out the possibility of their being caused by a contamination from the major side lobe of the antenna array. Therefore, one must conclude that the differences in absorption observed between 12°N and 12°S during the above interval represent real differences confirming the patchiness of auroral absorption. The College magnetogram for October 10, 1962, given in Figure 25, shows large negative bays in the H-trace at the same time that intense absorption was recorded by the riometers.

5.3.2 The Event of October 16, 1962

The cosmic radio-wave absorption measured by 12°N,S and 40°N,S riometers on October 16, 1962 is plotted against local time in Figure 26. The sudden absorption increase at 0041 hrs coincided with the sudden brightenning of aurora as seen by the photometers (see Figure 21). At the above time the absorptions in 40°N and 40°S directions were close to 1.0 db whereas those in the 12°S and the 12°N directions were 2.5 and 1.7 db respectively. The above observation suggests that the

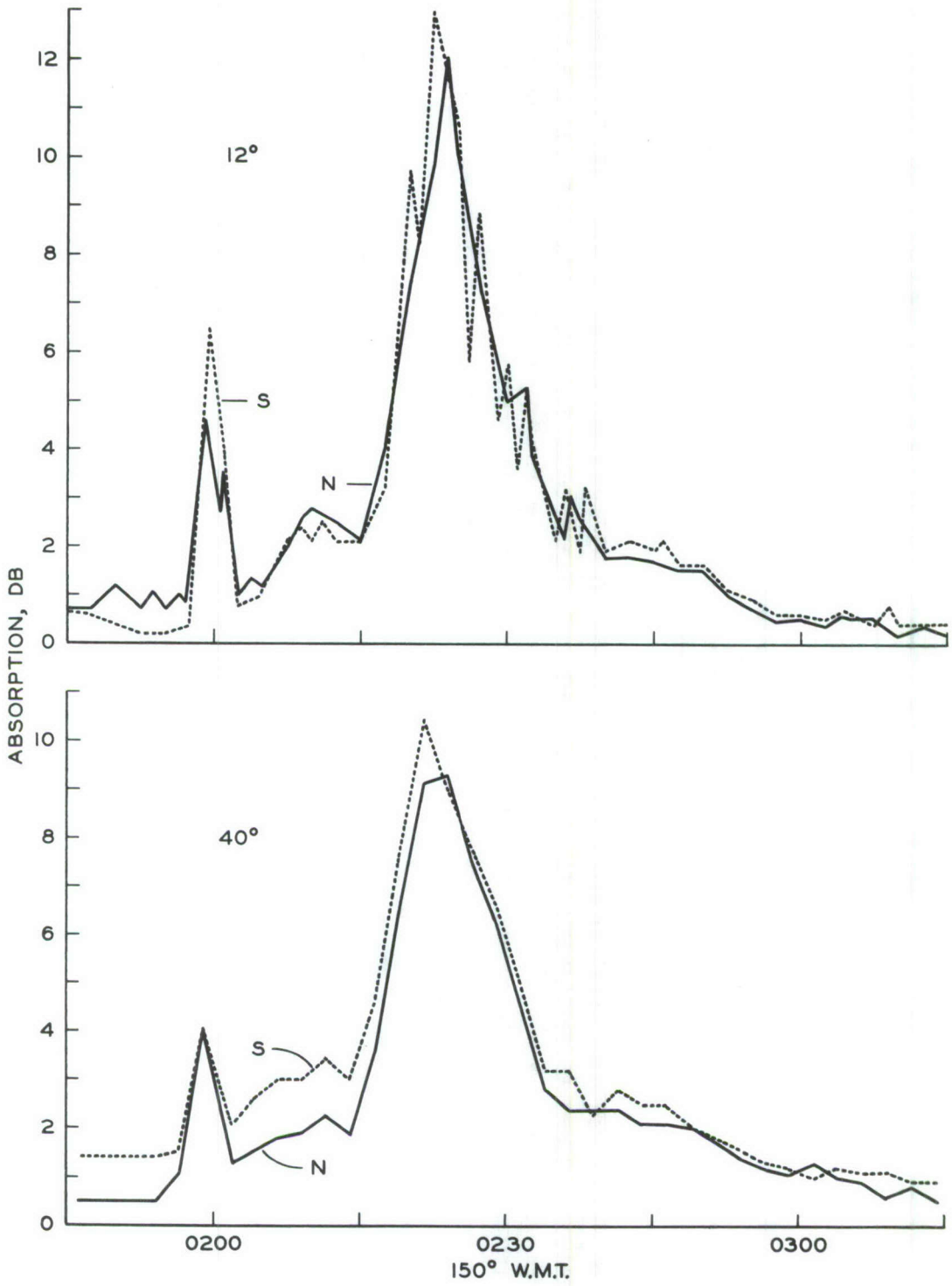

Fig. 24. Variations in absorption of radio-waves originating from different parts of the sky as measured by 40°N,S and 12°N,S riometers on Oct. 10, 1962 showing the wide spread character of the absorption event.

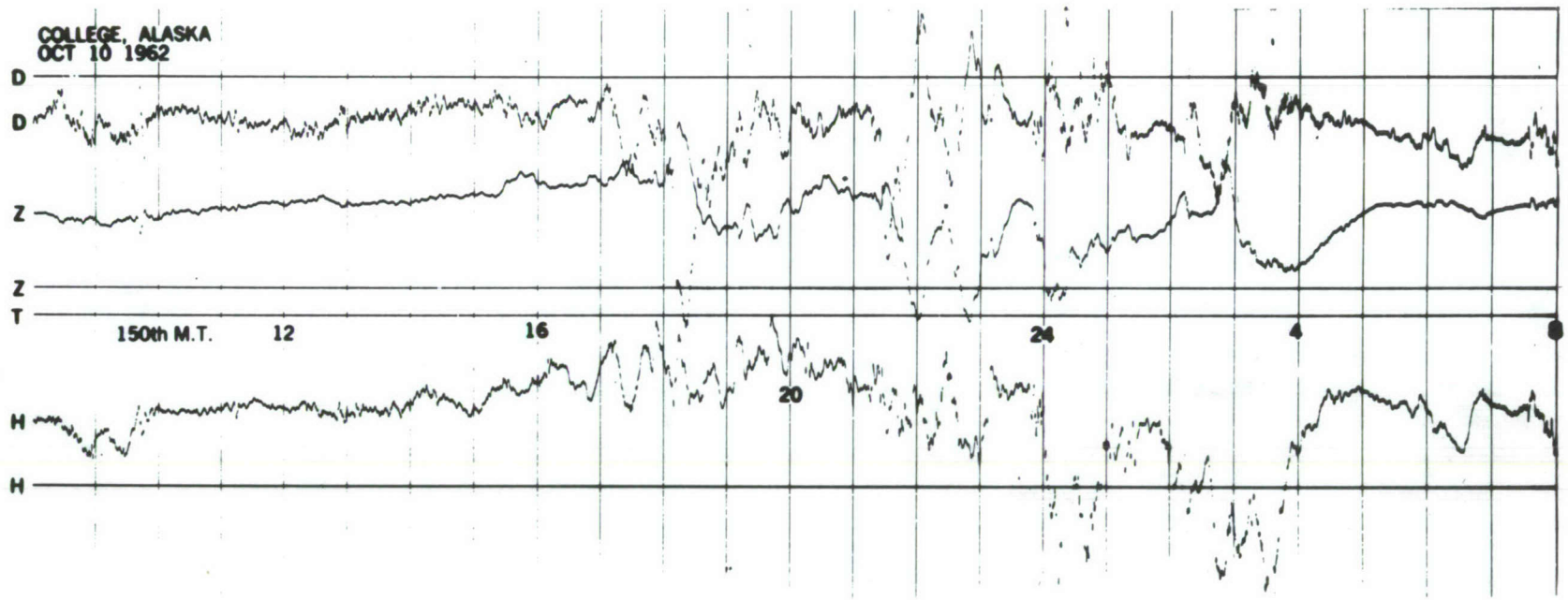

Fig. 25. College magnetogram of Oct. 10, 1962 showing large negative bays in the H-trace coincident with the time of occurrence of the absorption event.

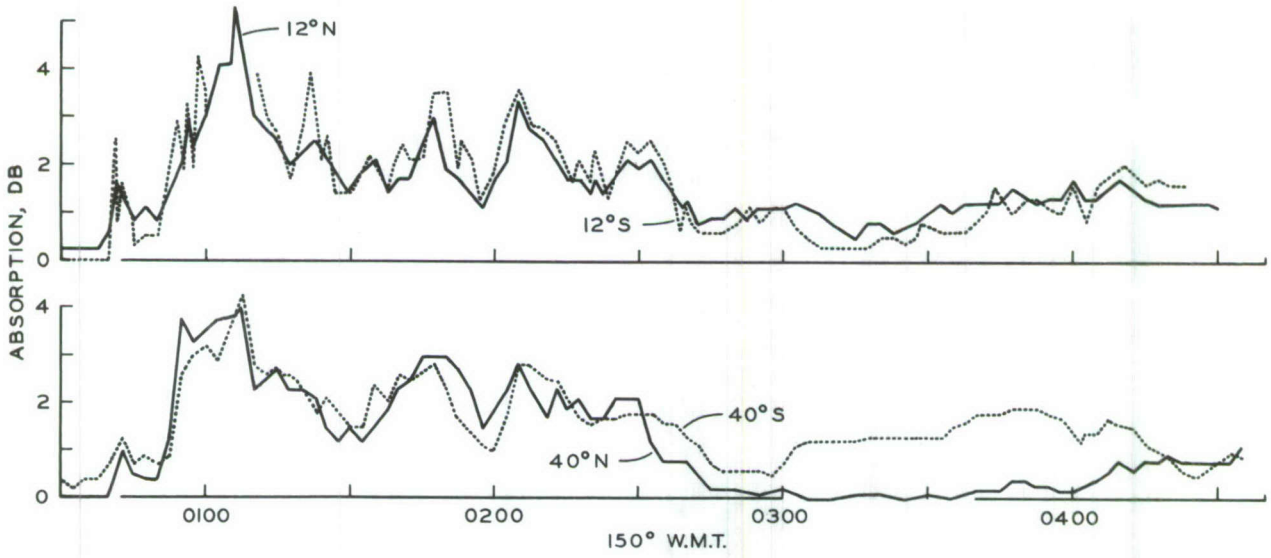

Fig. 26. Variations in absorption of radio-waves originating from different parts of the sky as measured by 40^{o}N,S 12^{o}N and 12^{o}S riometers on Oct. 16, 1962 showing a non-uniform SAI (sudden absorption increase) followed by dissimilar changes in absorption in different directions.

observed difference of 0.8 db in absorptions between 12°N and 12°S directions, represents the actual difference at that time. Between 0050-0100 hrs, the absorption in the 12°S direction showed large fluctuations that were not accompanied by similar fluctuations in 12°N and 40°N directions. Therefore, the differences in absorption between 12°N and 12°S observed during the above period are interpreted as genuine differences. Another case of genuine difference occurred at 0121.5 hrs when the 12°S and 12°N absorptions were 3.9 db and 2.5 db while the absorptions in 40°N,S directions were both equal to 2.2 db. In the above situation, as the absorptions in 40°N and 40°S directions were equal, it is logical to expect that the absorptions in 12°N and 12°S directions were equally effected by their respective major side lobes. It is therefore interpreted that at the above time there was a genuine difference of 1.4 db in absorption between 12°S and 12°N directions. Comparing Figure 26 with the photometer records of Figure 21 it may be noticed that increased absorption at 0121.5 hrs in the 12°S direction was not accompanied by any noticeable increase in auroral luminosity in that direction. This statement again confirms the observation made in the beginning of this section where it was stated that in the SVIA phase of an absorption event, there appears to be no apparent correlation between absorption and auroral luminosity fluctuations.

5.3.3 The Event of October 25-26, 1962

In Figure 27, the absorption measured by 12°N,S riometers on October 25-26, 1962, is plotted against the relative

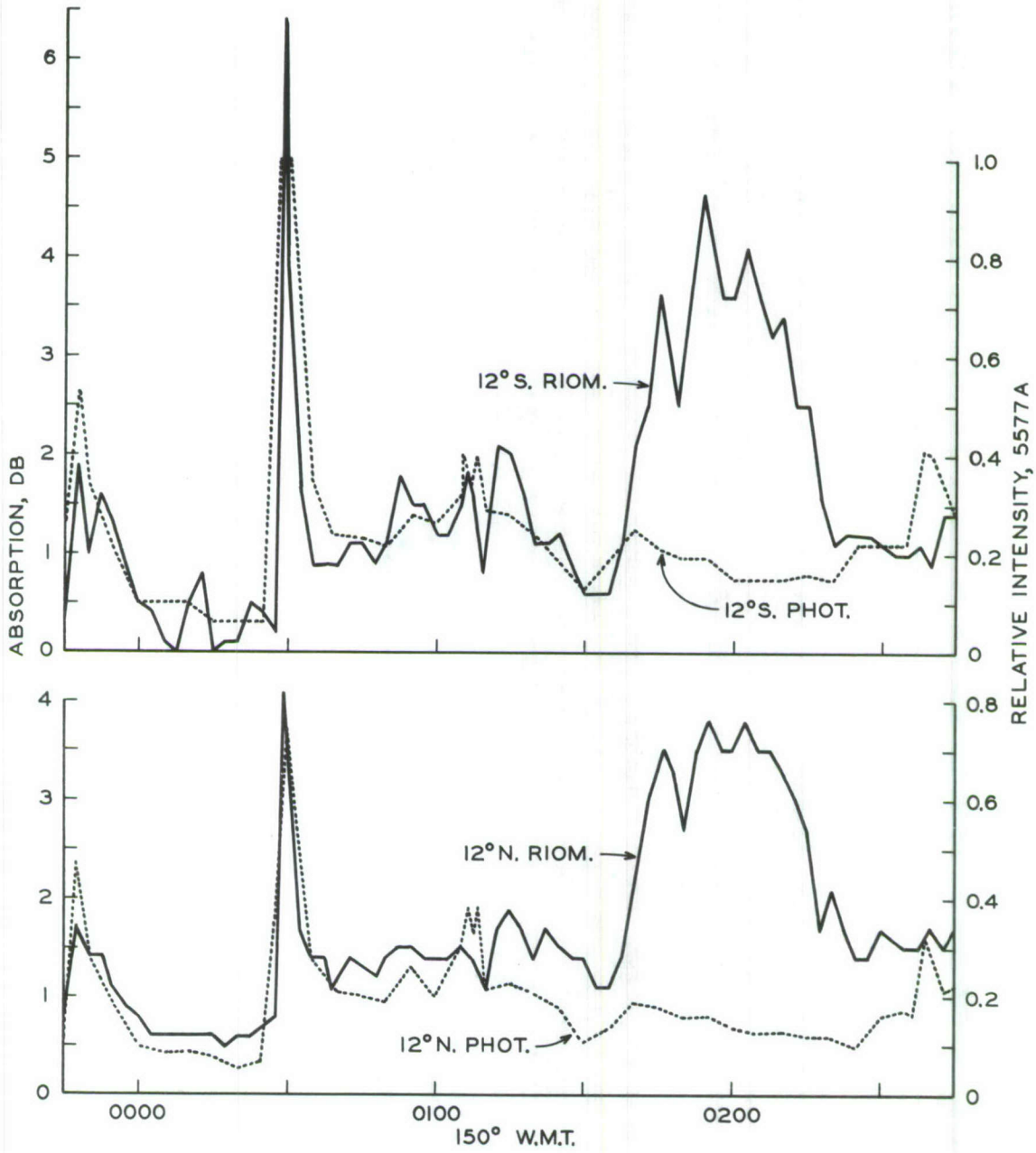

Fig. 27. Variation of absorption measured by 12^{o}S,N riometers and the relative λ 5577 Å intensity observed by 12^{o}N,S photometers on Oct. 25-26, 1962. The correspondence between auroral intensity and absorption is very good till the time of break-up which happens approximately at 0030 hrs in this case.

intensity of λ5577A observed by 12°N,S photometers during the same period. The absorption event of October 25-26 is an extremely interesting event because the various phases of the event are well separated and easily recognizable.

Referring to Figure 27, it will be noticed that the absorption in the 12°N direction decreased smoothly during 2345-0127.5 hrs with the auroral intensity. During the same period, the absorption in the 12°S direction showed a few minor fluctuations which were not accompanied by similar fluctuations of the auroral intensity. The uncorrelated absorption fluctuations are easily explained as the 40°N riometer showed similar fluctuations at the same time which implies that those observed by 12°S riometer represent a contamination by the 40°N side lobe of the antenna array.

Both north and south photometers registered a sudden increase in λ5577A intensity between 0027.5-0029 hrs which was associated with the break-up phase of the auroral display. The 12°S and 12°N riometers recorded SAIs at this time and the absorption and auroral intensity peaks occurred simultaneously. The south photometer went off scale at 0028 hrs, whereas, the north photometer observed a considerably lower intensity at this time. The same behavior was reflected in the north and south riometers as the former recorded a peak absorption of 4.1 db, whereas, the latter showed 6.4 db at the same time. The rates of increase of absorption were 2.5 db/min and 4.1 db/min respectively. From 0029 hrs to approximately 0035 hrs both the 12°N and 12°S auroral intensities decreased with 12°N,S absorption.

In Figure 27, the SVIA (slowly varying intense absorption) phase started at approximately 0135 hrs. During the SVIA phase it should be noted that absorption and auroral intensity appear to be unrelated phenomena. The extremely high ratio of absorption to auroral intensity is especially striking. As mentioned in section 5.2, the occurrence of SVIA appears to be limited to post midnight hours.

5.3.4 The Event of October 26-27

The event of October 26-27, 1962 was rather unusual in the sense that the SVIA (slowly varying intense absorption) phase was not observed immediately after the break-up but after a delay of several hours. The SAI (sudden absorption increase) associated with the break-up occurred at 2052 hrs and soon the cosmic noise signal returned to its normal value. The slowly varying intense phase started at about 0200 hrs and there was no absorption immediately preceding it. This condition implies that the SVIA phase is, most probably, a separate absorption event by itself and the reason it was not identified as such in previous cases was that in those cases its occurrence closely followed that of SAI and was therefore considered to be a part of the same event.

In order to portray the differing characteristics of the break-up type absorption and that of SVIA, the 12^{o}N,S absorption and auroral intensities are plotted in Figure 28 for both. The top portion of the figure refers to the pre-break-up and break-up phases whereas the bottom portion refers to the slowly varying intense phase (SVIA). As before, the auroral intensity

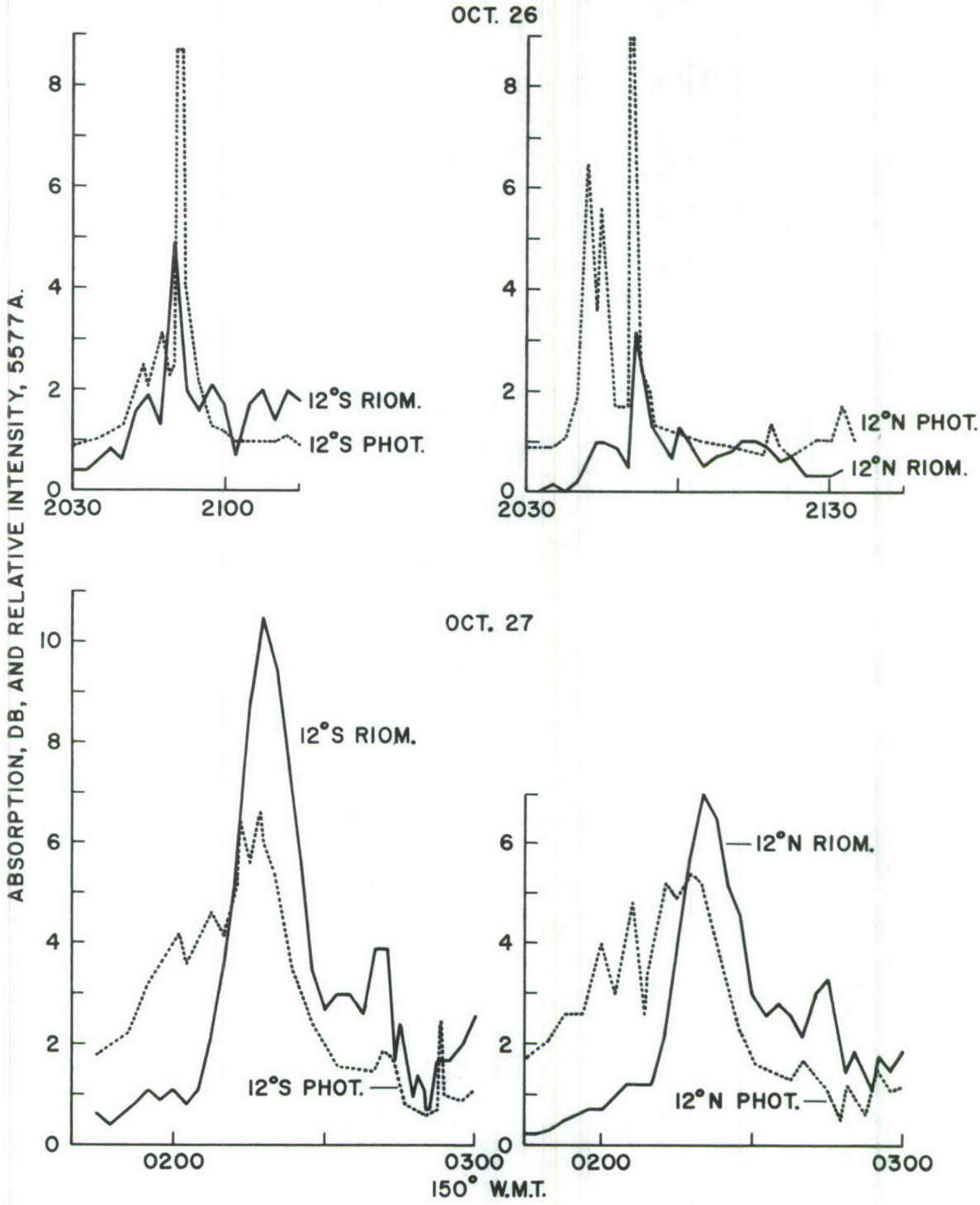

Fig. 28. Variation of absorption measured by 12°S,N riometers and the relative λ 5577Å intensity observed by 12°S,N photometers on Oct. 26-27, 1962 showing a time lag of several hours between the occurrence of SAI (sudden absorption increase) associated with the break-up of aurora and the intense absorption which usually follows it immediately.

correlates very well with absorption in the former phases, but the correlation is poor in the latter phase. In particular, the considerably higher ratio of absorption to auroral intensity is especially striking in the SVIA phase as compared to that in the break-up phase. The above observation suggests that either the physical mechanisms responsible for the two types of absorption are quite different from each other or there is a considerable difference in the energy spectrums of the primary particles responsible for these absorption events. A complete discussion of the physical mechanisms responsible for various features of absorption events will be given in Chapter VII.

In order to show the widespread character of the SVIA event of October 26-27, the absorption measured in 12°N,S and 40°N,S directions is plotted against time in Figure 29. The peak absorption in 12°N and 40°N,S directions was of the order of 6 db but that in the 12°S direction was more than 10 db. It is not possible to say whether the observed difference of 4 db between 12°S and 12°N directions at the peak of SVIA represents the actual difference, because of the occurrence of intense absorption in the direction of the side lobes. Figure 29 shows that SVIA is quite a wide spread event.

5.3.5 The Event of December 18, 1962

The event of December 18, 1962 was briefly discussed in section 5.3 in connection with the relation between visual aurora and absorption. Here the non-uniform nature of the SAI associated with auroral break-up is discussed. The absorption in 40°N,S and 12°S directions plotted in Figure 30 shows a

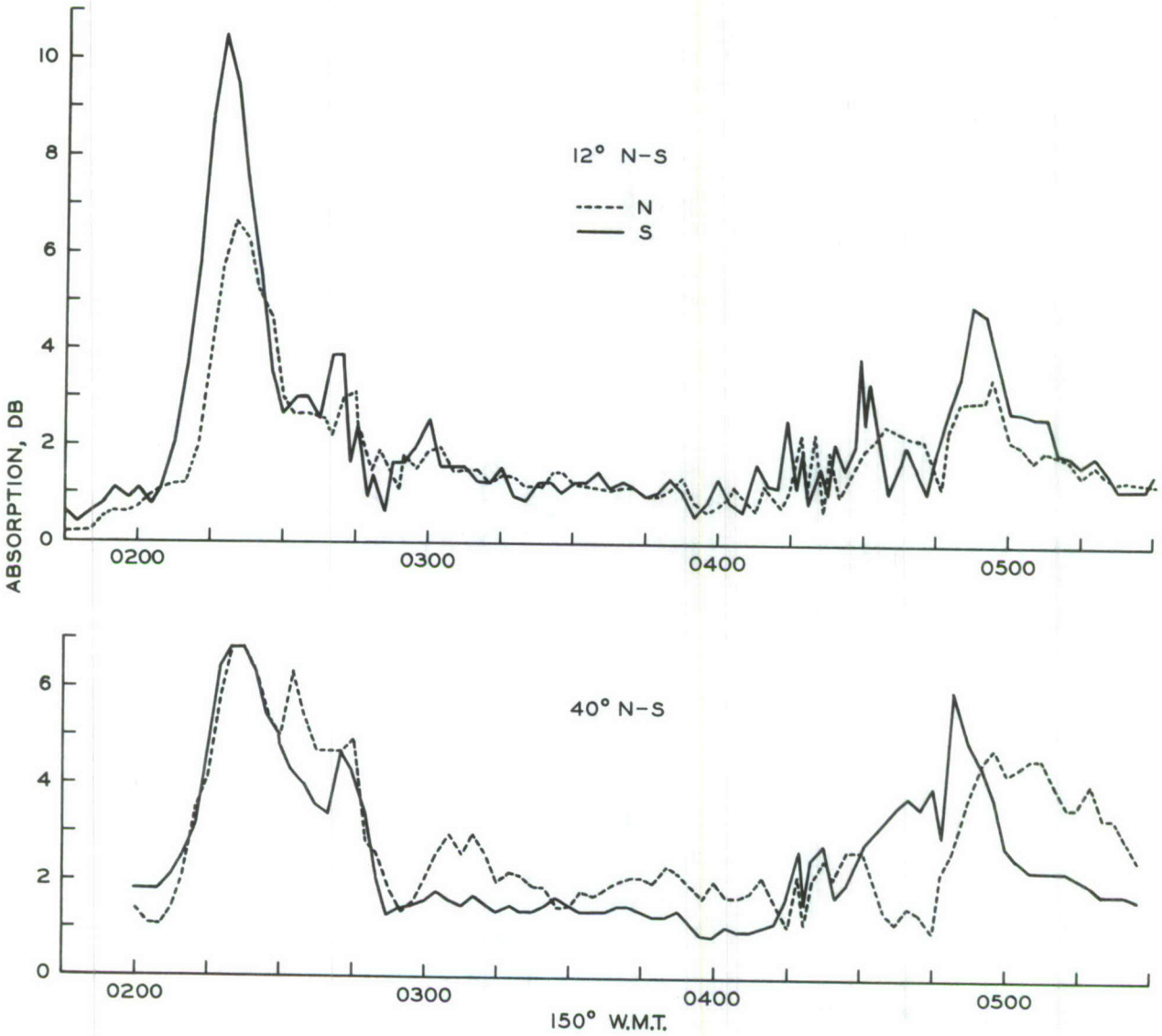

Fig. 29. Variations in absorption of radio-waves originating from different parts of the sky as measured by 40^{o}N,S and 12^{o}N,S riometers on Oct. 27, 1962 showing the wide spread character of the absorption event.

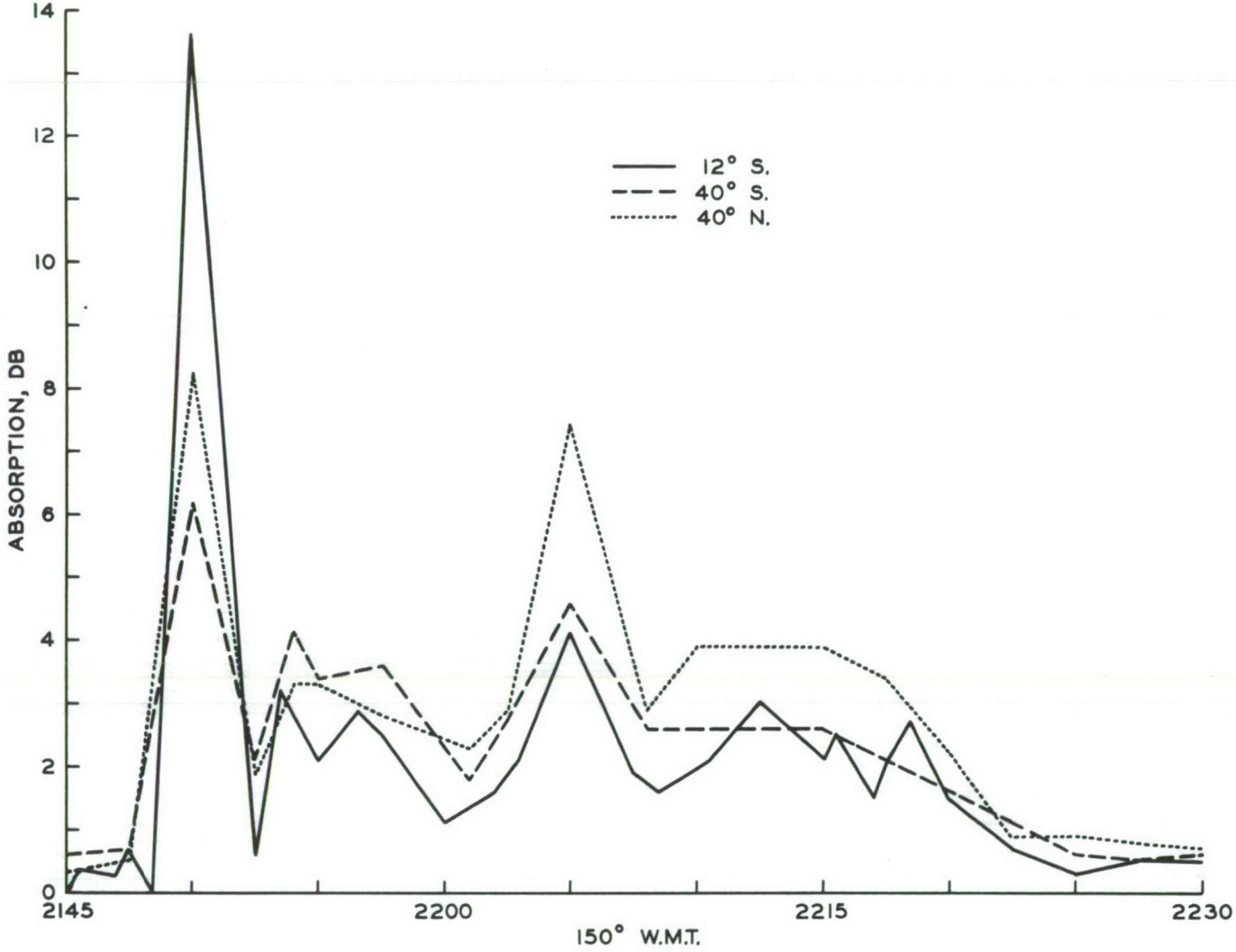

Fig. 30. Variations in absorption measured by 40°N,S and 12°S riometers on Dec. 18, 1962 showing a non-uniform SAI (sudden absorption increase). The absorption measured by 12°S riometer at the peak of SAI is several db higher than that measured by 40°N,S riometer.

non-uniform sudden absorption increase. Unfortunately, the absorption in 12°N direction could not be obtained because of equipment failure. At 2150 hrs, the absorptions in 40°S, 40°N, and 12°S directions were respectively 6, 8, and 13.6 db. It is not possible to say whether the apparent difference of 5.6 db between 12°S and 40°N directions represents the real difference in absorption or not. It is possible, however, to show that at 2150 hrs the absorption in the former direction must have been genuinely greater than that in the latter because of the following reason. Note that fifteen minutes later at 2205 hrs the absorption in the 40°N direction was close to 8 db whereas both 40°S and 12°S registered only about 4 db. This result implies that at 2205 hrs the contribution of the 40°N side lobe to the absorption observed by the 12°S riometer was definitely not very large. It may now be argued that in a period of fifteen minutes a significant decrease or increase in the contribution of the 40°N side lobe to the total cosmic noise signal observed by the 12°S riometer is not possible, owing to the fact that the change in the brightness temperature in the 40°N direction due to rotation of the earth in the above period will be negligibly small. Therefore, one concludes that at 2150 hrs also, the 40°N side lobe did not significantly contribute to the absorption observed by the 12°S riometer, which implies that at this time the absorption in the 12°S direction was genuinely much higher than that in 40°N or 40°S direction.

5.3.6 The Event of January 31, 1963.

The absorption in 40°N,S and 12°N,S directions observed during the unusual event of January 31, 1963 is shown in Figure 31.

The event is unusual in the sense that the various phases associated with a typical aurorally associated absorption event are not identifiable. The absorption varied rapidly in an irregular manner throughout the night and during part of the day. During a considerable portion of the event the absorption in the 40°S direction was appreciably greater than that in the 40°N direction. Genuine differences of as much as 2 db are noticeable between the absorptions in 12°S and 12°N directions.

5.4 ABSORPTION AND AURORAL COVERAGE OF THE RECEIVING ANTENNA BEAM.

The previous section was devoted mostly to a simultaneous study of absorption and relative intensity of the green auroral line for selected cases. An important variable which needs to be considered in a simultaneous study of radio-wave absorption and auroral luminosity is the fraction of the receiving antenna beam covered by the luminosity. Unfortunately, a photometer does not provide any information about the above variable as the auroral intensity recorded by the photometer at a given time may be attributed either to a bright aurora covering a small fraction of the photometer beam or to an aurora of lower luminosity covering the major portion. In order to study the effect of auroral coverage of the receiving antenna beam on radio-wave absorption, it is necessary to use all-sky camera photographs for comparison.

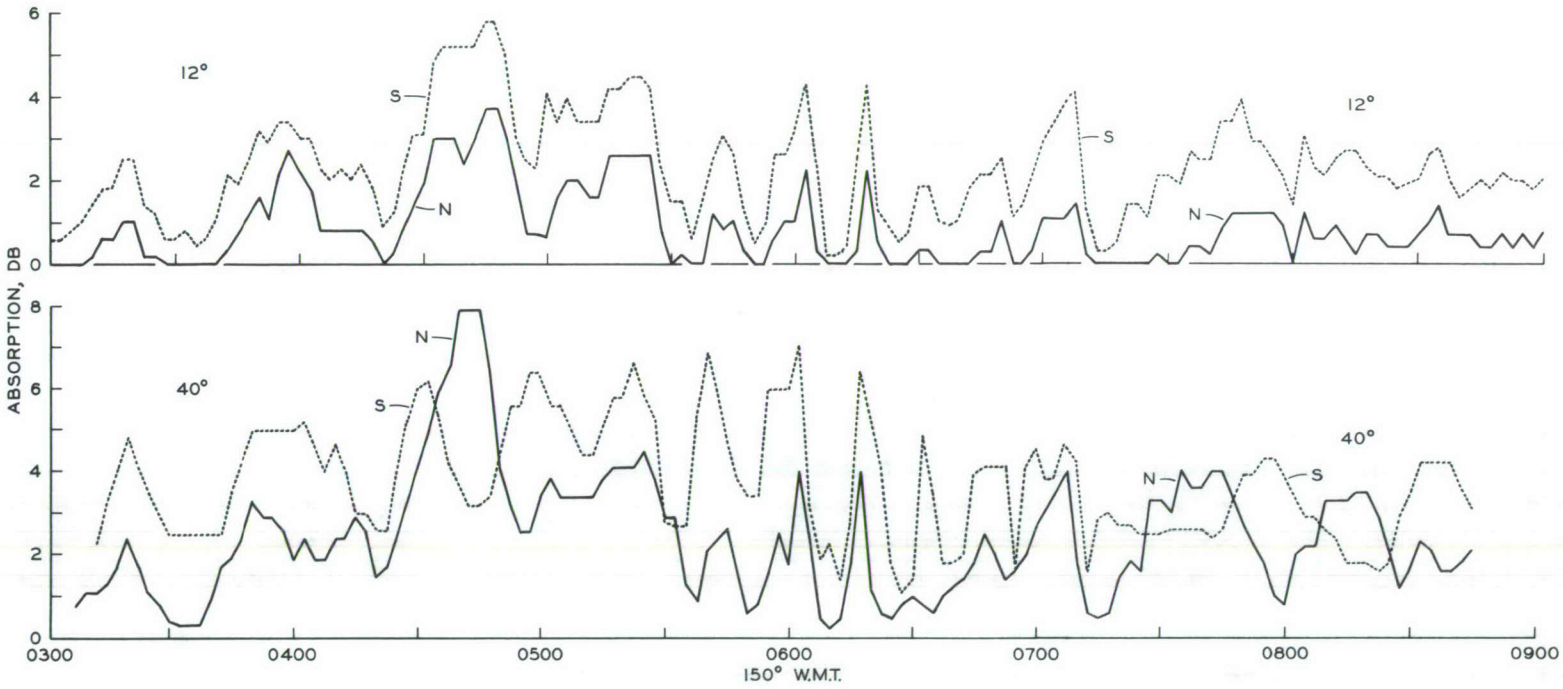

Fig. 31. Variations in absorption measured by 40°N,S and 12°N,S riometers during the unusual auroral event of Jan. 31, 1963. The event is unusual in the sense that the normal pattern of a typical auroral event as given in Fig. 17 is not applicable to it.

Unfortunately, for most of the important events discussed in the previous section, the all-sky camera data could not be used because of cloudy weather. Therefore, one was forced to include relatively weak absorption events which were observed on clear nights and for which all-sky photographs were usable. Following is a detailed study of such selected events.

5.4.1 The Event of October 8, 1962.

In Figure 32a, the absorption in 12°N and 12°S directions is shown as a function of local time. The corresponding all-sky camera photographs are shown in Figure 33.

At 0015 hrs an auroral arc lay close to the horizon in the south. Between 0015-0020 hrs it moved northward, became suddenly bright at 0020 hrs, and covered the beams of 12°S and 12°N positions of the antenna. Referring to Figure 32a, it may be seen that the absorption in 12°S and 12°N directions showed a sudden and pronounced increase during the same period. Between 0021-0023 hrs, the auroral luminosity decreased and the absorption in both directions also showed a pronounced decrease. At 0025 hrs, the luminosity increased again and was accompanied by increased absorption in both directions. The luminosity decayed between 0030-0045 hrs and the absorption in 12°N and 12°S directions also showed a gradual decline.

The above analysis shows a close association between the auroral luminosity and radio-wave absorption in the pre-midnight hours.

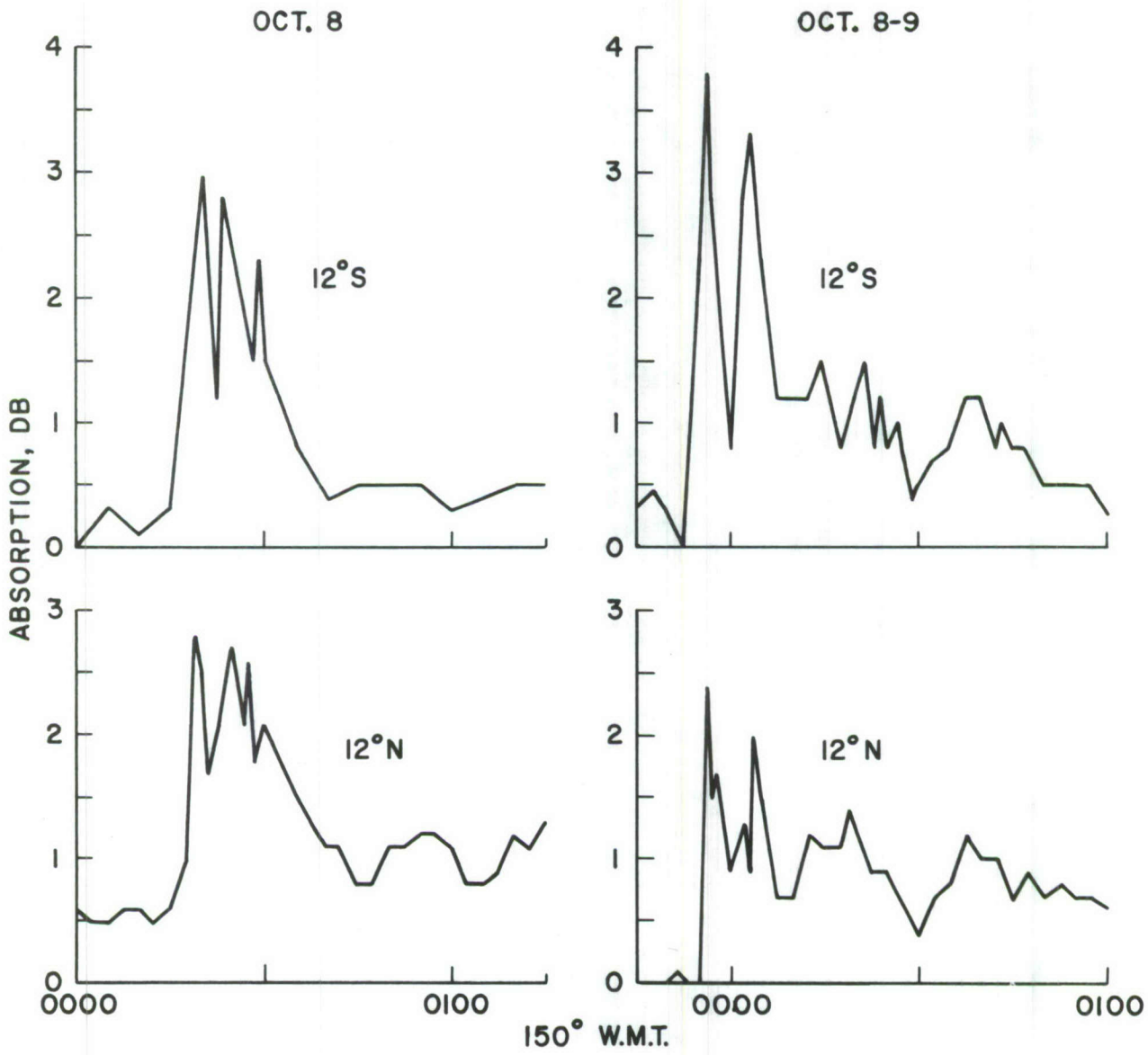

Fig. 32-a. The absorption event of Oct. 8, 1962. Comparing all-sky photographs for this event given in Fig. 33 with the absorption, one finds a good correlation between absorption and the occurrence of bright and active aurora.

Fig. 32-b. The absorption event of Oct. 8-9, 1962. Comparing absorption with the all-sky photographs for this event given in Fig. 34, a one to one correspondence between the SAI (sudden absorption increase) and auroral break-up is found.

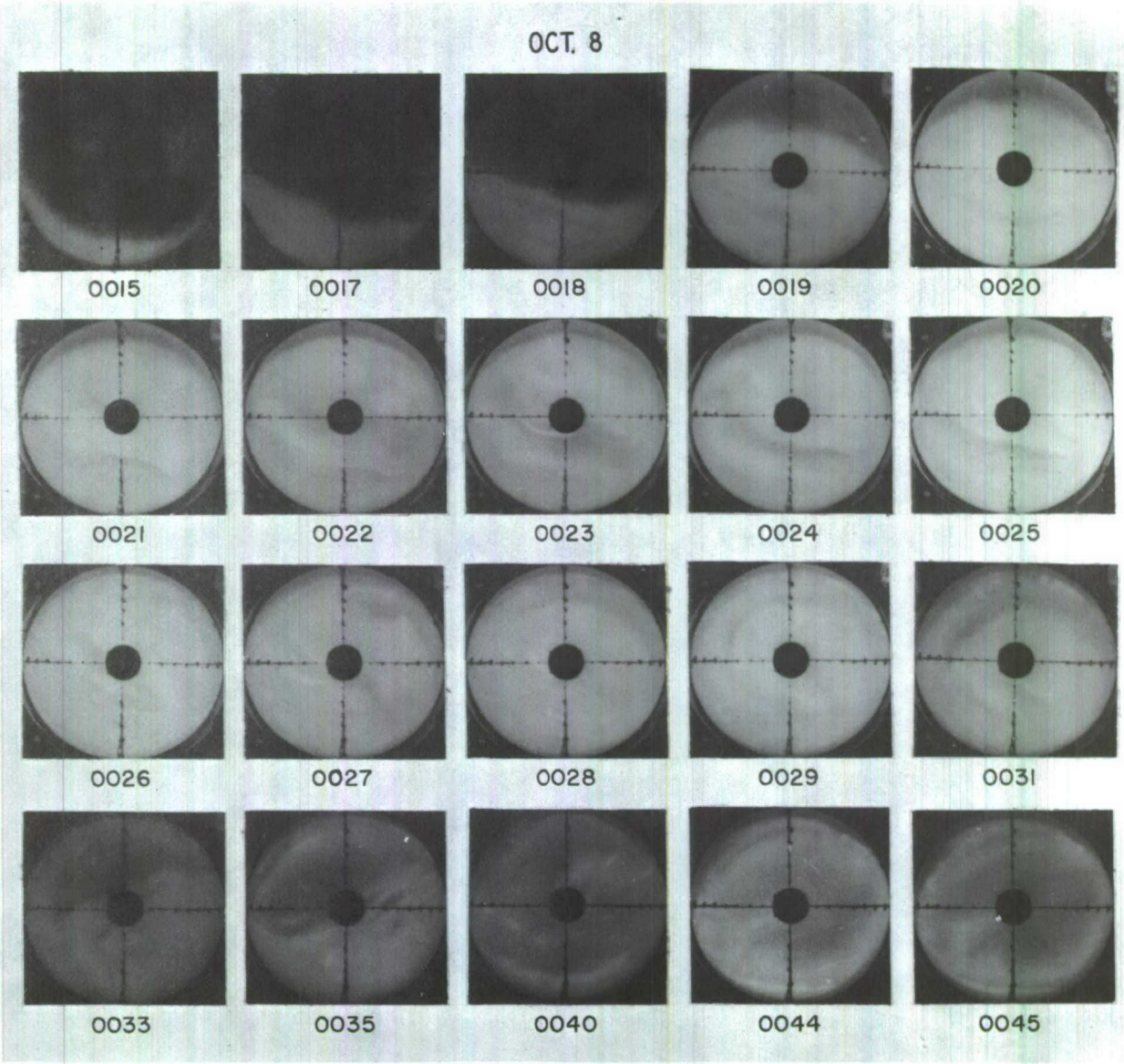

Fig. 33. All-sky photographs taken during the auroral event of Oct. 8, 1962. Compare Fig. 33 with Fig. 32-a.

5.4.2 The Event of October 8-9, 1962.

The event of October 8-9, plotted in Figure 32b, also shows a close relation between visible aurora and absorption. The all-sky camera photographs for the period of intense activity are shown in Figure 34.

At 2353 hrs there was a faint auroral arc in the south. At 2355 hrs the arc became suddenly active and bright, and covered part of the 12°S antenna beam, whereas, none of the 12°N beam was covered. At this time, the absorption in the 12°S direction increased to 2 db while that in the 12°N direction remained negligible. Between 2355-2357 hrs aurora extended to the north and covered both 12°S and 12°N beams. The absorption in the 12°N direction then showed a sudden increase and the peak absorption occurred at the same time in both directions. In this case, the peak value of absorption appeared to have occurred one minute after the occurrence of peak luminosity. The sudden fall in absorption between 2357-000 hrs followed the decrease in luminosity. At 0002 hrs, the aurora became suddenly bright again and the absorption in both north and south directions showed sudden increases at the same time. From 0003 hrs onwards the auroral luminosity decreased and so did the absorption. Between 0004-0025 hrs there was faint and diffuse aurora over most of the sky, and the absorption was close to 1 db in both directions. The auroral luminosity decreased in an area of the sky close to 12°S and 12°N beam positions between 0025-0030 hrs and both riometers showed recoveries at this time. The sky was again covered with aurora between 0032-0039 hrs which was followed by absorption increase.

Fig. 34. All-sky photographs taken during the auroral event of Oct. 8-9, 1962. Compare Fig. 34 with Fig. 32-b.

5.4.3 The Event of November 22, 1962.

The original riometer record of the absorption event of November 22 shown in Figure 35 shows many interesting characteristics which are worth describing in detail. In view of the fact that the interesting portions of the event occupied a long time interval, it is not possible to present all-sky camera photographs for the entire event.

At 0015 hrs an auroral arc was seen in the south, and it appeared to be moving northward. As the arc became brighter and occupied a major portion of the 40°S antenna beam, the absorption in that direction showed a pronounced increase and reached a peak value of about 2.8 db, while at the same time the peak absorption in the 40°N direction was only 0.5 db. In this case, the pronounced difference in absorptions between 40°S and 40°N directions is explained by the difference in auroral coverage of the respective antenna beams. Between 0045-0050 hrs, the 40°S riometer trace showed a recovery whereas the 40°N riometer trace showed increasing absorption. The above condition was found to be associated with large scale motion of aurora from the south to the north.

The most interesting part of the event is that from 0300 hrs onwards. At 0335 hrs the 40°N riometer trace underwent a sudden drop while there was absolutely no change in the level at 40°S. This condition was found to be associated with sudden brightening of the aurora in the north.

At 0345 hrs the absorptions in 40°N and 40°S directions were 3.4 and 2.7 db respectively. The all-sky camera photographs for

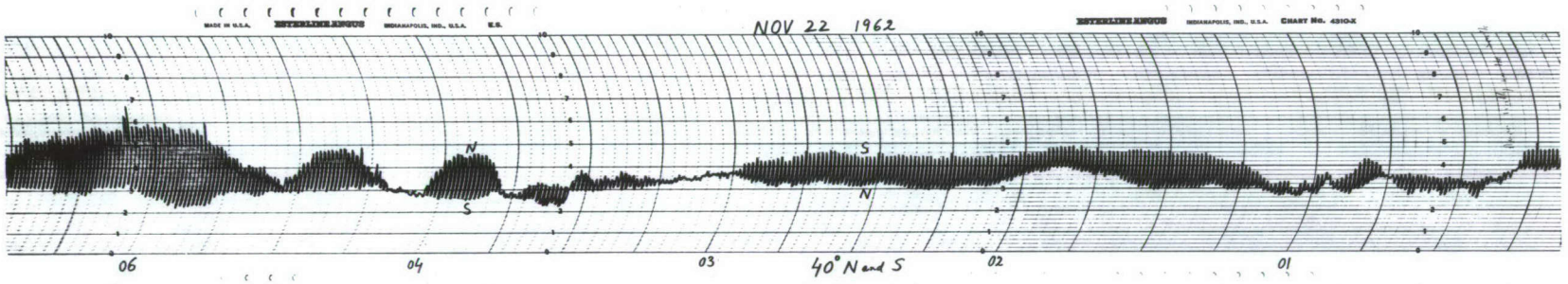

Fig. 35. Original 40°N,S riometer record for Nov. 22, 1962 showing strong, periodic recoveries between 0345-0430 hrs in the north which are not observed in the south. Comparing Fig. 35 with all-sky photographs for this event given in Fig. 36-a, the recoveries are found to be associated with periodic removal of a peculiar auroral cover from the northern sky while the southern sky remained under it.

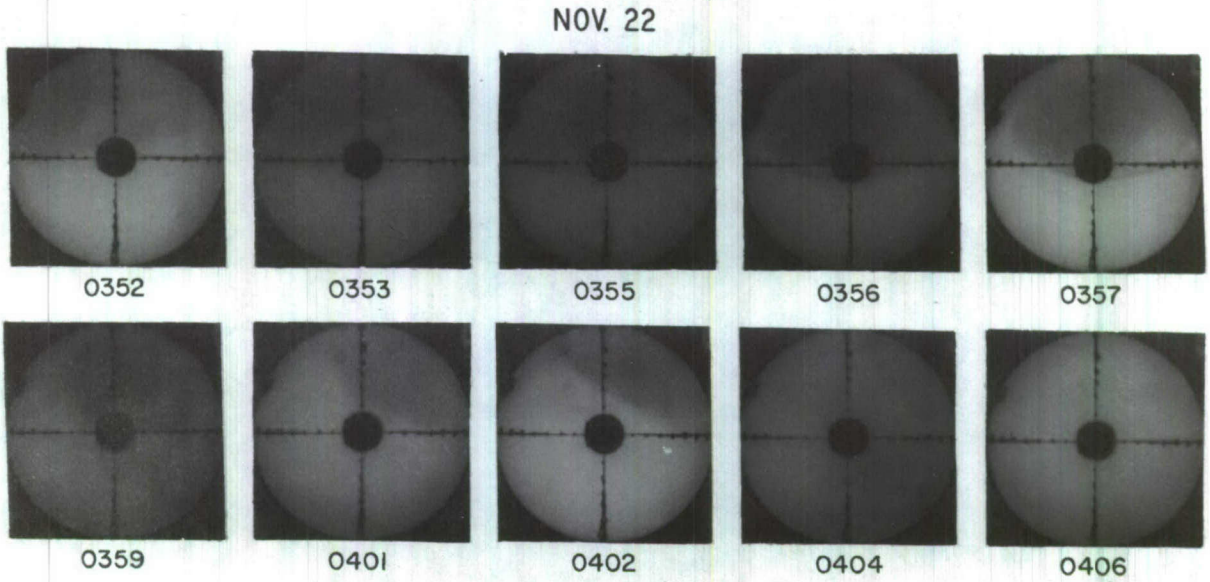

Fig. 36-a. All-sky photographs taken during strong and localized recoveries of Nov. 22, 1962. Compare Fig. 36-a with Fig. 35.

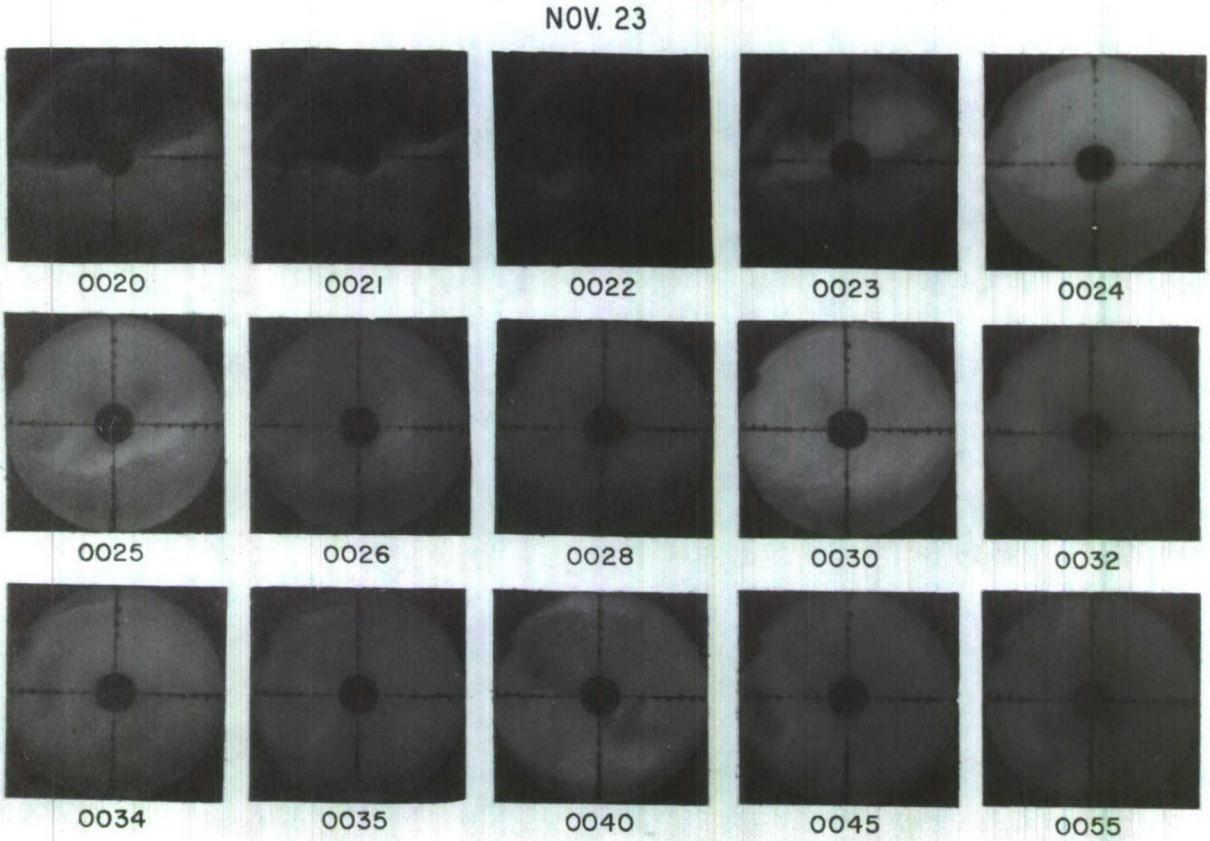

Fig. 36-b. All-sky photographs taken during the localized SAI (sudden absorption increase) of Nov. 23, 1962. Note that in the early part of the auroral event the bright and active part of the display was confined to a limited region of the northern sky.

the period 0352-0406 hrs, presented in Figure 36a, show diffuse aurora over almost all of the sky at the beginning. During 0353-0400 hrs the auroral coverage of the 40°N beam decreased and at the same time the absorption in that direction also showed a pronounced recovery from 3.4 db to 0.9 db. Between 0400-0406 hrs, the aurora again started to cover the 40°N beam and the absorption followed the same pattern. The absorption in the 40°S direction remained constant at 2.7 db throughout the above period.

5.5 CLASSIFICATION OF SAIs

In previous sections it was shown that the SAI is invariably associated with sudden brightening of the aurora or with the auroral break-up. The SAIs, in general, may be divided into three categories which are:

(a) uniform
(b) non-uniform
(c) localized.

The event of October 10, 1962 shown in Figure 24 is an example of a uniform sudden absorption increase. In such events, the SAI is observed over a large area of the sky and the peak absorptions in different directions are nearly equal.

As the name suggests, a non-uniform SAI is one which is observed over a large area of the sky but with varying intensity in different directions. The event of October 16, 1962, shown in Figure 26, is an example of a non-uniform SAI. The absorptions at the peak of SAI are considerably higher in 12°N,S directions as compared to those in 40°N,S directions.

In a localized SAI, the absorption increase takes place over a relatively limited region of the sky. The original 40°N,S riometer record of November 23, 1962 shown in Figure 37, is a clear case of a localized SAI. Note that the SAI was observed in the 40°N direction but not in the 40°S direction.

Of all sudden absorption increases, the localized SAIs are the most intriguing events. The next section is devoted to a detailed study of such events, in conjunction with all-sky photographs.

5.6 DETAILED STUDY OF LOCALIZED SAI EVENTS IN CONJUNCTION WITH ALL-SKY CAMERA PHOTOGRAPHS.

Having established the existence of localized SAIs, one wishes to study the peculiar auroral display associated with the sudden absorption increase in a limited region of the sky. In this section all-sky photographs taken during selected localized SAIs are studied in detail in an attempt to understand the cause of the peculiar absorption pattern.

5.6.1 The Event of November 23, 1962.

Figure 36b gives the all-sky photographs for the localized SAI of November 23 whose original riometer records were presented in Figure 37.

Referring to Figure 36b, it may be seen that the 40°S beam was covered by faint aurora at 0021 hrs while there was no aurora in the 40°N beam. Figure 37 shows that during the above period the 40°N riometer did not show any absorption while the 40°S riometer showed 0.5 db. The fact that the absorption in the south was greater than that in the north during the above period

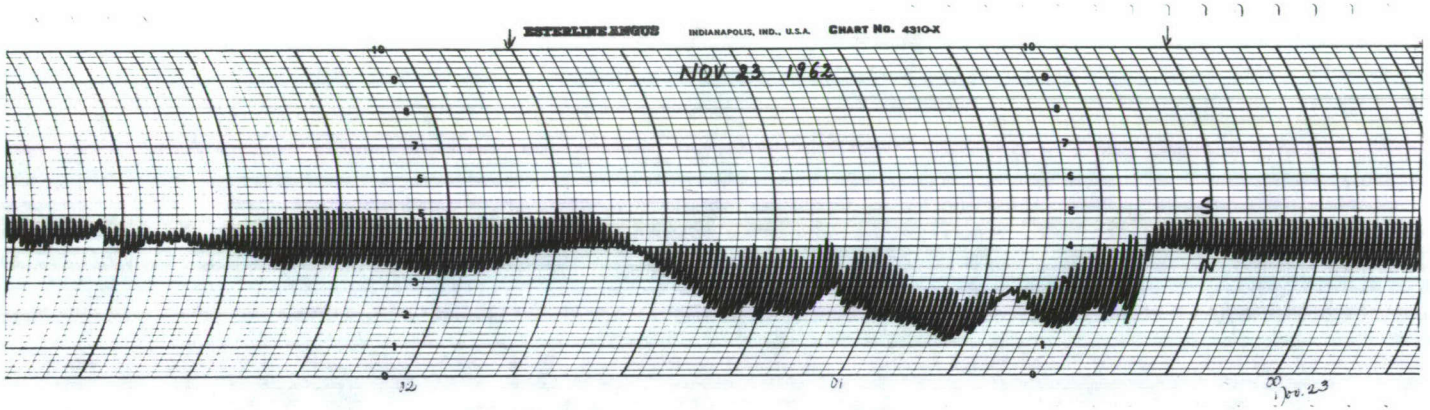

Fig. 37. Original 40°N,S riometer record for Nov. 23, 1962 showing an intense SAI (sudden absorption increase) recorded in the North but not in the south. Comparing Fig. 37 with 36-b, the localized SAI is found to be associated with the bright and active part of the auroral display which happened to be over a limited region of the northern sky. The slight increase in absorption as shown by 40°S riometer record at the time of SAI in the north may be attributed to increased brightness of the background sky. The conclusion reached from Figs. 36-b and 37 is that strong absorption is limited to bright and active part of an auroral arc, and that there is no reason to believe that absorption is more wide spread than visual aurora.

is explained by the difference in auroral coverage of the respective antenna beams.

At 0023 hrs a faint arc suddenly became bright and active in the north. One minute later the arc covered the entire 40°N antenna beam, and its brightness continued to increase. Although there was a pronounced increase in the brightness of the southern sky at the time when break-up happened in the north, the 40°S beam itself was free of the bright and active part of the display. The absorption in the 40°N direction increased suddenly from 0.1 db to 4.2 db between 0022.5-0024 hrs. During the same period the increase in absorption in the 40°S direction was only from 0.4 to 1.1 db. The sudden absorption increase of 4 db in the north between 0022.5-0024 hrs was associated with the break-up of aurora within the 40°N antenna beam, whereas the slow increase of 0.7 db in the south may be attributed to the increase in the brightness of the faint aurora which covered the 40°S beam at that time.

The above observation suggests that a localized SAI is observed only when an auroral arc becomes bright and active in a limited region of the sky. One also concludes that the sudden absorption increase is observed when the bright and active aurora covers a significant portion of the receiving antenna beam. Another extremely important conclusion drawn from the event of November 23 is that almost all the absorption in the break-up phase of an auroral display is confined to its bright and active part and that there is no reason to suspect that absorption is more wide spread than the visual aurora itself.

The SVIA phase (slowly varying intense absorption) of the event started soon after the break-up. In this phase i.e. from 0025 hrs onwards, diffuse surfaces appeared over all the sky except in the southern edge of the photographs. As the diffuse surfaces extended to the south and covered more and more of 40°S antenna beam, the absorption in the 40°S direction also increased. At 0035 hrs the absorptions in 40°N and 40°S directions were respectively 4.7 and 2.5 db although the auroral luminosity was considerably less than that of the early phases of the display. The above result confirms the earlier result, obtained by using photometer data, that in the SVIA phase the ratio of absorption to auroral luminosity is much higher than that during the SAI phase.

At 0040 hrs both 40°N and 40°S directions showed 3 db absorption. Between 0042.5-0050 hrs, the absorption in the north slowly increased to 6.3 db, whereas that in the south stayed relatively constant. Referring to the all-sky photographs of Figure 36b, it may be seen that there was no noticeable increase in the brightness of the northern sky during the above period. The 12°N,S photometers also did not register any increase in the auroral intensity between 0045-0050 hrs. Once again, the above observation confirms the result of section 5.3 which indicated that absorption and auroral intensity fluctuations are not correlated in the SVIA phase.

Referring to Figure 37 it may be seen that the signal returned to its normal level at about 0145 hrs. Between 0230-0300 hrs, strong pulsating auroral intensity was recorded by the

photometers while the absorption on both 40°N and 40°S direction was negligibly small.

5.6.2 The Event of November 15, 1962.

The absorption event of November 15, 1962 shown in Figure 38 is a clear example of a localized sudden absorption increase. The all-sky photographs taken during the event are given in Figure 39a.

Referring to the all-sky photographs of Figure 39a, a thin quiet arc, observed in the south at 2226 hrs, later started moving towards the north. At 0029, hrs the arc covered a major portion of the 12°S antenna beam and also part of the 40°S antenna beam. During the above period both 12°N and 40°N antenna beams did not contain any part of the arc. Referring to the absorption graph for this event given in Figure 38, it may be seen that the absorptions in 12°N,S and 40°N,S directions at 2229 hrs were respectively 0.7, 0.2, 0.2, 0.5 db. The difference of 0.5 db in absorptions between 12°S and 12°N observed at the above time definitely represents a genuine difference because of the fact that negligibly small absorptions existed in the direction of major side lobes at that time. The observed difference of absorption between 12°N and 12°S directions is consistent with the difference in auroral coverage of the two beams, i.e. the beam that showed more absorption was almost fully covered with aurora whereas there was no aurora in the beam which showed little absorption. It should also be noted that the absorption caused by the quiet arc was less than 1 db even though it filled the entire antenna beam. This observation strongly suggests that

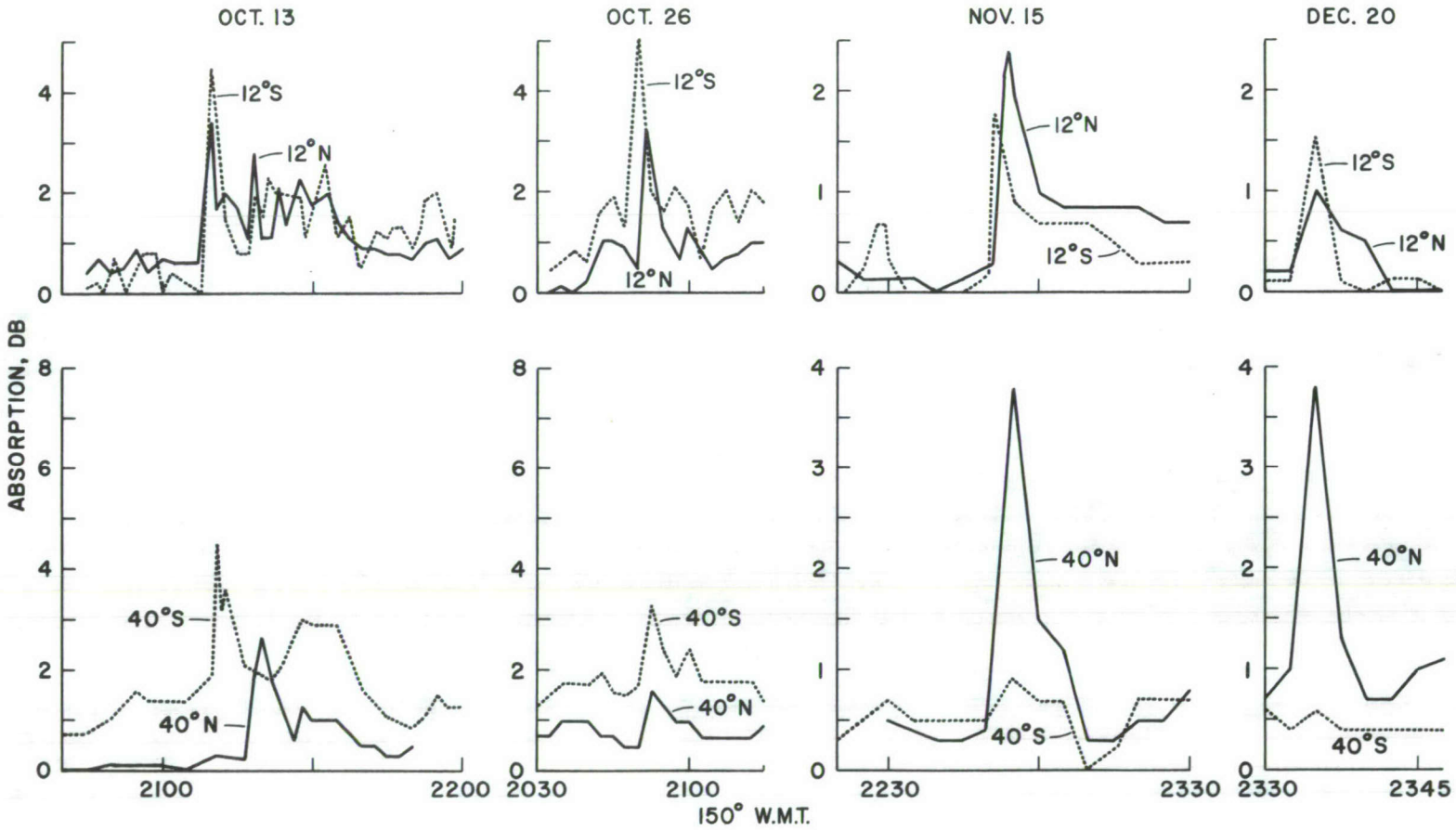

Fig. 38. Variations in absorption of radio-waves as measured by 40°N,S and 12°N,S riometers for selected events showing localized or non-uniform SAI (sudden absorption increase). Compare Fig. 38 with Figs. 39-a and 39-b.

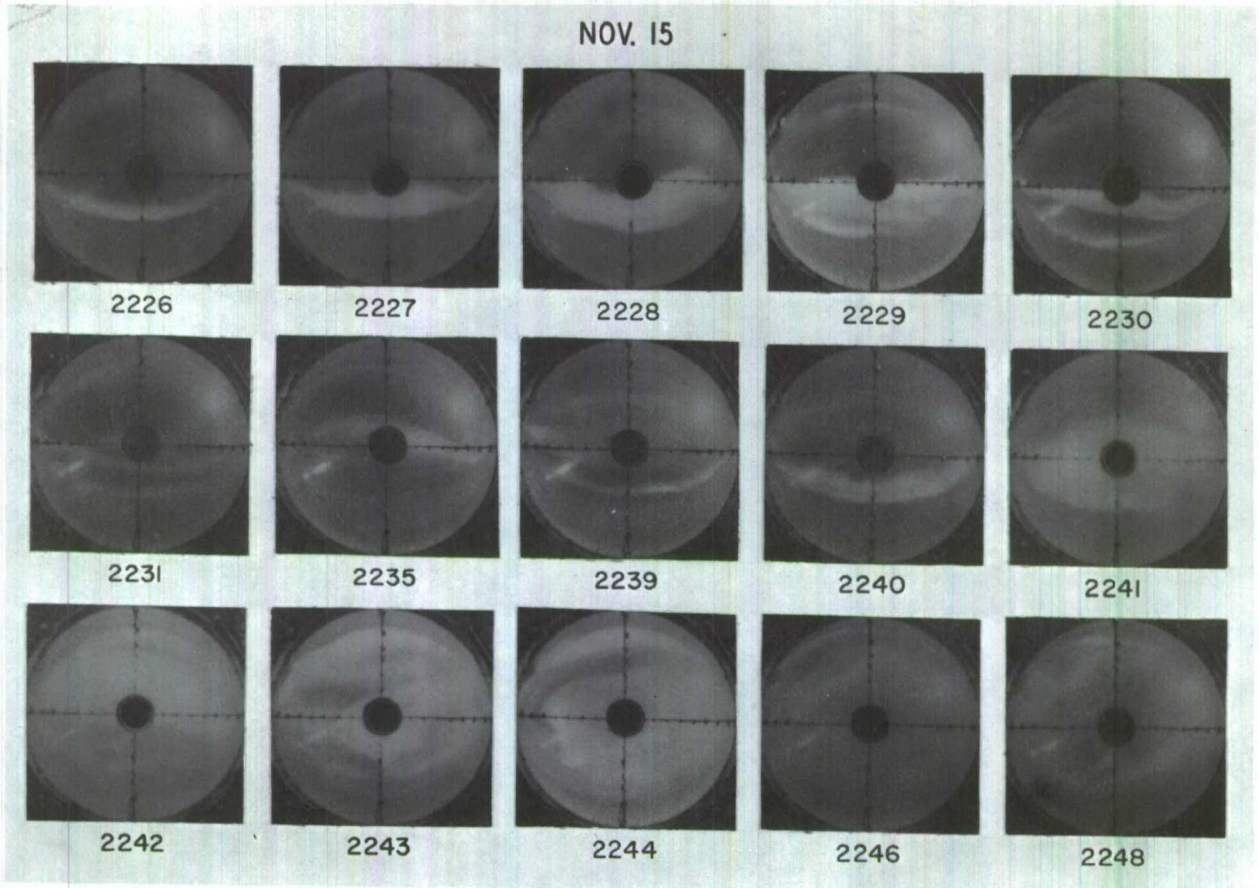

Fig. 39-a. All-sky photographs taken during the localized SAI (sudden absorption increase) of Nov. 15, 1962. Compare Fig. 39-a with the absorption on Nov. 15, 1962 given in Fig. 38.

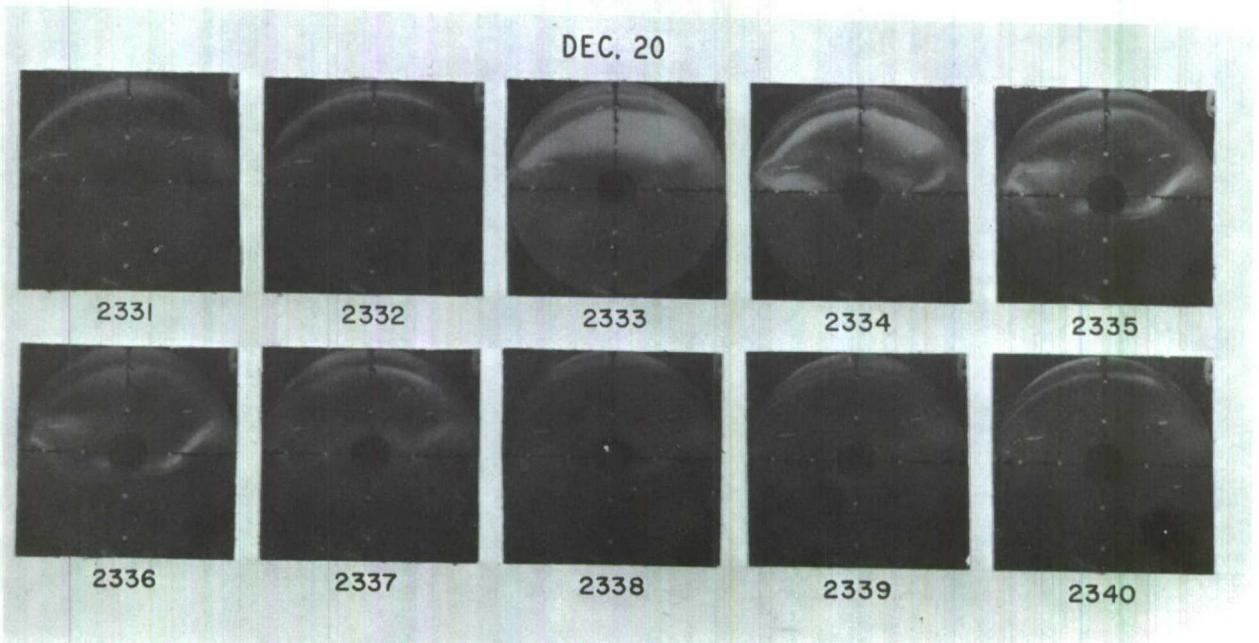

Fig. 39-b. All-sky photographs taken during the localized SAI (sudden absorption increase) of Dec. 20, 1962. Compare Fig. 39-b with the absorption on Dec. 20, 1962 given in Fig. 38.

while correlating absorption magnitudes with aurora it is necessary to differentiate between the quiet and active phases of the auroral display. One also concludes from the above observation that the absorption in presence of quiet arcs is limited to the visual auroral form only.

At 2231 hrs, the arc started to decrease in luminosity, and disappeared a few minutes later. The 12°S absorption decreased also in the above period and the cosmic noise signal returned to its normal level at about 2232 hrs.

Referring to Figure 39a, a thin arc was again seen in the south at 2239 hrs. The arc suddenly became bright and active in a localized region of the sky near the zenith at 2241 hrs. The 12°S beam was fully covered with bright and active aurora between 2240-2241 hrs, whereas the 12°N beam was only partially covered at the same time. The absorption in the 12°S direction increased by more than 1.5 db between 2240-2240.5 hrs, whereas the increase in both 12°N and 40°N directions did not start until 2241 hrs. It is therefore reasonable to conclude that at 2240.5 hrs there was a genuine difference of 1.5 db between the absorption in 12°S and 12°N directions, and that the difference in absorptions was consistent with the difference in auroral coverage of the two antenna beams.

The all-sky photographs of Figure 39a indicate that at 2242 hrs both 12°N and 40°N antenna beams were covered with bright and active aurora, while there was only faint aurora in 12°S and 40°S antenna beams. Referring to the absorption graph of Figure 38 it may be seen that both 12°N and 40°N riometers

registered a sudden absorption increase at this time, while the 12^{o}S riometer showed a sudden recovery from its sudden increase which had occurred 1½ minutes earlier. The absorption in the 40^{o}S direction did not show the sudden increase which was seen in all other directions i.e. 40^{o}N, 12^{o}N, 12^{o}S. However, the 40^{o}S riometer observed a slow increase of 0.5 db during the above period. The slow increase is attributed to the increase in the brightness of the faint aurora which covered the 40^{o}S antenna beam. One therefore concludes that at 2242 hrs the absorption in the 12^{o}N direction was genuinely greater than that in the 12^{o}S direction by more than 1 db. The marked difference in absorption at this time is explained by the fact that the beam which showed more absorption had bright and active aurora, whereas the other beam which showed less absorption had only faint aurora.

The analysis of the event of November 15 again strongly suggests that, both in the quiet as well as active phases of auroral arcs, absorption is limited to visual auroral forms only.

5.6.3 The Event of December 20, 1962.

The short event of December 20, 1962, shown in Figure 38, is another clear example of a localized sudden increase in absorption. The all-sky photographs for this event are shown in Figure 39b.

At 2232 hrs, a faint auroral arc was visible in the north. The luminosity of the faint arc increased suddenly at 2233 hrs and occupied a sizable portion of the 40^{o}N antenna beam while there was no aurora in 12^{o}S, 12^{o}N, and 40^{o}S antenna beams. The

absorption in the 40°N direction increased suddenly to 3.8 db at 2333.5 hrs, whereas, that in the 40°S direction stayed constant at 0.5 db. It should be noticed that, unlike the events of November 23, and November 15, in this event no increase in the brightness of the southern sky occurred with the break-up in the north. This explains why in the two events mentioned above, the 40°S beam showed a noticeable increase in absorption when break-up occurred in the north beam, whereas, no such increase was observed in the event under discussion when similar brightening of the aurora took place in the north.

While only a small fraction of the 12°N beam was covered with bright and active aurora between 2333-2335 hrs, there was absolutely no aurora in the 12°S beam. The fact that the latter showed more absorption than the former is interpreted as being caused by the contribution of the major side lobe which in this case happened to be filled with bright and active aurora. Had there been no side lobe pick up, the absorption in the 12°S direction would have been close to that in 40°S direction i.e. about 0.5 db.

It is therefore logical to conclude that, at 2235 hrs, the observed difference between absorptions in 12°S and 12°N directions does not represent the actual difference. It is more likely that the true absorption in the 12°N direction was greater than that in the 12°S direction by at least 1/2 db.

5.6.4 Discussion of the Event of October 13, 1962 and Deduction of Gross Auroral Features Associated with it.

The event of October 13, 1962, shown in Figure 38, is rather unusual in the sense that the sudden absorption increases occurred on both 40°S and 40°N beams but were separated by a few minutes. When the sudden absorption increase occurred on 40°S, both 12°N and 12°S beams also recorded sudden increases at approximately the same time, although the effect on the 12°S beam was more pronounced than that on the 12°N beam. The 40°N beam, on the other hand, showed only 0.2 db absorption at this time. It is quite probable that the absorption observed on the 12°N beam at 2110 hours might have been higher than the actual absorption on account of the fact that strong absorption was taking place at that time in the direction of its major side lobe i.e. at 40°S. On the other hand, the absorption of 4.5 db observed on the 12°S beam at 2110 hrs must be the actual absorption in that direction owing to the fact that its major side lobe was virtually free of any absorption at that time. Therefore, it is concluded that at 2110 hrs the absorption in the 12°S direction was greater than that in the 12°N direction by at least 1.2 db.

Between 2118-2120 hrs, while the 40°S beam was recovering from its sudden increase which occurred at 2110 hrs, the 40°N beam showed a sudden absorption increase which was observed as a strong increase by the 12°N beam and as a relatively weak increase by the 12°S beam. Using the reasoning of the previous

paragraph, it is concluded that at 2120 hrs the absorption in the 12°N direction was truly greater than that in the 12°S direction by at least 1 db.

Due to cloudy weather, the all-sky photographs for this event were not usable. However, using the riometer data, it is quite possible to visualize the auroral motions which gave rise to the above absorption pattern. The auroral motions between 2050-2130 hrs, as deduced from the riometer records, are presented below.

At 2050 hrs there was a quiet arc moving northward. It covered the entire 40°S beam at 2100 hrs. The arc became suddenly bright and active between 2108-2110 hrs in a broad region of the sky enclosing the 40°S and 12°S beams and possibly a small fraction of the 12°N beam. The bright and active part of the display definitely did not extend to the north more than a few degrees beyond the zenith. The brightness of the arc decreased between 2110 and 2115 hrs.

Between 2118 and 2120 hrs an auroral arc suddenly became bright and active in an area enclosing the 40°N and the 12°N beams. The bright and active part of the display definitely did not extend to the southern sky.

Obviously, the information obtained by riometers about auroral features is not as complete as that obtained by the all-sky camera. The purpose of the example given above is merely to point out that under cloudy conditions when all-sky camera records are not usable, it is still possible to deduce certain gross features of the display by observing radio-wave absorption

in different parts of the sky by means of narrow beam antennas. The technique may further be improved by increasing the coverage of the sky by using a chain of narrow beam antennas pointed at different parts of the sky.

5.6.5 The Event of April 5-6, 1962.

In Figure 40, the observed absorption in 12°N and 12°S directions is plotted against local time. Continuous visual auroral observations were made on this night between 2300-0030 hrs.

At 2315 hrs, a northward moving auroral arc was noticed in the south. The arc kept moving northward and suddenly became bright and active at 2322-2323 hrs, when it covered part of the 12°S beam. At this time there was no aurora in the 12°N direction. Referring to Figure 40 it may be seen that the absorption in the 12°S direction showed a sudden increase at about 2323 hrs. The absorption in the 12°N direction showed a much slower and smaller rise at the same time, which may be attributed to the contribution of the major side lobe situated at 40°S. Later on, the aurora moved northward and became suddenly bright and active at 2339-2340 hrs when it partially covered the main beam of the antenna in the 12°N position. The absorption in the 12°N position showed a sudden increase at 2340 hrs whereas in the 12°S direction no such increase occurred.

5.7 SUMMARY OF RESULTS

In this chapter the spatial and temporal variations of nighttime radio wave absorption were extensively studied in conjunction with the spatial and temporal intensity variations of

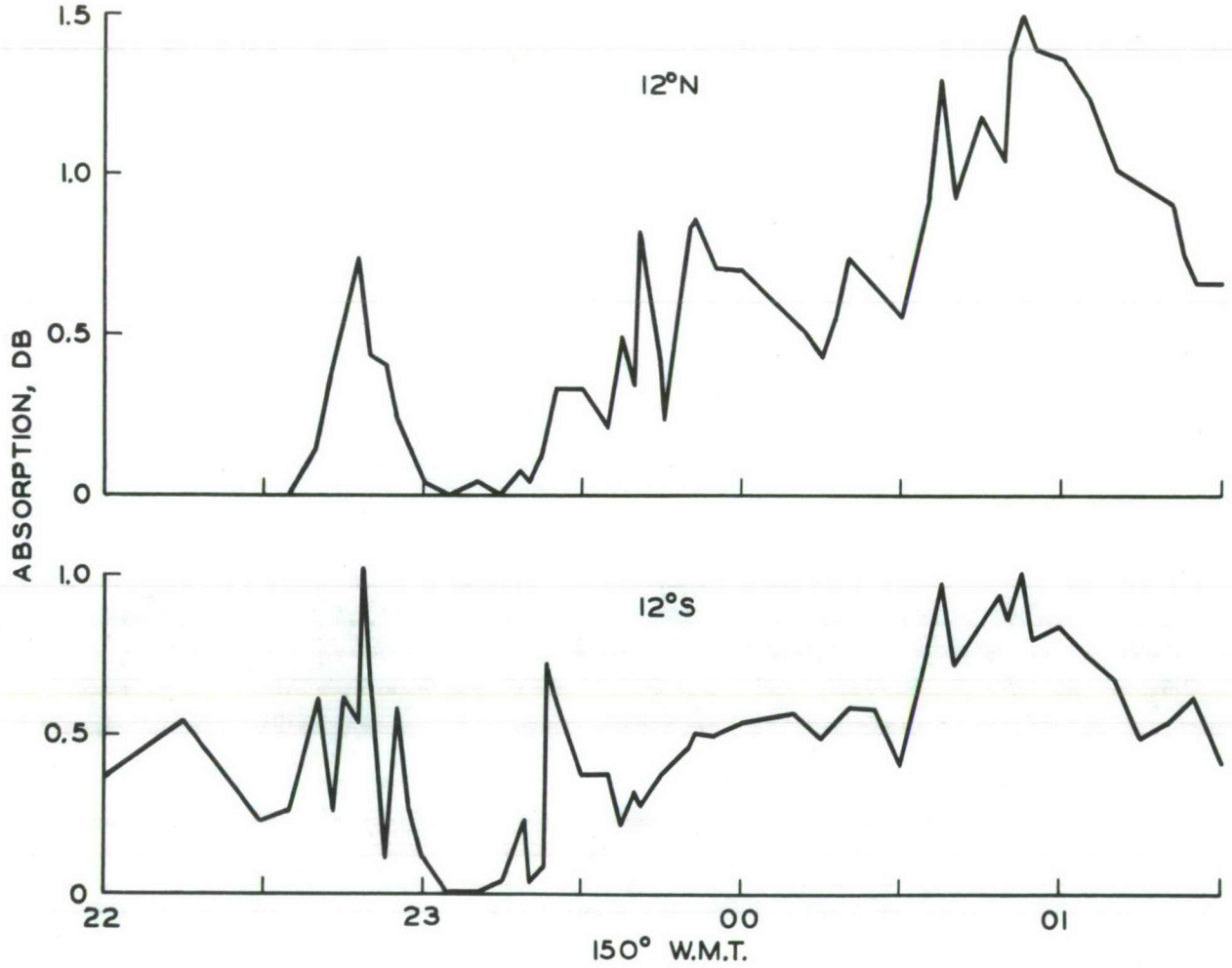

Fig. 40. Variations in absorption of radio-waves as measured by 12°N,S riometers on April 5-6, 1962 showing two extremely localized SAIs (sudden absorption increase). Visual observations as well as all-sky photographs indicated sudden brightenning of auroral arcs in limited regions of the sky.

λ5577A and also in conjunction with all-sky photographs. The results obtained are summarized below.

5.7.1 Simultaneous Study of Radio-Wave Absorption and λ5577A INTENSITY FLUCTUATIONS.

(1) A peak to peak correspondence between absorption fluctuations and intensity fluctuation of λ5577A was found in the pre-midnight hours. The sudden absorption increase, or SAI, was invariably found to be associated with sudden brightening of aurora or with the break-up phase.

(2) The correlation between absorption and auroral intensity fluctuations in the post midnight hours was sometimes good but sometimes extremely poor. It was found that the poor correlation existed only when a particular type of absorption event was observed. For identification purpose, this type of absorption was named SVIA or "slowly varying intense absorption". One peculiarity of this type is that the ratio of absorption to auroral intensity during an event is between 10-100 times higher than that which exists at the time of break-up.

(3) Genuine differences of as much as 2.5 db were occasionally noticed between absorptions in 12^{o}N and 12^{o}S directions. The aurorally associated absorption was sometimes found to be greater in the north and sometimes in the south. Because of a large number of ambiguous cases a statistical analysis of the absorption differences between 12^{o}N and 12^{o}S was not made.

By a simultaneous study of absorption suffered by radio waves originating from different parts of the sky and the all-sky camera photographs, certain interesting results were obtained which are as follows:

5.7.2 Quiet Phase of the Auroral Display

The radio-wave absorption associated with the quiet phase was found to be less than a db or so and was found to be limited to the luminous arc. Thin arcs which did not cover an appreciable fraction of the antenna beam did not cause any noticeable absorption. Only those quiet arcs which covered a large fraction of the antenna beam caused significant absorption. Even when the beam of the 12^{o}S antenna was fully covered with a quiet arc the absorption was found to be less than a db. The above observations do not support the view that the absorbing region is spread over a larger area of the sky than that occupied by the luminous arc itself.

5.7.3 The Bright and Active Phase

The SAIs or sudden absorption increases were found to be associated with auroral arcs that became suddenly bright and active. It was found that the SAIs could be classified into three categories,

(a) uniform (b) non-uniform (c) localized.

The localized SAIs were studied in detail in conjunction with all-sky photographs. It was found that the localized SAIs were associated with auroral arcs which suddenly became bright and active in a localized region of the sky. Moreover it was found that SAI was observed in a given direction only when the beam of the antenna used for cosmic noise signal reception enclosed a significant portion of the bright and active aurora. The above observation suggests that strong absorption is limited to that region of the sky where bright and active part of the display lies.

It was shown by an example that it is possible to deduce gross features of auroral displays in the pre-break-up and break-up phases by observing absorptions in different parts of the sky. The technique may be further improved by providing a continuous coverage of absorption taking place along the magnetic meridian using several narrow beam antennas pointed at different directions.

5.7.4 The Post Midnight Phase of the Display Associated with SVIA.

During a clear night when a mild SVIA was in progress, the all-sky photographs indicated faint and diffuse aurora over all the sky. In the post-midnight phase, absorption increases were not necessarily accompanied by increased luminosity. The ratio of absorption to auroral luminosity was found to be considerably higher during the post midnight phase than the corresponding ratio at the time of auroral breakup; a result which agrees with the earlier result obtained by a simultaneous study of absorption and λ5577A intensity fluctuations.

CHAPTER VI

A CLASS OF PECULIAR DAYTIME EVENTS

6.1 INTRODUCTION

It was mentioned briefly in Chapter I that the absorption frequently observed during the daytime at high latitudes, shows characteristics similar to those shown by the nighttime aurorally associated absorption and therefore, is also referred to as auroral absorption, although no visual aurora is associated with it. The so called daytime auroral absorption is often more intense than that which occurs during the night. The above observation led Chapman and Little to suggest that the higher absorption prevalent during the day may be explained because of the photodetachment process which is operative only during the day. The above authors carried out calculations of the expected day and night absorptions by assuming the midnight particle flux to be twenty times the noon flux. Their calculations showed that the photodetachment process could account for higher absorption during the day even though the daytime particle flux was assumed to be much smaller than the nighttime flux.

In this chapter, evidence will be presented to show that some of the daytime absorption events exhibit entirely different characteristics from those showed by the nighttime events and therefore one is not justified in using the name auroral absorption for them. The entirely different characteristics of the daytime events to be discussed in this chapter suggest that their causative mechanism is probably not the same as that of a typical aurorally associated absorption event. A difference of the causative mechanism could either imply ionization by two different

kinds of primary particles, i.e. electrons and protons, or ionization by primary particles of the same kind but having vastly different energies. In any case, it is obvious that the reasoning of Chapman and Little cannot be applied for daytime absorption events which show different characteristics from the nighttime events. Their calculations can explain only those cases of higher daytime absorption for which one is sure that the relevant primary particles are of the same kind and of approximately of the same energy as those responsible for the nighttime absorption.

6.2 DAYTIME ABSORPTION EVENTS POSSIBLY OF NON-AURORAL ORIGIN

Figure 41 gives the original 40°N,S and 12°S riometer records for November 6, 1962, showing an absorption event that exhibits characteristics entirely different from those of a nighttime aurorally associated event.

Referring to the results of Chapter V, it will be recalled that all nightime absorption events show irregular fluctuations in absorption which are more pronounced during one phase of the event than in the other. Moreover, the aurorally associated absorption was sometimes found to be greater in the north and sometimes in the south. It was also shown that a pronounced negative bay in the H-trace of the magnetogram is invariably associated with the typical aurorally associated absorption.

The daytime absorption event of November 6, 1962 conforms to none of the above description. In fact both its appearance and characteristics are closer to a polar cap absorption event than to an aurorally associated absorption event.

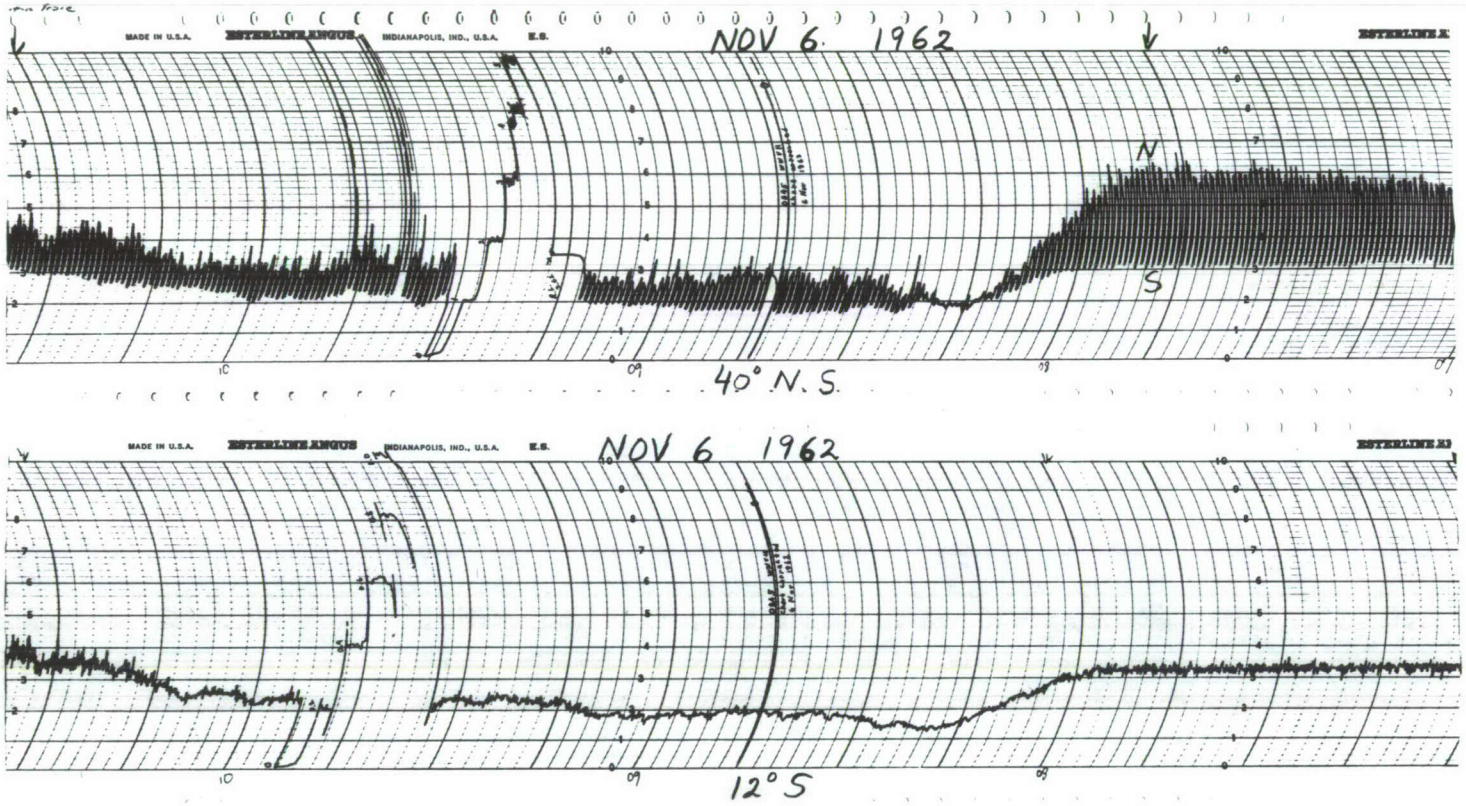

Fig. 41. Original 40°N,S and 12°S riometer records illustrating a peculiar daytime event which exhibits a consistent tendency of occurrence between 8 A.M.-10 A.M. The event also is peculiar in the sense that it is almost completely devoid of rapid fluctuations in the signal level which are invariably found in nighttime events. Unlike auroral absorption events which are associated with large negative bays in the H-trace, the peculiar daytime event illustrated in Fig. 41 is not connected with any noticeable increase in magnetic activity, with the possible exception of micropulsations.

The characteristics of the peculiar daytime event are as follows:

(1) The absorption increase is very smooth, gradual and devoid of any fluctuations. Usually there are no fluctuations in absorption during the event, and whenever fluctuations do occur they appear to be superimposed on a smooth trend.

(2) The absorption in the 40°N direction, is considerably greater than that in the 40°S direction, throughout the event.

(3) The most favored time of occurrence appears to be between 0800-1000 hrs, local time.

(4) The event is accompanied by weak magnetic activity or no magnetic activity.

6.2.1 The Event of October 16, 1962.

The daytime absorption event of October 16, 1962 is shown in Figure 42. Note the absence of large fluctuations, which are characteristic of all nighttime events, and the slow and smooth onset of the event. The absorption in the 40°N direction started to increase a few minutes earlier than that in the 12°S and 12°N directions. At the peak of the event i.e. at 0923 hrs, the absorption in the 40°N direction was greater than that in 40°S direction by more than 2.5 db, while at the same time the absorption in the 12°S direction was greater than that in the 12°N direction by 1.5 db. According to the analysis of section 4.12, the actual difference in absorption between 12°S and 12°N is ambiguous. Most probably, the higher absorption in the 12°S direction was caused by a greater contamination by the 40°N side lobe which registered an absorption of close to 8 db.

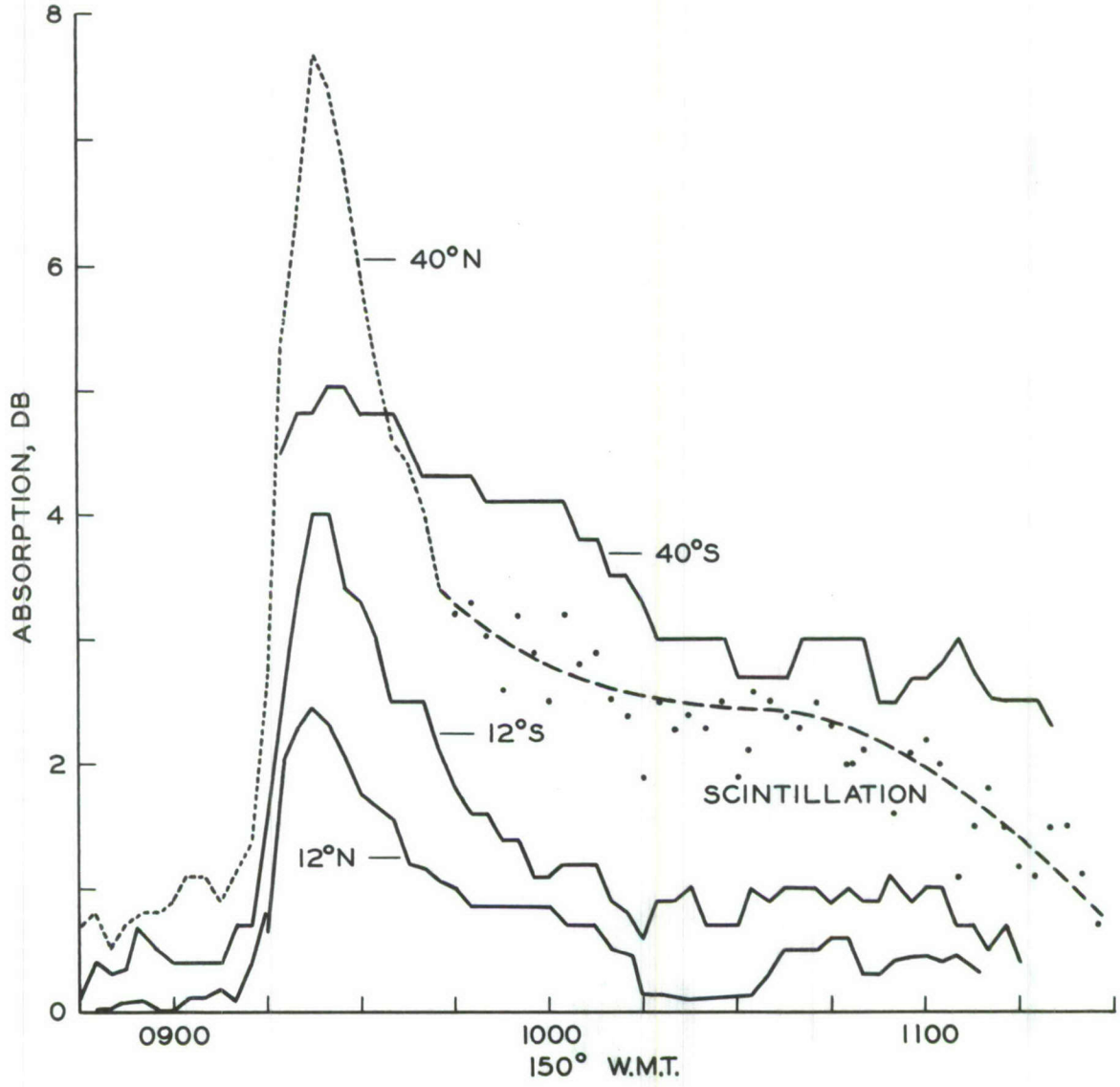

Fig. 42. Variations in absorption of radio-waves measured by 40°N,S and 12°N,S riometers on Oct. 16, 1962 illustrating the characteristics of the peculiar daytime event. Compare with Fig. 43.

Figure 43 gives the College magnetogram for October 16, 1962. Comparing Figure 43 with the absorption event given in Figure 42, it will be noticed that there was no pronounced magnetic activity in the early morning hours when the above event was observed.

6.2.2 The Event of October 22, 1962

The daytime absorption event of October 22, 1962, given in Figure 44, is the most intense event belonging to the special category of daytime events being discussed in this section.

The absorption increase in this event was smooth as usual but was considerably slower than the event discussed previously. Between 1220-1320 hrs large fluctuations in absorption occurred which appeared to be superimposed on a smooth event. The absorptions in the 12°N and 12°S directions appeared to be equal between 1145-1215 hrs, although differences of more than 3 db existed between the 40°S and 40°N directions. Referring to the analysis of section 4.12, it follows that the true absorptions in the former directions may not have been equal on account of the fact that the 12°S position was contaminated more by the 40°N side lobe than the 12°N position was by the 40°S side lobe. Later on after about 1215 hrs, the absorption in the 12°S direction appeared to rise above that in the 12°N direction and continued to be higher throughout the rest of the event except at the very end.

The higher values of absorption in the 12°S direction as compared to that in the 12°N direction, throughout most of the event, are interpreted as being caused by a strong contamination from the 40°N side lobe. It is therefore concluded that the

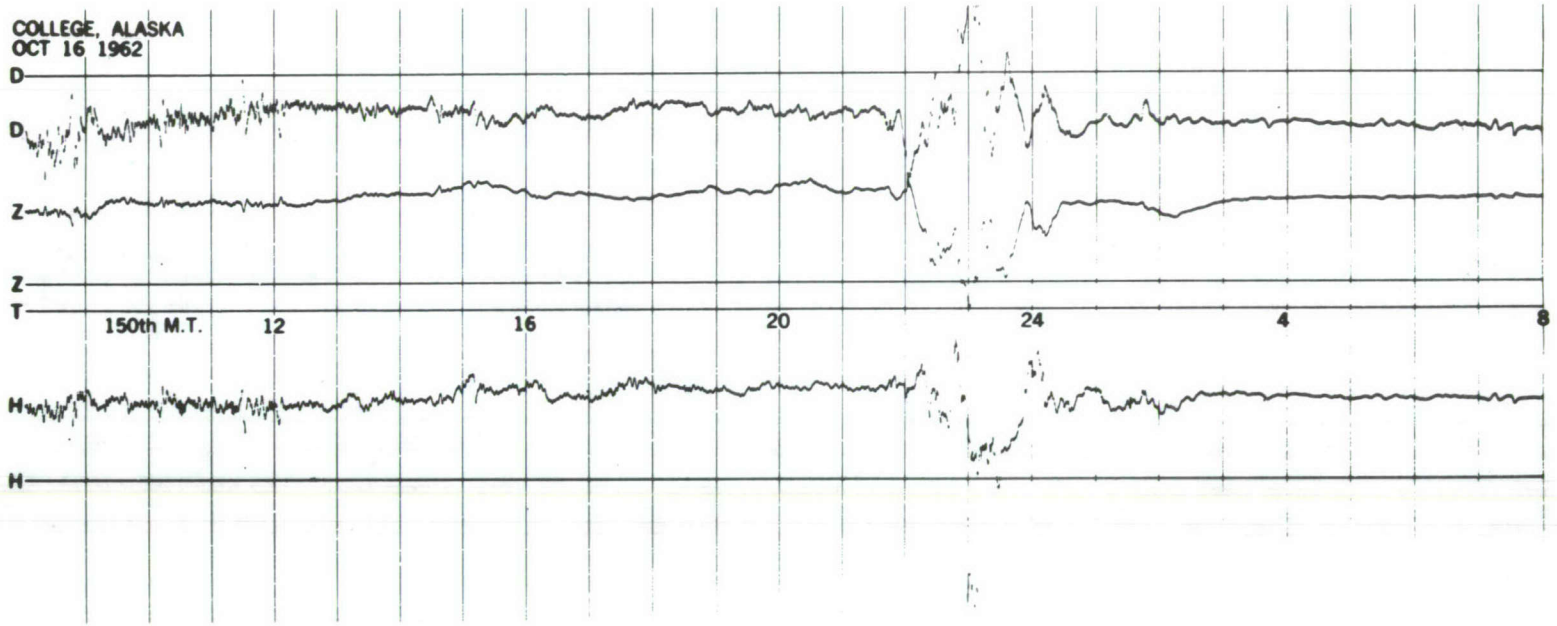

Fig. 43. College magnetogram for Oct. 16, 1962. Note the absence of any pronounced magnetic activity during the duration of the absorption event of Fig. 42.

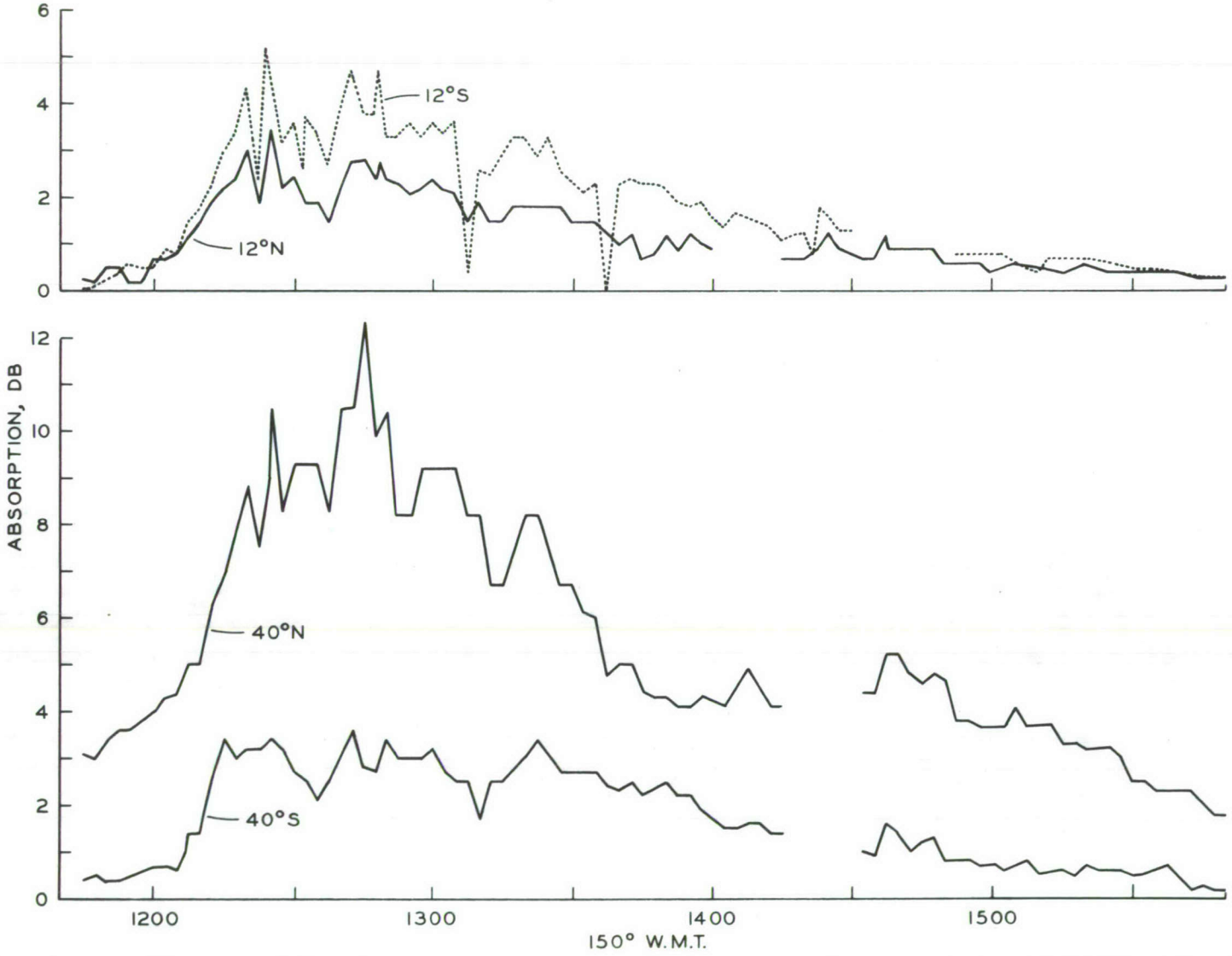

Fig. 44. The absorption event of Oct. 22, 1962. Fig. 44 illustrates a case of later than usual occurrence of the peculiar daytime event.

observed differences between the 12°S and the 12°N directions during this event do not represent the true differences existing at that time.

The enormous differences in absorption between the 40°N and 40°S directions are very striking. Note that at 1245 hrs, there existed a difference of 9.5 db between the absorptions in the two directions. The above observed difference represents the largest of all differences observed so far between the 40°S and the 40°N directions. Throughout the event, the absorption in the 40°N direction was considerably greater than that in the 40°S direction.

Referring to the nighttime events discussed in the previous chapter, it will be recalled that a typical aurorally associated event shows irregular variations and more or less a random character. During the same event the absorption in the 40°S direction may exceed that in the 40°N direction on several occasions and vice versa. The absorption graphs for the two directions may intersect several times during the same event implying random variations of the absorbing mechanism.

Referring to Figure 44, it may be seen that the event under discussion does not conform to any of the above characteristics of an aurorally associated event, and therefore one is justified in concluding that their causative mechanisms are not the same.

6.2.3 The Event of February 13, 1963

The absorption event of February 13, 1963, shown in Figure 45a, appears to be a departure from the smooth and regular absorption increases encountered in previous events. However, the general trend of the 40°N absorption is definitely that of a

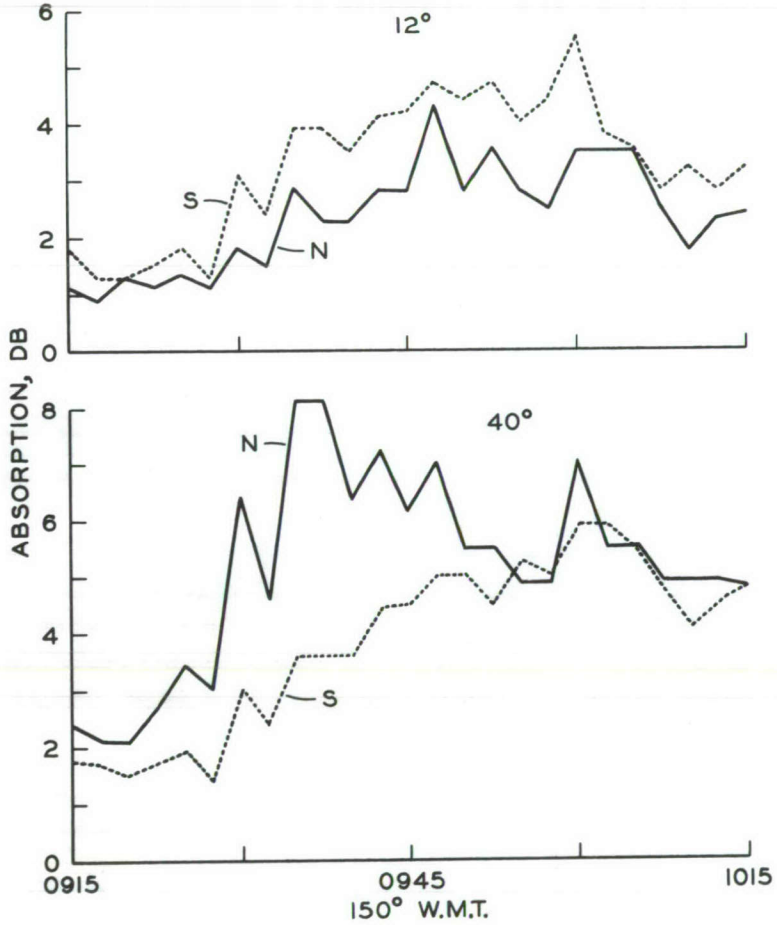

Fig. 45-a. The absorption event of Feb. 13, 1963 illustrates the case of fluctuating absorption superimposed on a smooth absorption event.

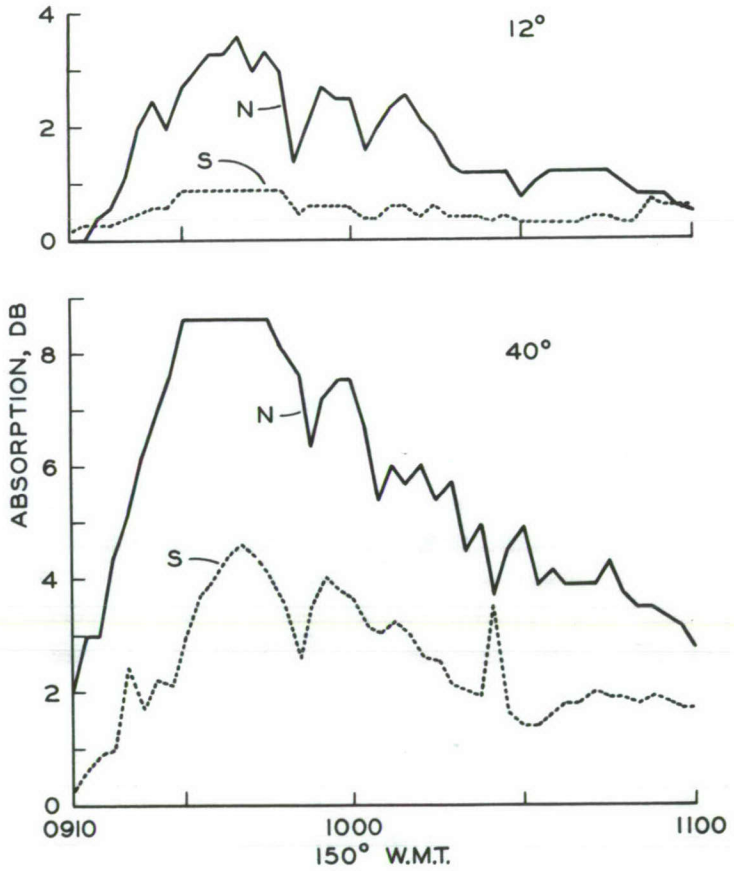

Fig. 45-b. The absorption event of Jan. 14, 1963. Note the existence of genuine differences in absorption between 12°N and 12°S with a peak value of as high as 2.5 db.

gradual increase on which irregular fluctuations seem to be superimposed. It appears from the absorption graph that two different physical processes were responsible for the D-region ionization during the event of February 13, 1962. One of the processes appears to have caused the slow and gradual increase in absorption, while the other process superimposed the characteristic fluctuations of auroral absorption. It is tentatively suggested that the slow and gradual increase in absorption was caused by protons, whereas, electrons were responsible for the irregular fluctuations.

6.2.4 The Event of January 14, 1963.

The daytime absorption event of January 14, 1963, shown in Figure 45b, also belongs to the category of special daytime event being discussed in this chapter. The above event is especially interesting because of the fact that the absorption in the 12^{o}N direction was genuinely higher than that in the 12^{o}S direction throughout most of the event. The maximum difference of 2.5 db in absorptions between the above two directions occurred at about 0940 hrs. At the same time, the absorption in the 40^{o}N was greater than that in the 40^{o}S direction by about 4 db.

The pattern of absorption observed on this day may be explained by a gradual decrease in the flux of primary particles from the north to the south.

6.2.5 The Event of October 17, 1962.

The weak daytime event of October 17, 1962, shown in Figure 46, was observed in the 40^{o}N direction but not in the 12^{o}S, 12^{o}N, or 40^{o}S directions. It should be noticed that the time of

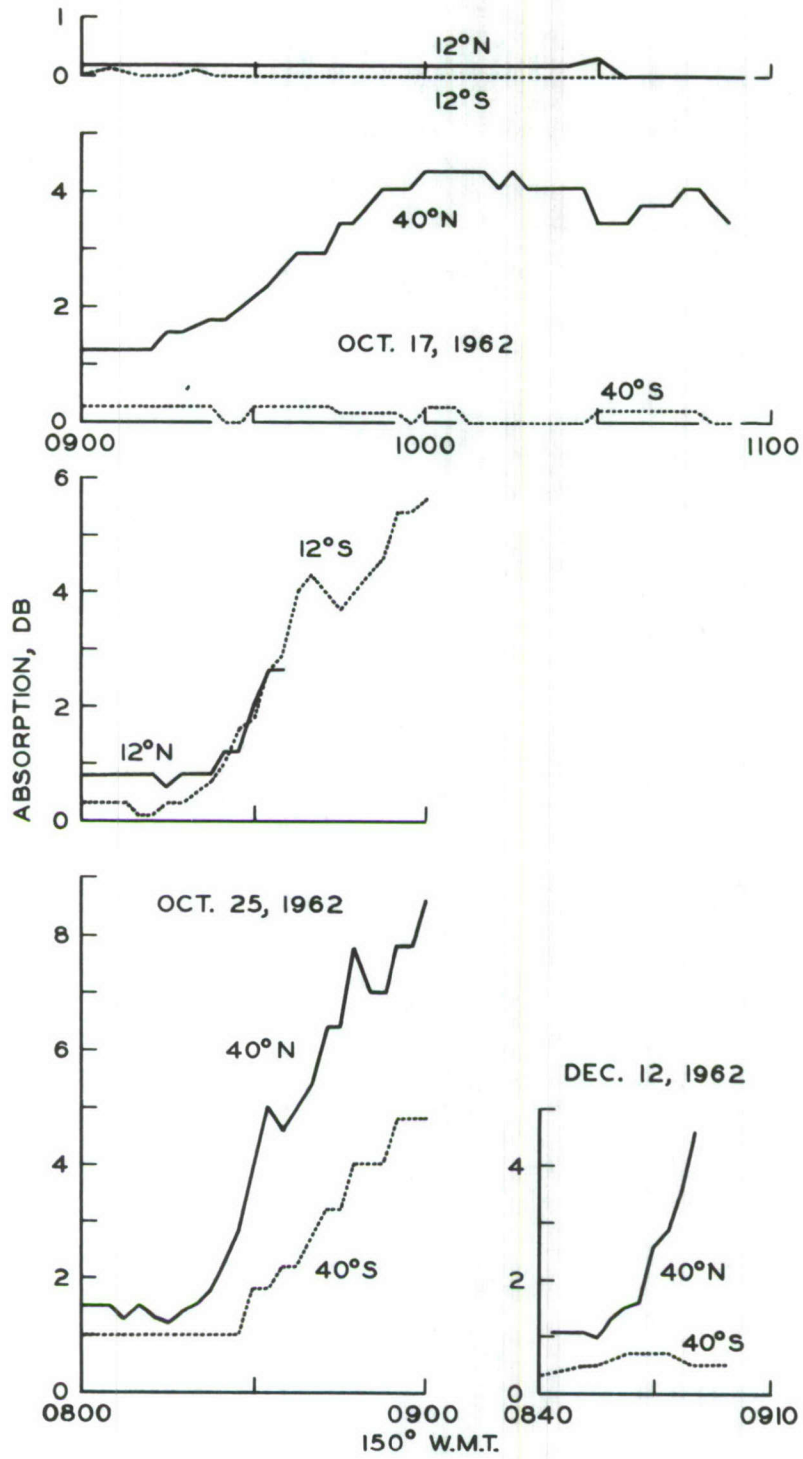

Fig. 46. The absorption events of Oct. 17, Oct. 26 and Dec. 12, 1962 illustrating consistent occurrence of higher absorption in the north than in the south between the hours 8 AM - 10 AM.

occurrence, i.e. 0900-1100 hrs, the smooth and gradual onset, and the fact that the absorption in the 40°N direction was greater than that in the remaining three directions by more than 4 db, suggests that the above event belongs to the special category of daytime events being discussed in this section.

The only possible interpretation of the occurrence of absorption in the 40°N direction and not in any other is that the primary particles responsible for the D-region ionization during the above event precipitated to the north of College and that there was a cutoff in the precipitation somewhere between the 12°N and 40°N directions. The possible nature of the cutoff will be discussed later in Chapter VII.

6.2.6 The Event of October 25, 1962.

Figure 46 gives the early part of the daytime absorption event of October 25, 1962. The later part of the event, showing the recovery, was unfortunately lost due to calibration of the riometers at that time.

Referring to Figure 46, it may be seen that the smooth and gradual absorption increase occurred first in the 40°N and the 12°S direction followed by an increase in the 12°N and 40°S directions after about 3 minutes and 8 minutes respectively. The earlier increase in the 12°S direction as compared to that in the 12°N direction was obviously due to side lobe contamination. Throughout the event, the absorption in the 40°N direction was greater than that in the 40°S direction with a maximum difference of about 3.8 db. The absorptions in the 12°S and the 12°N directions did not appear to be too different in the early phase of

the event. According to the analysis of section 4.12, however, it does not necessarily follow that the true absorptions in the above directions were also equal at that time, on account of the ambiguity of the side lobe contribution.

6.2.7 The Event of December 12, 1962.

Figure 46 gives the initial phase of the daytime event of December 12, 1962 which was observed in the 40°N direction and not in the 40°S. The later part of the event was unfortunately lost because of routine calibration of riometers, usually done between 0800-0900 hrs. The smooth and gradual absorption increase, the time of its occurrence, the absence of magnetic activity, and the fact that the absorption in the 40°N direction was much greater than that in the 40°S direction, all conform to the characteristics of the peculiar daytime event which was described in the beginning of section 6.2.

6.3 SUMMARY OF RESULTS

The daytime events discussed in this chapter belong to a group which exhibits the following characteristics:

(1) Slow and smooth onset usually devoid of random fluctuations.
(2) Lack of pronounced magnetic activity at the time of onset.
(3) Persistent occurrence between 0800-1100 hrs.
(4) Absorption to the north of College much greater than to the south throughout the event.

The possible causative mechanisms of this class of events will be discussed in the next chapter.

CHAPTER VII

DISCUSSION OF RESULTS, CONCLUSIONS, AND RECOMMENDATIONS FOR FUTURE WORK

7.1 INTRODUCTION

In this chapter the results obtained in the previous chapters will be discussed and compared with those of other workers.

Different workers disagree concerning the simultaneity of occurrence of absorption and visual aurora. Some workers, [Holt and Omholt (1960), Gustaffson and Ortner (1962)], having obtained good correlation between absorption and the auroral intensity fluctuations at λ5577A, have ventured to suggest that the primary particles responsible for the D-region ionization, which in turn causes radio-wave absorption, must be the same as those that cause auroral excitations. On the other hand Kavadas (1961) found very little connection between the occurrence of intense absorption and the appearance of discrete auroral forms in the receiving antenna beam.

It was shown in Chapter V that a typical aurorally associated absorption event exhibits certain discrete phases. It was also shown that some of the absorption phases are closely linked with the phases of the auroral display, as the fluctuations of absorption during these phases correlate well with those of λ5577A intensity. One particular type of absorption event observed in the post midnight hours, however, consistently showed no correlation with auroral intensity fluctuations. Moreover a significent increase in the ratio of absorption to λ5577A intensity. was especially striking whenever the above event occurred.

In the light of the above results, one would like to know what can be inferred about the physical mechanisms of aurorally associated absorption in general, and about those of its various phases in particular.

The first step towards understanding the main physical process of auroral absorption is to know the relative contributions of X-rays and primary electrons to the total absorption. The above step will not only enable one to pinpoint the process which is of prime importance, but will also hopefully end the controversy which has been going on for several years regarding the role of bremsstrahlung X-rays in the D-region ionization.

Having selected the one physical process which is of utmost importance, the next step would be to consider the variations required in the said process, i.e. changes in flux and energy spectrum etc., in order to explain the various phases of an absorption event. The third and most important step is to show that the deduced changes in the flux or the energy spectrum are in reasonable agreement with the results of various particle measurements made by use of rockets.

7.2 DISCUSSION OF RESULTS

7.2.1 Absorption and Visual Aurora.

The results presented in Chapter V, after a detailed study of radio wave absorption in conjunction with the intensity variations of λ5577A radiation and all-sky photographs, indicated a close association between absorption and some phases of the auroral display. In particular, for all cases studied, it was

found that the absorption associated with both quiet as well as bright and active phases of the display was limited to luminous regions of the sky only. There was no evidence to indicate that the absorption in the presence of discrete auroral forms covered a wider area than that covered by luminous aurora. The above observation seems to contradict a statement by Chapman and Little (1957) implying that the radio-wave absorption is more widespread over the sky than is the visible aurora. It is not clear from their statement whether they were referring to discrete auroral forms generally prevalent in the pre-midnight hours or to the diffuse broken-up aurora of post-midnight hours. In the latter case, there is no disagreement between the results of this investigation and their statement on account of the fact that poor correlation was generally found between absorption and auroral luminosity in the post-midnight hours. However, in the former case the experimental results obtained by the present investigation seem to differ markedly from their statement.

The result obtained in Chapter V pertaining to the insignificant absorption caused by the pre-break-up or quiet auroral forms, agrees with that of Little and Lienbach (1958). The above authors also found that the break-up phase of aurora was not necessarily associated with strong absorption. From the results of the present investigation, it follows that a sudden absorption increase is invariably associated with the break-up provided a significant portion of the receiving antenna beam is filled with the bright and active part of the display. Although the magnitude of the peak absorption varied between 1-13 db, from one break-up to the

other, the sudden absorption increase associated with the break-up was unmistakably identifiable in all cases studied.

Heppner, Byrne, and Belon (1951), Little and Leinbach (1958), and Campbell and Leinbach (1961) reported the incidence of strong absorption in a large number of cases when pulsating or flaming aurora was present in the sky. Major (1954), who observed the occurrence of polar blackouts in the southern hemisphere at Macquarie Island in conjunction with auroral displays, also confirmed the results of Heppner et al. Owing to cloudy skies in almost all the nights which showed strong absorption in the post midnight hours during the course of the present study, it was not possible to relate the absorption with the type of aurora present in the sky. However, the frequently observed auroral luminosity fluctations and the absorption data did not show a one to one correspondence. Several cases of strong absorption with no pulsating aurora and strong pulsating aurora with only weak absorption were noticed. The above observation does not necessarily contradict the result of Heppner et al as they themselves did not find a one to one correspondence between the occurrence of the two phenomena. It seems quite probable that the strong post-midnight absorption discussed by these authors is the same event which has been referred to as SVIA in the present study.

Holt and Omholt (1960) found a good correlation in Norway between the absorption measured by a wide beam antenna and the intensity fluctuations of the green auroral line. The above authors plotted the absorption and the relative intensity at λ 5577A for selected nights and found a considerable change in

the slope of the best fitting straight line from one night to the other. They argued that the change of the slope is indicative of a change in the primary electron spectrum. It would be recalled that, in the course of the present study, a significant increase in the ratio of absorption to auroral intensity, from the break-up to the slowly varying intense absorption phase, was found in all cases discussed in Chapter V. The observation referred to above seems to confirm Holt and Omholt's result with the exception that in the present study significant changes in the ratio of absorption to auroral intensity were noticed during the same night, whereas the above authors noticed changes from one night to another. The full implications of the change in the ratio, from one phase of the event to another, will be considered in detail under the discussion of physical mechanisms.

Holt, Landmark, and Lied (1961) operated a network of five closely spaced riometer stations in Norway, all of which used 3-element Yagis as the receiving antennas. The above authors studied an auroral absorption event in conjunction with all-sky photographs and found good agreement between absorption and the auroral activity at each station. However, these authors indicated that in general the correspondence between auroral activity and absorption was not one to one. The lack of association between auroral activity and absorption, if observed by the above authors during pre-break-up and break-up phases of the display, may be explained by the fact that their use of wide beam antenna at each station resulted in a considerable overlap between the antenna beams of the five stations. It should be emphasized here

that a wide beam antenna such as a 3-element Yagi receives cosmic noise signals from a much wider area of the sky than that intercepted by the half power cone. The above statement is even more true if regions of higher sky temperatures happen to be situated outside the 3 db beamwidth of the antenna. In such cases, if a bright and active arc happens to be just outside the half power beam covering a region of high brightness temperature, considerable absorption may be observed although the auroral activity may appear to be outside the antenna beam (half power).

The results of the present study, indicating a close association between the occurrence of bright and active aurora in the antenna beam and absorption, are not in good agreement with those obtained by Kavadas (1961) at Saskatoon, Canada. His receiving antenna consisted of a linear array of 16 folded dipoles and had beamwidths of 6.5^{o} and 72^{o} in the north-south and east-west directions respectively. In order to explore the absorption differences between adjacent areas of the sky and their relation with visual auroral features, Kavadas switched the main beam periodically to 3^{o} on either side of the zenith, in the north-south plane. The above author found a close association between the occurrence of absorption and aurora in some cases, whereas no such relation was found in others. Kavadas has not given detailed particulars of the events and therefore it is not possible to say whether those events which showed poor correlation with auroral activity are the same as the SVIA events of the present study, which exhibit similar behavior. He described a particular case in which the absorption increase was noted when

the auroral arc was to the north outside the antenna beam. Superficially it seems that the above observation is very similar to some of the cases discussed in Chapter V section 4.12, which were explained by a strong side lobe contamination. However, it is not possible to say this with certainty in the above case, as Kavadas has neither given the magnitudes and positions of the side lobes, nor has he given any indication that the radiation pattern of his array was measured.

The localized sudden absorption increases of the present study are probably the first to be discussed extensively but are by no means the first to be reported. Jelly, Mathews, and Collins (1961), observed one such event at Churchill on September 18, 1959, by using two separate antennas, one of which was directed towards the zenith and one of which was directed towards the north celestial pole. The zenith riometer recorded an absorption of 8 db at 2200 hrs, whereas the north polar riometer showed no absorption. The above authors however, did not attempt to study the event in detail in conjunction with the auroral features existing at that time.

7.3 THE RELATIVE CONTRIBUTIONS OF X-RAY AND PRIMARY ELECTRON IONIZATION TO THE AURORAL ABSORPTION.

It should be recalled that the X-ray photon spectrum and the resultant rate of electron production deduced in Chapter III were based on the assumption that monoenergetic electrons of 10 kev energy and of 8×10^{10} cm^{-2} sec^{-1} monodirectional flux were incident over a large area of the ionosphere. The calculations of the X-ray intensity took into account the polar diagram of X-ray emission and the energy loss of primary electrons as a

result of collisions. It was shown that as far as the ionization of the D-region is concerned, X-rays in the energy range 1-10 kev are far more important than those of much higher energy.

Using the results of the generalized magnetoionic theory given in Chapter II, the expected radio wave absorption at 36 Mc/s will be calculated in this section for (a) a D-region ionized by monoenergetic and monodirectional electrons of 10 kev energy and of 8×10^{10} cm^{-2} sec^{-1} flux, (b) a D-region ionized by the X-ray spectrum generated as bremsstrahlung of the above electrons.

The calculations for case (a) proceeded in the following steps.

(1) The rate of electron production per electron, (q), was deduced from Figure 6 page 68 for various heights above ground.

(2) The total rate of electron production was obtained by multiplying the q values by the flux.

(3) Using Table 4 page 76, the equilibrium electron density profile was determined.

(4) The ionosphere, between the stopping height of the electrons and 100 km, was divided into slabs of 1 km thicknesses. The absorption suffered by a radio wave of 36 Mc/s frequency, while passing through each of these slabs, was determined by multiplying the electron density at the mid-point of the slab by the appropriate value of Adb/km (Absorption in db per km) tabulated by Chorbajian et al.

(5) The total absorption suffered by the wave was determined by summing up the individual contributions of all the slabs.

The calculations for the case (b) proceeded in similar steps except that since the total rate of electron production due to the X-ray spectrum was already calculated in Chapter III, steps (1) and (2) were not needed. In case (b), the ionosphere between 60-100 km was divided into slabs of 2 km thickness and the total absorption was calculated in essentially the same steps.

The result of calculations are as follows:

Total absorption as a result of ionization of the D-region by the primary electrons = 5.0 db

Total absorption as a result of the D-region ionization by the X-rays generated as bremsstrahlung of the primary electrons = 0.14 db

The ratio of the absorptions caused by the two processes is close to 40:1, which means that ionization by primary electrons is the process which contributes to most of the auroral absorption. Moreover the contribution of X-rays generated as bremsstrahlung of the primary electrons, is too small to be detected even under extreme cases.

The above result appears to be in sharp contrast with that of Chapman and Little (1957), who sought to explain the seemingly wider-than-visual characteristic of auroral absorption on the basis of the D-region ionization by bremsstrahlung X-rays. The above mentioned authors have apparently based their calculations on a height independent X-ray photon flux value of 10^5 cm^{-2} sec^{-1} and have disregarded the continuous X-ray spectrum. Both of these assumptions are severe approximations which are open to

question. The rough calculations made by Chapman and Little showed that a daytime absorption of 9.25 db and a nighttime absorption of 2.4 db can be attributed to the action of the X-rays.

7.4 THE POSSIBLE CHANGES IN THE ENERGY SPECTRUM AND FLUX OF THE PRIMARY PARTICLES FROM ONE ABSORPTION PHASE TO ANOTHER.

Having established the preponderance of one of the two physical processes which could cause auroral absorption in general, one wonders what changes the said process must undergo in order to cause the various distinguishable phases of absorption. In particular, one would like to know what the transition from one absorption phase to another entails in terms of the changes in the flux and the energy spectrum of the primary electrons.

In order to give a satisfactory answer to the above question, the absorption expected as a result of the D-region ionization caused by primary electrons of energy 10-100 kev was calculated in accordance with the steps given in the previous section for different values of electron flux ranging between 10^3-10^{11} electrons cm^{-2} sec^{-1}. The calculated values of the total absorption in decibels for a radio wave of 36 Mc/s are given in Table 7.

It should be emphasized here that the above calculated values are sensitive to the values of rate coefficients used, to the atmospheric model employed, and to the collision frequency profile assumed.

Table 7.

Electron Energy kev	Flux Particles cm^{-2} sec^{-1}	10^3	10^4	10^5	10^6	10^7	10^8	10^9	10^{10}	10^{11}
10					.02	.06	.18	.57	1.82	5.74
20					.15	.48	1.52	4.82	15.23	
30				.12	.37	1.18	3.73	11.80		
50			.09	.29	.93	2.94	9.29			
100		.07	.23	.73	2.32	7.33				

The total (computed) absorption in decibels at 36 Mc/s associated with primary electrons of various energies and fluxes.

7.4.1 The Energy Spectrum and Flux of Primary Electrons Responsible for Pre-Break-up Absorption and SAI.

The close relation between auroral luminosity and absorption both in the quiet and bright and active phases suggests that the primary particles causing the D-region ionization and resulting radio wave absorption are the same as those which cause auroral excitation, i.e. they have energies of less than 20 kev or so. The above conclusion is also supported by the fact that in both of the above phases, absorption was found to be limited to the luminous regions of the sky. Had there been a significant contribution to the D-region ionization by electrons of much higher energy than 20 kev at the time when discrete auroral forms were present in the sky, it would have been possible at times to detect absorption outside a discrete arc. Referring to Table 7, it may be seen that if the flux of electrons in the energy range 50-100 kev were of the order of 10^6 electrons cm^{-2} sec^{-1},

the resulting absorption could be as high as 2 db, whereas the corresponding increase in the intensity of λ3914 would be negligibly small according to rough calculations by Chamberlain (1960). In the light of above discussion it seems logical to conclude that the absorption associated with the quiet as well as bright and active phases of the display are caused by electrons of less than 20 kev energy. The differing characteristics exhibited by absorption in the two phases may be explained by a pronounced change in the flux of these low energy electrons. Referring to Table 7 it may be seen that a flux of 10^7-10^8 electrons cm^{-2} sec^{-1} in the energy range 10-20 kev can adequately account for the absorption associated with the quiet phase. The sudden increase in absorption coincident in time and space with the sudden increase in auroral luminosity at the time of break-up suggests a sudden increase in the number of electrons of less than 20 kev energy. Again referring to Table 7, it follows that if the quiet arc electron flux of 10^7-10^8 electrons cm^{-2} sec^{-1} suddenly increased to some value between 10^9-10^{10} electrons cm^{-2} sec^{-1} momentarily, all cases of SAIs discussed in Chapter V can be adequately explained.

The above conclusion is in fair agreement with the results obtained by McIlwain who measured the primary particle flux by firing a rocket into a bright and active auroral arc at Fort Churchill. The results of his measurements indicated that the particle flux decreased suddenly above 10 kev but did not increase rapidly towards low energies in the vicinity of 4 kev, indicating a flat energy spectrum more or less. The above observation led McIlwain to conclude that 75% of the auroral luminosity in that

particular case must have been due to nearly monoenergetic electrons of 6 kev energy. The absence of electrons of energies greater than 10 kev at the time when bright and active auroral forms were present in the sky, supports the conclusion that the associated sudden absorption increase must be entirely due to an increased number of electrons of less than 10 kev energy. A 10 to 100 fold increase in the quiet arc flux of low energy electrons is sufficient to explain all cases of sudden absorption increases associated with the sudden brightening of aurora or break-up encountered in Chapter V.

7.4.2 The Energy Spectrum of Primary Electrons During a SVIA

The significant increase in the ratio of absorption to the intensity at λ5577A and the lack of correlation between absorption and the auroral intensity fluctuations in the slowly varying intense absorption phase (SVIA) are both indicative of a hardening of the primary electron spectrum, possibly due to the injection of a large number of electrons in the energy range 30-100 kev. Referring to Table 7, it may be seen that most SVIA events may be explained if the integral flux of 30-100 kev electrons increased to about 10^7 electrons cm^{-2} sec^{-1}.

In support of the above conclusion, the flux measurements of McDiarmid, Rose, Budzinski (1961), made at Fort Churchill at the time when the zenith riometer showed an unmistakable SVIA, very similar to that of November 23, 1962, are quoted. The above mentioned authors fired a rocket soon after a sudden absorption increase had occurred, and measured a peak flux of 2×10^6 electrons cm^{-2} sec^{-1} for energies greater than 30 kev and with an

integral energy spectrum of $e^{-E/22}$ kev. The flux of protons of energy greater than 500 kev was found to be 6×10^2 particles cm^{-2} sec^{-1} $sterad^{-1}$ and was not correlated with the electron flux in space or in time. Unfortunately, information about electrons of lower than 30 kev energy could not be obtained.

Although both rocket flights were made at Fort Churchill, significant differences in the energy spectrum are detectable between the results obtained by McIlwain and those obtained by McDiarmid et al. McIlwain's results, obtained during a bright and active display, indicated an absence of electrons of greater than 10 kev energy, whereas those obtained by McDiarmid et al, during a mild SVIA, indicated a peak flux of 2×10^6 particles cm^{-2} sec^{-1}, of electrons of energy greater than 30 kev. It is therefore logical to conclude, that the transition from SAI phase (sudden absorption increase), associated with the bright and active display, to SVIA (slowly varying intense absorption) phase is the result of hardening of the energy spectrum of the primary particles caused by the injection of 10^6-10^7 electrons cm^{-2} sec^{-1} of energy greater than 30 kev. McDiarmid et al came to the conclusion that the measured particle flux was sufficient to account for the observed cosmic noise absorption.

7.5 DISCUSSION OF THE CLASS OF PECULIAR DAYTIME EVENTS

The results obtained in Chapter VI indicated that the daytime events discussed therein belonged to a separate group of absorption events whose characteristics are closer to the polar cap absorption than to the auroral absorption. However, the events

cannot be classified as weak polar cap events in view of the fact that the riometer at Thule did not show any absorption at the time when these events were observed. Moreover, unlike polar cap events, the peculiar daytime events were only of a few hours duration and no solar flares stronger than 1 were noticed on the dates of occurrence of the said events. Also, in view of their persistent occurrence between 0800-1100 hrs, it seems unlikely that these daytime events could be linked in any manner with the occurrence of solar flares.

It should be recalled that throughout the duration of the above class of events, absorption to the north of College was much greater than that to the south. The absorption event of October 22, 1962 showed a spectacular difference of 9.5 db between the absorptions in the 40°N and the 40°S directions. Numerous cases throughout the present study were noted in which the absorption belonging to the category under discussion occurred only in the 40°N direction and not in any of the remaining three directions, i.e. 12°N, 12°S, and 40°S. The above observation suggested that the precipitation of primary particles responsible for the absorption was cutoff somewhere between the 12°N and 40°N directions.

The main question, in the light of above discussion, concerns the possible causative mechanism of this class of daytime absorption events. It is quite clear that the causative mechanism of these events is not the same as that of the typical aurorally associated events discussed previously.

On account of their general resemblance with polar cap events and interpreting the cutoff exhibited by them as magnetic cutoff, it is suggested that the peculiar daytime events are caused by proton bombardment. It must be emphasized that a consistent occurrence of higher absorption in the north than in the south, as observed during these events, cannot be explained by electron precipitation. The idea of proton precipitation may seem to be a bit speculative, but it seems to be the only one which can adequately explain the various features of these events.

7.6 CONCLUSIONS

The following conclusions are based on the experimental results of Chapter V and VI and the discussions thereof given in Chapter VII.

The nighttime radio-wave absorption observed at College, Alaska falls under two main categories which are as follows.

The absorption belonging to the first category is observed at any time during the evening between 2000-0200 hrs, correlates well with the intensity fluctuations at λ5577A and is limited to luminous regions of the sky. The above category includes the absorption associated with the quiet as well as bright and active phases of the auroral display. The primary electrons responsible for the absorption belonging to Category I are definitely of less than 20 kev energy, possibly even less than 10 kev. According to the results of McIlwain's rocket flight, the primary particles may even be monoenergetic with about 6 kev energy. The various phases of absorption under the first category are explained by a

change in flux rather than by a change in the energy spectrum of the primary particles. A flux of 10^7-10^8 electrons cm^{-2} sec^{-1} in the 10-20 kev energy range is adequate to explain the absorption caused by a quiet arc. A sudden 10-100 fold increase in the above flux is adequate to explain the sudden absorption increase associated with the sudden brightening of aurora or break-up.

The absorption falling under the second category is observed only in the post-midnight hours, varies relatively slowly with time, and does not correlate with the intensity fluctuations of λ5577A. The rate of absorption increase is typically of the order of 0.5-1 db/min, persists for a long period of time, and causes very intense absorption. The ratio of absorption to λ5577A intensity is considerably higher for events of Category II than of Category I. It can be said with certainty that the contribution of electrons of less than about 20 kev energy to the absorption of Category II is negligibly small, and that almost all the absorption is due to electrons in the energy range 30-100 kev. It is estimated that a flux of 10^7-10^8 electrons cm^{-2} sec^{-1} in the energy range 30-100 kev can adequately explain all cases studied. The above conclusion is in good agreement with the rocket results of McDiarmid et al who obtained a peak flux of 2×10^6 during a relatively weak absorption event belonging to Category II.

Theoretical considerations showed that the absorption associated with the D-region ionization caused by bremsstrahlung X-rays is too small to be seriously considered. It is therefore

concluded that the aurorally associated absorption is solely due to the action of primary electrons.

Differences of as large as 2.5 db, frequently observed between absorptions at two adjacent areas of the sky such as 12^{o}S and 12^{o}N, suggest the patchiness of auroral absorption. It is concluded that the patchy character of auroral absorption is the result of patchy precipitation of primary particles.

The close association found between discrete auroral forms and absorption suggests that gross features of the auroral displays can be deduced by observing radio wave absorption by means of narrow beam antennas pointed at different directions along the magnetic meridian. In particular if the primary electrons associated with the bright and active phase of the display are assumed to be monoenergetic of about 10 kev energy [McIlwain (1960)], it follows that a fair estimate of the particle flux can be made from the observed value of peak absorption. The above observation is indicative of the enormous potentialities of narrow beam riometers, in the hitherto unexplored field of primary particle data deduction from absorption measurements alone.

The daytime radio wave absorption observed at College, Alaska also may be divided into two categories.

The absorption belonging to the first category varies irregularly in space and time and is similar in character to the nighttime absorption in general.

The absorption belonging to the second category occurs most frequently between 0800-1000 hrs, varies regularly both in space

and in time and is similar in character to the polar cap absorption. During an absorption event of the second category, the absorption to the north of College is several decibels higher than that to the south of College.

The differing characteristics exhibited by the absorptions belonging to the first and the second category strongly suggest different causative mechanisms, possibly electron and proton bombardment respectively.

7.7 RECOMMENDATIONS FOR FUTURE WORK

The results of the experimental investigation described in this dissertation have been very encouraging and fruitful in general. However, at several stages during the course of the study the need for a more sophisticated experimental approach was felt. The above feeling mainly stemmed from the fact that the narrow beam antenna used in the experimental study had strong side lobes because of electrical beam switching, and the contamination from these introduced an element of ambiguity in the interpretation of data. The use of the "side lobe monitors" resolved the ambiguity only in a small fraction of the total number of cases, while the majority of cases remained unresolved.

In the light of above discussion it is strongly recommended that in the future narrow beam arrays used in cosmic noise absorption studies, the level of the side lobes should be at least 15 db down. To meet the above requirement, it would be necessary to use large sized arrays whose individual elements will have much narrower beams than that of a 3-element Yagi. The twin 6-element

Yagi antenna used as a "side lobe monitor" appears to be an ideal choice for this purpose. It is estimated that a 6 x 6 array using twin 6-element Yagis will have a half power beamwidth of about 6^{o} and a main beam to side lobe power ratio of greater than 15 db.

On account of the approaching sunspot minimum, the aurorally associated absorption events are expected to be considerably weaker on the average. It is recommended that the frequency selected for the narrow beam riometer should be low enough so that a large number of events could be studied. The operation of a narrow beam array at some location to the north, such as Fort Yukon, in addition to one at College, is advisable.

The problems relating to the interpretation of riometer data, obtained by using a 3-element Yagi antenna, have already been adequately described elsewhere in the dissertation. It is strongly recommended that the 3-element Yagi antennas used at regular field stations be replaced as soon as possible with antennas of significantly narrower beamwidth, such as the twin 6-element Yagi. The satisfactory operation of two side lobe monitor antennas with a single riometer demonstrated that without loss of useful data it is possible to explore the absorption in two different regions of the sky with the same riometer. The operation of two antennas at each field site with a single riometer would result in a continuous measurement of absorption in two different parts of the sky at the same place and at the same time. By suitably directing the two antennas at each field site, it is possible to obtain a continuous coverage of the absorption taking place throughout the auroral zone.

The pronounced increase in the ratio of absorption to λ5577A intensity, from one type of auroral event to another is considered to be an important result. It is recommended that photometers with a wide dynamic range be used in the future to determine the above ratio.

The peculiar daytime event discussed extensively in Chapter VI does not seem to be aurorally associated. In order to determine its causative mechanism, it is recommended that balloons equipped with particle detectors be flown at the time when such an event is in progress.

The present study has adequately demonstrated that what is generally known as auroral absorption, consists of several distinguishable categories and sub-categories. However, the data on which the present study is based, was not spread over a long enough period to warrant a morphological study of each category and sub-category of high latitude absorption. In view of the above, it is strongly recommended that the observational program be continued preferably incorporating the suggested improvements relevant to the narrow beam antenna, so that a sound morphological study could be made in the future. By a sound morphological study, the author means a morphological study which individually takes into account the various distinguishable categories of auroral absorption and not that which considers the so called auroral absorption as a whole.

Sooner or later, one is bound to find that ground based equipment alone, no matter how sophisticated, is inadequate to unravel all of the mysteries of the aurora borealis and its associated geophysical effects. It is recommended for future work that balloons and rockets be seriously considered as complementary tools of research.

Appendix 1

Evaluation of $I = \int_0^{2\pi} \int_0^{\pi} \frac{\sin^3\theta}{(1-\beta\cos\theta)^4} \, d\theta \, d\phi$

Consider $\int_0^{\pi} \frac{\sin^3\theta}{(1-\beta\cos\theta)^4} \, d\theta = \int_0^{\pi} \frac{\sin\theta \sin^2\theta}{(1-\beta\cos\theta)^4} \, d\theta$

Integrating the above expression by parts

$$= \left[-\frac{1}{3\beta} (1-\beta\cos\theta)^{-3}\sin^2\theta \right]_0^{\pi} + \frac{1}{3\beta} \int_0^{\pi} \frac{2\sin\theta\cos\theta}{(1-\beta\cos\theta)^3} \, d\theta$$

$$= \frac{2}{3\beta} \int_0^{\pi} \frac{\sin\theta\cos\theta}{(1-\beta\cos\theta)^3} \, d\theta$$

$$= -\frac{1}{3\beta^2} \left[(1-\beta\cos\theta)^{-2}\cos\theta \right]_0^{\pi} - \frac{1}{3\beta^2} \int_0^{\pi} \frac{\sin\theta}{(1-\beta\cos\theta)^2} \, d\theta$$

$$= -\frac{1}{3\beta^2} \left[\frac{-1}{(1+\beta)^2} - \frac{1}{(1-\beta)^2} \right] + \frac{1}{3\beta^3} \left[(1-\beta\cos\theta)^{-1} \right]_0^{\pi}$$

$$= \frac{1}{3\beta^2} \frac{2(1+\beta^2)}{(1-\beta^2)^2} - \frac{1}{3\beta^3} \left[\frac{1}{1-\beta} - \frac{1}{1+\beta} \right]$$

$$= \frac{4}{3(1-\beta^2)^2}$$

Therefore $I = \frac{8\pi}{3(1-\beta^2)^2}$

Appendix 2

Evaluation of the integral $$\int_0^{2\pi}\int_0^{\frac{b}{\sqrt{\pi}}} \frac{br}{n(r^2+b^2)^{3/2}}\left[1-\frac{(\ell r\cos\theta+mr\sin\theta-bn)^2}{r^2+b^2}\right] dr d\theta$$

Expand the integrand and integrate over θ

$$=\int_0^{2\pi}\int_0^{\frac{b}{\sqrt{\pi}}} \frac{br}{n(r^2+b^2)^{3/2}}\left[1-\frac{\ell^2r^2\cos^2\theta+m^2r^2\sin^2\theta+b^2n^2+r^2\ell m\sin 2\theta-2\ell rbn\cos\theta-2mrbn\sin\theta}{r^2+b^2}\right] dr d\theta$$

$$=\int_0^{\frac{b}{\sqrt{\pi}}} \frac{br}{n(r^2+b^2)^{3/2}}\left[2\pi-\frac{\pi(r^2\ell^2+r^2m^2+2b^2n^2)}{r^2+b^2}\right] dr$$

$$=\frac{2\pi b}{n}\int_0^{\frac{b}{\sqrt{\pi}}} \frac{rdr}{(r^2+b^2)^{3/2}} - \frac{\pi b(1-n^2)}{n}\int_0^{\frac{b}{\sqrt{\pi}}} \frac{r^3\,dr}{(r^2+b^2)^{5/2}} - 2\pi b^3 n\int_0^{\frac{b}{\sqrt{\pi}}} \frac{rdr}{(r^2+b^2)^{5/2}}$$

Now

$$\int_0^{\frac{b}{\sqrt{\pi}}} \frac{rdr}{(r^2+b^2)^{3/2}} = \left[-(r^2+b^2)^{-1/2}\right]_0^{\frac{b}{\sqrt{\pi}}}$$

$$\int_0^{\frac{b}{\sqrt{\pi}}} \frac{rdr}{(r^2+b^2)^{5/2}} = \left[-1/3\,(r^2+b^2)^{-3/2}\right]_0^{\frac{b}{\sqrt{\pi}}}$$

$$\int_0^{\frac{b}{\sqrt{\pi}}} \frac{r^3dr}{(r^2+b^2)^{5/2}} = \int_0^{\frac{b}{\sqrt{\pi}}} 1/2\,\frac{2r\cdot r^2}{(r^2+b^2)^{5/2}}\,dr$$

$$= \left[-1/3(r^2+b^2)^{-3/2}\ r^2\right]_0^{\frac{b}{\sqrt{\pi}}} + 1/3\int_0^{\frac{b}{\sqrt{\pi}}} \frac{2r}{(r^2+b^2)^{3/2}}\ dr$$

$$= \left[-1/3(r^2+b^2)^{-3/2}\ r^2\right]_0^{\frac{b}{\sqrt{\pi}}} - 2/3\left[(r^2+b^2)^{-1/2}\right]_0^{\frac{b}{\sqrt{\pi}}}$$

Combining all the three integrals the main expression reduces to:

$$\frac{2\pi}{n}\left[1-\frac{1}{\sqrt{1+\frac{1}{\pi}}}\right] - \frac{2\pi}{3}n\left[1-\frac{1}{\left(1+\frac{1}{\pi}\right)^{3/2}}\right] + \frac{1}{3n}\left[\frac{1-n^2}{\left(1+\frac{1}{\pi}\right)^{3/2}}\right] + \frac{2\pi}{3n}(1-n^2)\left[\frac{1}{\sqrt{1+\frac{1}{\pi}}}-1\right]$$

which may be simiplified to $\frac{.761}{n} - .660\ n.$

APPENDIX III

The Analysis of a Four-Element Antenna Array with a Constant Phase Lag Between Adjacent Elements and with Currents in the Ratio 1/2 : 1 : 1 : 1/2.

The polar diagram of a 4-element linear antenna arry, in which there is a constant phase lag, $\emptyset$, from one antenna to the next and in which the currents are 1/2 I_o, I_o, I_o, 1/2 I_o from one end of the array to the other, is to be calculated.

Let

d = antenna separation in wavelengths

λ = wavelength

$\psi = \frac{2\pi d}{\lambda} \cos \alpha - \emptyset$

α = angle measured from the array axis

$F(\alpha)$ = polar diagram of the individual elements of the array.

The field strength E is given by the expression

$$E = I_o F(\alpha) \left| \left[1/2 + e^{j(\frac{2\pi d}{\lambda} \cos \alpha - \emptyset)} + e^{2j(\frac{2\pi d}{\lambda} \cos \alpha - \emptyset)} + 1/2\, e^{3j(\frac{2\pi d}{\lambda} \cos \alpha - \emptyset)} \right] \right|$$

$$= I_o F(\alpha) \left| \left[1/2 + \cos \psi + \cos 2\psi + 1/2 \cos 3\psi + j\,(\sin \psi + \sin 2\psi + 1/2 \sin 3\psi) \right] \right|$$

$$|E|^2 = \frac{I_o^2}{4} F^2(\alpha) \left[10 + 16 \cos \psi + 8 \cos 2\psi + 2 \cos 3\psi \right]$$

$$= \frac{I_o^2}{2} F^2(\alpha) \left[5 + 8 \cos (\frac{2\pi d}{\lambda} \cos \alpha - \emptyset) + 4 \cos 2 (\frac{2\pi d}{\lambda} \cos \alpha - \emptyset) + \cos 3 (\frac{2\pi d}{\lambda} \cos \quad - \emptyset) \right]$$

If $F(\alpha)$ is a slowly varying function of α, the maximum in $|E|^2$ occurs for $\frac{2\pi d}{\lambda} \cos \alpha_m - \phi = 0$, which gives $\alpha_m = \cos^{-1} (\frac{\lambda \phi}{2\pi d})$.

Substituting the value of ϕ in terms of α_m, we get

$$|E|^2 = \frac{I_o^2}{2} F^2(\alpha) \left[5 + 8 \cos\left\{ \frac{2\pi d}{\lambda} (\cos \alpha - \cos \alpha_m) \right\} + 4 \cos \left\{ \frac{4\pi d}{\lambda} (\cos \alpha - \cos \alpha_m) \right\} + \cos \left\{ \frac{6\pi d}{\lambda} (\cos \alpha - \cos \alpha_m) \right\} \right] .$$

The polar diagram $F(\alpha)$ of a dipole is given by the expression

$$F(\alpha) = \frac{\cos (\frac{\pi}{2} \cos \alpha)}{\sin \alpha}$$

Using the above value of $F(\alpha)$, $|E|^2$ was calculated as a function of α, for $d = 1.1\lambda$ and for $\alpha_m = 78^\circ$. The calculated values are plotted in Figure 8.

The polar diagram $F(\alpha)$ of the 3-element Yagi, Telrex model 0S309/35, was obtained from manufacturers' specifications. Using the $F(\alpha)$ for the 3-element Yagi, $|E|^2$ was similarly calculated for the Yagi array as for the dipole array, and is shown in Figure 8.

The polar diagrams of the dipole and the Yagi arrays were also calculated for the case of zero phase shift, i.e., when $\phi = 0$ or $\alpha_m = \pi/2$, and are shown in Figure 8 for comparison. In order to show the loss of the main beam power as a result of the beam tilt, the polar diagrams for the case of constant phase shift have been normalized with respect to those of zero phase shift.

REFERENCES

Agy, V., The location of the auroral absorption zone, J. Geophys. Research, 59, 267-272.

Akasofu, S-I., Large scale auroral motions and polar magnetic disturbances, J. Atmospheric and Terrest. Phys. 19, 10-25, 1960.

Anderson, K. A., Soft radiation events at high altitude during the magnetic storm of August 29-30, 1957, Phys. Rev. 111. 1397-1405, 1958.

Anderson, K. A. and Enemark, D. C., Balloon observations of X-rays in the auroral zone II, J. Geophys. Research 65, 3521-3538, 1960.

Appleton, E. V. and Chapman, F. W., The collisional friction experienced by vibrating electrons in ionized air, Proc. Phys. Soc. (London) 44, 246- , 1932.

Appleton, E. V., Naismith, R. and Ingram, L. J., British radio observations during the second international polar year 1932-1933, Phil. Trans. Roy. Soc. 236, 191-259, 1937.

Baily, D. K. Disturbances in the lower ionosphere observed at VHF following the solar flare of 23 Feb. 1956 with particular reference to auroral zone absorption, J. Geophys. Research 62 (3) 431-462, 1957.

Baily, D. K., Abnormal ionization in the lower ionosphere associated with cosmic ray flux enhancements, Proc. Inst. Radio Engrs., 47, 255-266, 1959.

Bates, D. R., Theory of the auroral spectrum, Ann. Geophys. 11, 253, 1955.

Bethe, H. A., Handbuch der Physik, Julius Springer, Berlin Vol. 24, 1933.

Bhavsar, P. D., Scintillation counter observations of auroral X-rays during the geomagnetic storm of May 12, 1959, J. Geophys. Research 66, 679-692, 1961.

Bialecke, F. P. and Dougal, A. A., Pressure and temperature variation of the electron-ion recombination coefficient in nitrogen, Jour. Geophys. Res. 63, 539, 1958.

Brown, R. R., Hartz, T. R., Landmark, B., Leinbach, H. and Ortner, J., Large scale electron bombardment of the atmosphere at the sudden commencement of geomagnetic storms, J. Geophys. Research, 66, 1035-1041, 1961.

Brown, R. R., Balloon observations of auroral zone X-rays, J. Geophys. Research, 66, 1379-1388, 1961.

Campbell, W. H. and Leinbach, H., Ionospheric absorption at times of auroral and magnetic pulsations, J. Geophys. Research, 66 25-31, 1961.

Chamberlain, J. W., Physics of the aurora and airglow, International Geophys. Series, Vol. II, Academic Press, 1960.

Chapman, S., The absorption and dissociative or ionizing effect of monochromatic radiation in an atmosphere on a rotating earth, Proc. Phys. Soc. London 43, 26-45, 483-501, 1931.

Chapman, S. and Cowling, T. G., The mathematical theory of non-uniform gases, Camb. Univ. Press.

Chapman, S. and Little, C. G., The non-deviative absorption of high-frequency radio waves in auroral latitudes, J. Atmospheric and Terrest. Phys. 10, 20-31, 1957.

Chorbajian, J., Sugiura, M., Parthasarathy, R., Radio-wave absorption coefficients based on Sen-Wyller magneto-ionic formula, University of Alaska, Geophysical Institute Report No. UAG-R132, 1962.

Cox, J. W. and Davies, K., Statistical studies of polar radio blackouts, Can. J. Phys. 32, 743-756, 1954.

Dicke, R. H., The measurement of thermal radiation at microwave frequencies, Rev. Sci. Instr. 17, 268, 1946.

Evans, D. S., A pulsating auroral zone X-ray event in the 100 second period range, J. Geophys. Research, 68, 395-399, 1963.

Faire, A. C. and Champion, K.S.W., Measurements of dissociative recombination and diffusion in nitrogen at low pressures, Phys. Rev. 113, 1959.

Fermi, E., Nuclear Physics, Revised Edition, The University of Chicago Press, 1950.

Friedman, H., Physics of the upper atmosphere, Chap. IV, pp. 133-215, Edited by J. A. Ratcliffe, Published by Academic Press, 1960.

Gustaffson, G. and Ortner, J., Kiruna Geophysical Observatory, Scientific Report No. 2, Contract No. AF 61(052)-288, 1962.

Halliday, D., Introductory Nuclear Phys. II Edition, John Wiley & Sons Inc. 1960.

Harang, L., The auroral luminosity curve, Terrest. Mag. 51, 381-400, 1946.

Heitler, W., The quantum theory of radiation, III Edition 422 pp. Clarendon Press, 1954.

Heppner, J. P., Byrne, E. C., Belon, A. E., The association of absorption and E_s ionization with aurora at high latitudes, J. Geophys. Research 57, 121-134, 1952.

Hodgman, C. D., Handbook of Chemistry and Physics, Forty-second Edition, Published by the Chemical Rubber Publishing Co., 1961.

Holt, C., Landmark, B. and Lied, F., Analysis of riometer observations obtained during polar radio blackouts, J. Atmospheric and Terrest. Phys. 23, 229-243, 1961.

Holt, O., and Omholt, A., Auroral luminosity and absorption of cosmic radio noise, Norwegian Defence Research Establishment, Tech. Note No. 2, AF 61(052)-526, 1962.

Hunsucker, R. D. and Owren L., Auroral sporadic E ionization, J. Research Natl. Bur. Standards, 66D 581-592, 1962.

Huxley, L. G. H., The propagation of electromagnetic waves containing free electrons, Phil. Mag. 29, 313-329, 1940.

Huxley, L. G. H., Proc. Phys. Soc. (London) 68, 884, 1951.

Jancel, R. et Kahan, T., Mechanique statistique des plasmas electroniques lorentziens et ses applications a l'ionosphere, The Physics of the Ionosphere published by the Physical Society, London, 1955.

Jelly, D. H., Mathews, A. G. and Collins, C., Study of polar cap and auroral absorption, J. Atmospheric and Terrest. Phys. 23, 206-215, 1961.

Kane, J. A., Arctic measurements of electron collision frequencies in the D-region of the ionosphere, J. Geophys. Research 64, 133-139, 1959.

Kane, J. A., Re-evaluation of ionospheric electron densities and collision frequencies derived from rocket measurements of refractive index and attenuation, J. Atmospheric and Terrest. Phys. 23, 338-346, 1961.

Kavadas, A. W., (1961) Absorption measurements near the auroral zone, J. Atmospheric and Terrest. Phys. 23, 170-175, 1961.

Little, C. G., High latitude ionospheric observations using extraterrestrial radio waves, Proc. Inst. Radio Engrs. 42, 1700-1701, 1954.

Little, C. G. and Leinbach, H., Some measurements of high-latitude ionospheric absorption using extraterrestrial radio waves, Proc. Inst. Radio Engrs. 46 (1) 334-348, 1958.

Little, C. G., Leinbach, H., The Riometer - a device for the continuous measurement of ionospheric absorption, Proc. Inst. Radio Engrs. 47 (2) 315-320, 1959.

Machin, K. E. Ryle, M. and Vonberg, D. D., The design of an equipment for measuring small radio-frequency noise powers, Proc. Inst. Elec. Engrs. 99 Part III, 127-134, 1952.

Maehlum, B. and O'Brien, B. J., Study of energetic electrons and their relationship to auroral absorption of radio waves, J. Geophys. Research, 68, 997-1009, 1963.

Major, G., The association of pulsating and flaming auroras with complete ionospheric absorption at Macquarie Island, Australian J. Phys. 7, 471-476, 1954.

McDiarmid, I. B., Rose, D. C., and Budzinski, E., Direct measurement of charged particles associated with auroral zone radio-wave absorption, Can. J. Phys. 39, 1888-1900, 1961.

McIlwain, C. E., Direct measurement of particles producing visible auroras, J. Geophys. Research, 65, 2727-2747, 1960.

Meek, J. H., Attenuation of radio waves in the auroral zone, Radio Physics Laboratory, Report No. 5, Defence Research Board, Ottawa, Canada

Meredith, L. H., Gottlieb, M. B., Van, Allen, J. A. Direct detection of soft radiation above 50 kms in the auroral zone, Phys. Rev. 97, 201, 1955.

Minzner, R. A., Champion, K. S. W., and Pond, H. L., Air Force Surveys in geophysics, No. 115, ARDC Model Atmosphere 1959, Air Force Cambridge Research Lab.

Mitra, S. K., The upper atmosphere II edition 1952, The Asiatic Society, Calcutta, India.

Mitra, A. P. and Jones, R. E., The enhancement of ionospheric ionization during solar flares, J. Atmospheric and Terrest. Phys. 5, 104-106, 1954.

Montalbetti, R., Photoelectric measurements of hydrogen emissions in aurora and airglow, J. Atmospheric and Terrest. Phys. 14, 200-212, 1959.

Nicolet, M., The collisional frequency of electrons in terrestrial atmosphere, Phys. Fluids 2, 95-99, 1959.

Omholt, A., Ionization by auroral particles, Institute of Theoretical Astrophysics, University of Oslo, Scientific Report No. 6, 1960.

Panofsky, W. K. H. and Philips, M., Classical electricity and magnetism, Addison-Wesley Pub. Co. 1955.

Phelps, A. V., Fundingsland, O. T. and Brown, S. C., Microwave determination of the probability of collision of slow electrons in gases, Phys. Rev. 84, 559-562, 1951.

Phelps, A. V., Pack, J. L., Electron collision frequencies in nitrogen and in the lower ionosphere, Phys. Rev. Letters 3, 340-342, 1959.

Reid and Collins, Observations of abnormal VHF radio-wave absorption at medium and high latitudes, J. Atmospheric and Terrest. Phys. 14, (1,2) 63-80, 1959.

Romick, G. J., and Elvey, C. T., Variations in the intensity of the hydrogen emission line Hβ during auroral activity, J. Atmospheric and Terrest. Phys. 12, 283-287, 1958.

Sayers, J. Solar eclipses and the ionosphere, Pergamon Press, 1956, Recent laboratory studies of recombination cross-sections.

Sen, H. K., Wyller, A. A., On the generalization of the Appleton-Hartree magneto-ionic formulas, J. Geophys. Research, 65, 3931-3950, 1960.

Shain, C. A., Galactic radiation at 18.3 Mc/s, Australian J. Sci. Research A 4, (3), 258, 1951.

Shklovsky, I. S., Cosmic Radio Waves, Harvard University Press, Camb. Mass., 1960.

Sommerfeld, A., Ann. Phys. (Lpz) 11, 257, 1931.

Spencer, L. V., Theory of electron penetration, Phys. Rev. 98, 1597-1615, 1955.

Starr, A. T., Radio and radar technique, Isac Pitman & Sons, London, 1953.

Swift, D. W., The effect of solar X-rays on the ionosphere, J. Atmospheric and Terrest. Phys. 23, 29-56, 1961.

Thomas, J. A. and McNicol, R. W. E., A highly directive rotating array for the observation of field-aligned irregularities, Scientific Report No. 1, 1960, Contract No. AF 64(500)-9, University of Queensland, Brisbane, Australia.

Van Allen, J. A., Direct detection of auroral radiation with rocket equipment, Proc. Natl. Acad. Sci. 43, 57-62, 1957.

Wells, H. W., Polar radio disturbances during magnetic bays, Terr. Mag. Atmosph. Elect. 52, 315-320, 1947.

Winckler, J. R., Cosmic Ray Group, University of Minnesota, Tech. Report No. CR-40, 1960.

Winckler, J. R. and Peterson, L., Large auroral effect on cosmic ray detectors observed at 8g/cm^2 atmospheric depth. Phys. Rev. 108, 903-905, 1957.

Winckler, J. R. Peterson, L. E., Hoffman, R. and Arnoldy, R., Auroral X-rays cosmic rays and related phenomenon during the storm of February 10-11, 1958, J. Geophys. Research 64, 597-610, 1959.